# The future Climate of Bangladesh

**MET**report nr. 20/2025. ISSN: 2387–4201 Climate

Md. Bazlur Rashid, Kajsa Parding, Hans Olav Hygen, Afruza Sultana, Jan Even Øie Nilsen, S.M.Quamrul Hassan

METreport
nr. 20/2025

# The future Climate of Bangladesh

## Projections of the climate in Bangladesh for the 21st century

Md. Bazlur Rashid, Kajsa Parding, Hans Olav Hygen,
Afruza Sultana, Jan Even Øie Nilsen, S.M.Quamrul Hassan

| Title | Date |
|---|---|
| The future Climate of Bangladesh | 05.11.2025 |
| **Section** | **Report nr.** |
| 2387-4201 | 20/2025 |
| **Authors** | **Classification** |
| Md. Bazlur Rashid, Kajsa Parding, Hans Olav Hygen, Afruza Sultana, Jan Even Øie Nilsen and S.M.Quamrul Hassan | Free ● Restricted ○ |
| **Client** | |
| NORAD | |


**Abstract**

With its low altitude deltaic geography and densely populated, agriculture-based society, Bangladesh is among the most vulnerable countries in the world when it comes to climate change. Global warming is no longer an abstract threat in the far future, but has been observed and felt in recent decades as increasing temperatures and stronger and more frequent heatwaves. In this report, we examine how the climate will continue to unfold until 2100, using state-of-the-art climate model data (NEX-GDDP-CMIP6) to explore how various levels of greenhouse gas emissions could impact important aspects of climate and society. Assuming continued high emissions of greenhouse gases, Bangladesh would likely experience a warming of +1.5 °C to +4.5 °C. Heatwaves are expected to continue to rise in severity and frequency, and may in parts of Bangladesh be a threat throughout the year. There is also a significant risk of more extreme precipitation, which may result in local flooding and slides. The compound effects of sea level rise and storm surges, especially during cyclones, poses a threat to coastal communities. Climate change will affect all sectors of Bangladesh, and there is an urgent need for local climate adaptation and international climate mitigation measures to protect lives, livelihoods, and ecosystems in Bangladesh.

# Contents

Photo: Amdadphoto/Shutterstock

1

# Summary for policy makers

In the last century, the temperature on Earth has increased at an alarming rate. The primary cause is the increasing levels of greenhouse gases in the atmosphere, caused by human activity: the burning of fossil fuels, land use change and deforestation. The warming trend has been accompanied by an acceleration of the water cycle, changes in weather patterns, melting of the cryosphere, and severe impacts on ecosystems (Field et al., 2012; IPCC, 2021).

In Bangladesh, the effect of this warming trend has already been felt in stronger and more frequent heatwave conditions (defined in Bangladesh as three consecutive days with maximum temperature above 36 °C). In recent decades, heatwave days have been observed more often, both in the pre-monsoon season, which is known to be very hot, and in the monsoon season in which such heat has historically been a rare occurrence (Rashid et al., 2024).

Projections of the future climate of Bangladesh based on model output (the ensemble mean of 23 climate models from the NASA Earth Exchange Global Daily Downscaled Projections, NEX-GDDP-CMIP6) with a scenario of continued high emissions of greenhouse gases (SSP3-7.0) show the following main tendencies in the future:

**Mid-century (2041–2070):**

- The increase in daily mean temperature is projected to be between +1 °C and +2 °C, depending on the region and season, with the largest increase in the post-monsoon season.
- The daily maximum temperature is expected to increase by approximately +1.0 °C to +2.5 °C, with the largest increase in the post-monsoon season.
- The daily minimum temperature is projected to increase by approximately +2.0 °C to +3.0 °C, indicating a stronger warming at night than during the day.

**End of the century (2071-2100):**

- The increase in daily mean temperature is projected to be between +1.5 °C and +4.5 °C, with the largest increase in the winter season.
- The daily maximum temperature is expected to increase by +1.5 °C to +4.0 °C, with the largest increase in the winter season.
- The daily minimum temperature is expected to increase by +3.0 °C to +4.5 °C, with some regions like Rangpur and Rajshahi potentially experiencing extreme increases of over +5.0 °C.

The effects of the warming will be a further increase in heatwaves, and for some regions, especially in the western part of the country, heatwaves will have a strong presence in all seasons.

There is greater uncertainty for the precipitation in the future. Globally, a trend toward more total precipitation but a smaller area of the Earth with precipitation on a given day suggests

more heavy precipitation. For Bangladesh, where most of the precipitation is associated with the monsoon, total monsoon rainfall is projected to increase by about 15% (ensemble mean). Regional variations indicate that the northeastern parts of the country will receive the largest increase in precipitation. Combining this signal with the global signal of stronger precipitation showers, one may expect more extreme precipitation.

The global sea level is rising due to global warming. This increase is partly due to thermal expansion of sea water and partly due to melting of glaciers. The increase in global sea level is a slower process than the increase in air temperature, and is expected to continue for centuries. In the latest assessment report from the IPCC (AR6), global sea level rise projections under a high emission scenario (SSP5-8.5) are summed up to have a median of 0.77 m by the end of the 21st century with a likely range of 0.63 to 1.01 m. In Bangladesh, the compound effects of sea level rise, storm surges, and waves, especially during cyclones, could be devastating for coastal communities. Chronic sea level rise could displace around 0.9 million people in Bangladesh by 2050.

The warmer and wetter climate will affect all sectors of Bangladesh; e.g. there is an indication that the risk of dengue and malaria might increase. The sea level rise will worsen challenges with coastal flooding and salt intrusion, threatening agriculture, fisheries and drinking water supplies. High temperatures increase the risk of serious heat-related illnesses, both immediate and chronic, and heat waves pose a threat to labor health and productivity.

These examples of effects from global warming underscore the urgent need for local climate adaptation and international climate mitigation measures to protect lives, livelihoods, and ecosystems in Bangladesh. It's important to bear in mind that global warming is not a sector challenge, but a challenge that needs a cross-sectoral approach and thus requires strong collaboration on all levels of the society.

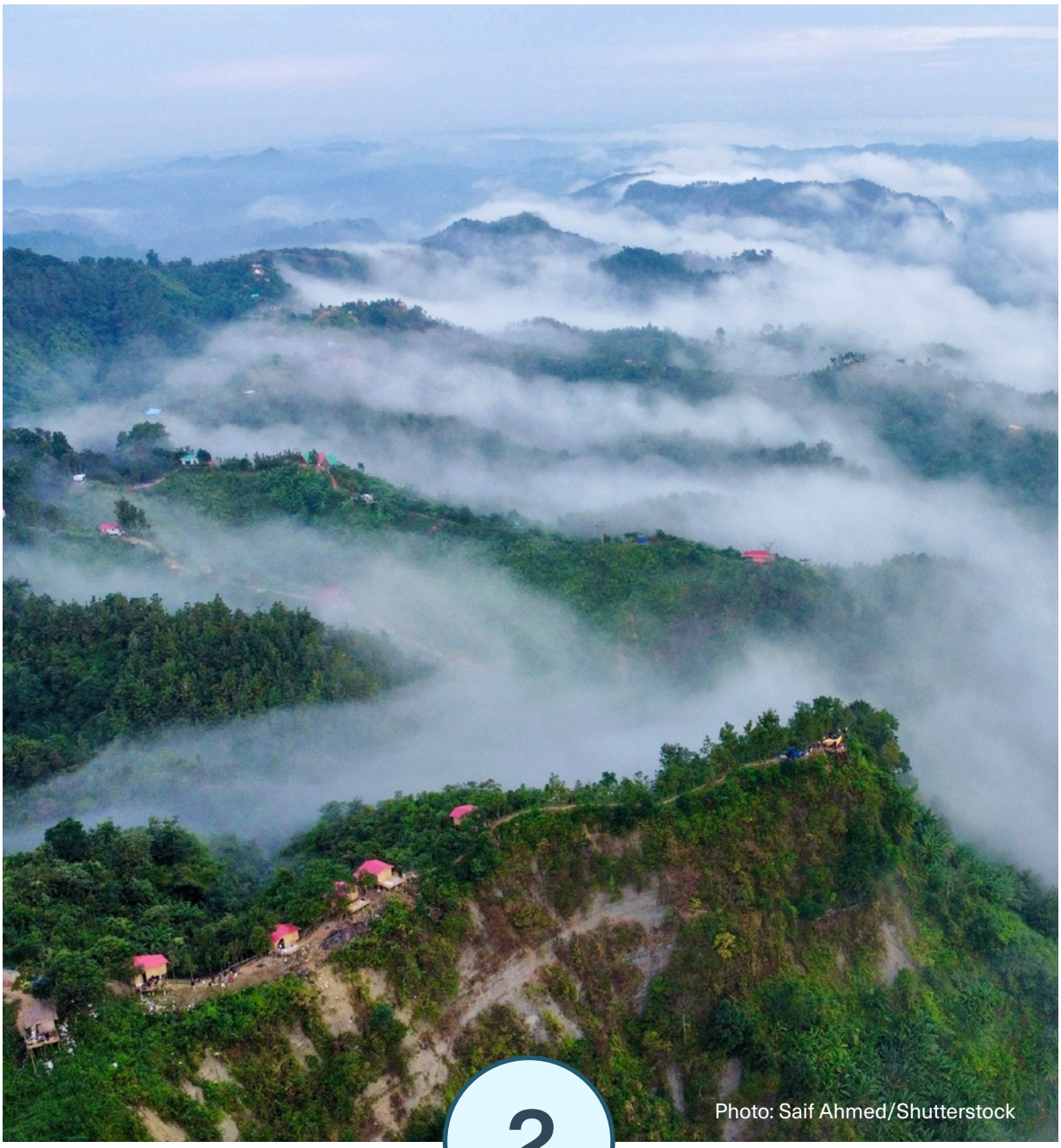

Photo: Saif Ahmed/Shutterstock

2

# Introduction

The climate on the Earth is changing at an unprecedented and alarming rate. Increasing levels of greenhouse gases have resulted in a global warming which is apparent in long-term data from the atmosphere and ocean and has had a measurable effect on the water cycle, biosphere, and cryosphere (Field et al., 2012). The global surface temperature for the time period 2011–2020 was 1.1 °C higher than during the historical period 1850–1900 (IPCC, 2021). Moreover, the last ten years (2015–2024) have been the ten hottest years on record since

direct reliable temperature measurements started to become available almost 200 years ago (NOAA, 2025). In Bangladesh, analysis of historical climate data from 1901 to 2022 reveals that the annual daily average surface air temperature has risen by nearly 2 °C over the past 120 years (Jihan et al., 2025).

Global warming is also associated with increased frequency and intensity of extreme events, including heatwaves, heavy rainfall events, floods, droughts, and wildfires (Clarke et al., 2022, IPCC, 2019). Climate change represents a severe threat to the health, safety and quality of life of humans and animals (Costello et al., 2009). Changes in the global climate are expected to continue over the coming century due to the continued burning of coal and fossil fuels and deforestation. The severity of the consequences will depend on the ability of humanity to rein in its greenhouse gas emissions.

Climate change is typically described in terms of the global mean temperature, but the associated changes in the climate system are not equally distributed across the globe. The highest social and mortality consequences of climate change tend to fall on the Global South, particularly on countries that have contributed the least to historical and current greenhouse gas emissions (Uddin, 2017; Bressler, 2021; Nordhaus, 2017). Bangladesh is one of the most vulnerable countries to climate change due to its low-altitude deltaic geography, which makes it highly vulnerable to sea level rise, and its densely populated, agriculture-dependent society (Hoque et al., 2019; Khanom, 2016; Mohammed et al., 2018). Regional changes such as land development and changes in land use have also affected the temperature and precipitation trends in Bangladesh since the last century (Fahad et al., 2017).

The Constitution of the People's Republic of Bangladesh clearly states an obligation to protect the environment that its citizens live in and depend on: "The State shall endeavor to protect and improve the environment and to preserve and safeguard the natural resources, bio-diversity, wetlands, forests and wildlife for the present and future citizens" (Act No. of 1972, Article 18A). In this report, we aim to gather information about how climate change could play out in Bangladesh until the end of the century, to provide a basis for informed decision-making and further research. The report is based on analyses of data from state-of-the-art global climate models, downscaled to fine spatial resolution, as well as findings from relevant scientific publications, including the latest report from the Intergovernmental Panel on Climate Change (IPCC, 2021).

The historical climate of Bangladesh has been examined and described based on observational data from stations in the country in Khatun et al. (2016), and changes in the climatological conditions in the period 1981–2023 were investigated in Rashid et al. (2024). In this report, we focus on the future and investigate how different emission scenarios could influence the climate of Bangladesh. The scenarios range from optimistic forecasts, where humans manage to reduce greenhouse gas emissions in the next few decades, to those that represent a failure to phase out fossil fuels at sufficient speed or at all. Towards the end of the century, the levels of greenhouse gas emissions result in vastly different outcomes in terms of warming and sea level rise. The diverging levels of projected climate change emphasize that the future is not set in stone and that this generation holds the power and responsibility for what the world will be like for decades and centuries to come.

Photo: Vectors and photos

3

# Data sources and methods

## Climate models and downscaling

Our collected knowledge about the climate system is based on a long history of scientific studies, theoretical and empirical, as described in Chapter 1.3 of the IPCC Sixth Assessment Report (AR6; IPCC, 2021). Much of the climate change and variations predicted by theory have been observed in historical records of the atmosphere, cryosphere, ocean and biosphere. Climate models provide a further opportunity to investigate the climate system and how it responds to internal variations and external forcings.

Climate projections are representations of possible outcomes of the Earth's climate for future decades (typically until 2100) as it is simulated based on assumed 'scenarios' for the

concentrations of greenhouse gases, aerosols, and other atmospheric constituents that affect the Earth's radiative balance. Climate projections are obtained by running numerical models of the Earth's climate, covering the whole globe or a selected region. These models are referred to as Global Climate Models (GCMs) or Regional Climate Models (RCMs). Climate models are based on equations that describe physical processes within and interactions between various parts of the Earth system, e.g., the transfer of solar and thermal radiation through the atmosphere, the atmospheric circulation and the water cycle. Chemical reactions in the atmosphere and ocean, and the interactions between the atmosphere, ocean and biosphere can also be included. Climate models that incorporate physical, chemical and biological processes and their interactions in the Earth System are known as Earth System Models.

GCMs are valuable tools for exploring possible global futures based on certain conditions e.g. climate scenarios, but the simulations should not be interpreted as predictions in the same way as weather predictions, e.g. for a specific outcome on a specific date. The coarse resolution of the GCMs make them unfit to explore the fine-scale heterogeneities of climate variability and change. Topographic features like mountains, glaciers, water bodies, infrastructure, land-cover characteristics and components of the climate system are in reality finer than the resolution of GCMs. However, these heterogeneities are often essential to the impact modelers and decision-makers who require information on potential impacts on crop production, hydrology, species distribution etc. Many methods have been developed to provide high-resolution information about climate change to meet society's requirements for risk assessment and decision-making.

The derivation of fine-scale climate information from GCM output is called downscaling. There are many downscaling methods, but they can broadly be divided into two groups: dynamical downscaling and empirical-statistical downscaling. Dynamical downscaling refers to the use of an RCM with higher spatial resolution, from 50 x 50 km down to 5 x 5 km or even less (Giorgi and Gutowski, 2015). Empirical-statistical downscaling (ESD) is based on establishing statistical relationships between historical and current large-scale atmospheric and local climate variables and then applying that statistical model to calculate future changes in local climate variables from GCM projections (Murphy, 2000; Schmidli et al., 2007; Benestad et al., 2008; Hewitson et al., 2014; Labeurthre et al., 2024). Both approaches are based on the assumption that the local climate is determined by the interactions between large-scale atmospheric characteristics (circulation, temperature, moisture, etc.) and local conditions (water bodies, mountain ranges, land surface properties, etc.).

Dynamical and empirical-statistical downscaling both have their strengths and weaknesses. RCMs are, just like GCMs, based on physics and provide a more consistent representation of multiple variables within the regional domain, but is more computationally expensive. Statistical downscaling can be used to produce location-specific climate projections for a particular station, while RCMs provide projections that are only as fine as the spatial grid of the model. Furthermore, since ESD methods are typically computationally efficient, they can be applied to large ensembles of GCMs (many model simulations) and multiple emission scenarios, describing different socio-economic developments and associated levels of greenhouse gases. The ESD approach depends on the critical assumption that the relationship between present large-scale and local climate is stationary under different forcing conditions in the simulated future (Zorita and von Storch, 1999).

## Emission scenarios

To capture a range of possible future developments in global society, demographics, economy, and technology, and their implications for greenhouse gas concentrations in the atmosphere, a new set of scenarios referred to as the Shared Socioeconomic Pathways (SSPs) was developed as part of Phase 6 of the Coupled Model Intercomparison Project (CMIP6) (Eyring et al., 2016).

The SSPs describe five distinct trajectories that global society could follow over the coming centuries (Meinhausen et al., 2020):

- **SSP1:** a future of sustainability-focused growth and equality;
- **SSP2:** a "middle of the road" scenario where trends follow historical patterns;
- **SSP3:** a world of regional rivalry and resurgent nationalism with worsening inequalities;
- **SSP4:** increasing inequalities and stratification across and within countries;
- **SSP5:** unconstrained growth in economic output fueled by intense use of fossil fuels.

Within each SSP, there are several possible emission scenarios that are compatible with the described socio-economic development, but mitigation and adaptation efforts are easier in some versions of the future than others. The level of emissions is reflected in the name of the scenarios in terms of the expected levels of increase in Earth's energy balance (radiative forcing) by the year 2100 (1.9 to 8.5 W/m2). For example, SSP1-2.6 is the sustainable growth scenario SSP1 with emissions that result in 2.6 W/m2 radiative forcing by the end of the century, and SSP3-7.0 is the regional rivalry scenario with emissions that results in a 7.0 W/m2 radiative forcing within the same time frame.

In this report, we consider the four 'Tier 1' emission scenarios that have been a top priority in the scenario model intercomparison project in CMIP6 (IPCC, 2021):

- **SSP1-2.6**, which is a low emission scenario, where CO2 emissions cut to net zero around 2050 and the likely global warming ends up in the range of 1.0–1.8 °C by 2100, meeting the target of limiting warming to 2 °C or less, but not the 1.5 °C target.
- **SSP2-4.5**, which is a medium emission scenario which results in a global mean warming in the range of 2.1–3.5 °C by the end of the century.
- **SSP3-7.0**, which is a high emission scenario, where CO2 emissions double by 2100 and the expected global mean temperature increases by 2.8–4.6 °C.
- **SSP5-8.5**, which may be considered an extreme scenario with tripled CO2 emissions by 2100 and a global warming of 3.3–5.7 °C.

The likelihood of the different scenarios was not quantified in the sixth IPCC report on climate change (IPCC, 2021). Rather, they were used to explore how different societal and political choices would impact the global climate and risks of climate related hazards.

The choice of a scenario is based on what one wants to study and achieve. As stated above, IPCC does not quantify or point to any of the scenarios as more likely than others. This lack of quantification by IPCC does not imply that all scenarios have the same likelihood. The lack of mitigation on a global scale so far basically eliminates the probabilities of the low emission scenarios. Similar to the unlikeliness of the low emission scenarios, the high emission scenarios, in particular SSP5-8.5, appears to be on the extreme side, thus leaving moderate scenarios like SSP2-4.5 and SSP3-7.0 as more likely future developments. The precautionary principle indicates, in the choice of a scenario, to err on the pessimistic side. Based on this argument, the scenario SSP3-7.0 will receive the most thorough examination, and we recommend using this as a basis for climate adaptation.

## Empirical-statistical downscaling, CMIP6-NEX-GDDP

For the empirical-statistical downscaling, the analysis in this report was based on the NASA Earth Exchange Global Daily Downscaled Projections (NEX-GDDP-CMIP6) data set, which provides statistically downscaled global climate model output on a common 0.25° x 0.25° (longitude by latitude, corresponding to 25 km x 28 km for Bangladesh) grid at daily temporal resolution (Thrasher et al., 2022). The NEX-GDDP-CMIP6 ensemble consists of simulations from 35 global climate models from CMIP6 (Eyring et al., 2016). However, not all models offer data for every emission scenario (SSP1-2.6, SSP2-4.5, SSP3-7.0, and SSP5-8.5) or for all meteorological variables considered in this report (namely daily precipitation sum, daily mean, maximum and minimum surface temperature). Based on both data availability and validation of the NEX-GDDP-CMIP6 data, through comparison with gridded observational data for Bangladesh, a subset of 23 models was selected for the analysis. The full and reduced NEX-GDDP-CMIP6 ensembles are listed in Table A1 of the Appendix, along with a description of the data validation process (Figures A1.1–A1.11).

In Chapter 4, the present day climate of Bangladesh is presented based on analysis and visualisation of the seasonal climate patterns of the NEX-GDDP-CMIP6 data for the reference period 1985–2014. A comparison of the ensemble mean of this data set to surface-based observations (Appendix 1, Figures A1.8–A1.11) showed that, for both precipitation and temperature, the seasonal cycle and spatial patterns closely follow the observed climatology, indicating that the model data give a realistic picture of the historical climate of Bangladesh.

## Time periods considered in the analysis

To avoid noise from effects of large-scale climate variability on shorter terms (years to decades), like the El Niño Southern Oscillation, it is common to divide and analyse the data in 30 year periods. The chosen time slices to be presented are:

- Historic reference: 1985–2014
- Mid-century: 2041–2070
- End of the century: 2071–2100.

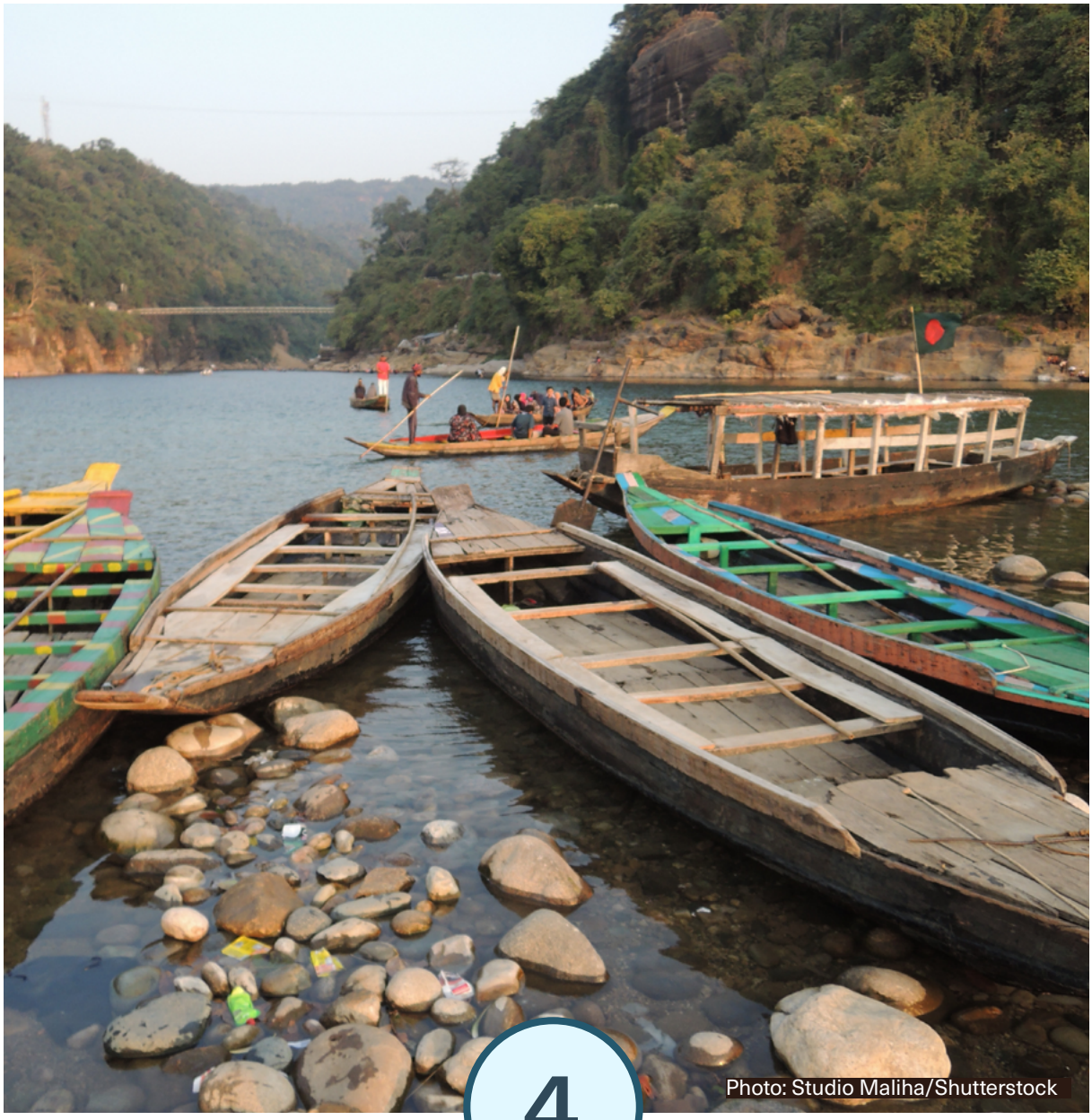

Photo: Studio Maliha/Shutterstock

4

# The present day climate of Bangladesh

Bangladesh is a low-lying country with a sprawling deltaic landscape in the south, where its coastline meets the Bay of Bengal. Most of the territory lies below 100 m in elevation (Figure 4.1), with the highest points located in the Chittagong Hills in the southeastern region bordering Myanmar. Covering an area of 148,460 km$^2$, Bangladesh has a population of over 170 million people, making it the most densely populated country in the world.

The weather and climate of Bangladesh can be divided into distinct seasons according to several different criteria. Here, we adhere to a definition commonly used in climate research: the pre-monsoon or summer season lasts from March to May, followed by the monsoon season from June to September, the post-monsoon from October to November, and winter from December to February.

## Pre-monsoon season or summer (March–May)

The pre-monsoon season in Bangladesh is characterised by high temperatures, with April and May being the hottest months of the year. During this season, the average temperatures range from 25 °C to 29 °C, depending on the region (Figure 4.2a). Daily maximum temperatures, a measure of the peak daytime temperature, range on average from 29 °C to 36 °C, with the highest values observed in the northwestern and southwestern parts of the country (Figure 4.3a). In contrast, daily minimum temperatures, which typically occur at night, range from 19 °C to 25 °C, displaying a slightly different spatial pattern: warmer conditions in the south and slightly cooler temperatures in the north (Figure 4.4a). The spatial distribution of daily mean temperatures (Figure 4.2a) reflects a combination of these patterns, with the north-south gradient of minimum temperatures and high daily maximum temperatures in the west resulting in generally hotter conditions in the southwest and cooler conditions in the northeast.

Due to the intense heating of the land during the daytime in the pre-monsoon season, surface heat low-pressure systems tend to develop over Bihar and West Bengal in India, as well as the northwestern part of Bangladesh. These low-pressure systems facilitate the incursion of moist air from the Bay of Bengal during the afternoon, creating favourable conditions for the formation of thunderclouds and severe convective storms. These events, known locally as Nor'westers ('Kalbaishakhi' in Bengali), are often accompanied by fierce squalls, thunder and heavy rainfall with hail.

On average, Bangladesh receives 418 mm of precipitation during the pre-monsoon season, accounting for just under 20% of its total annual rainfall (Figure 4.5a). Rainfall distribution is uneven, with eastern regions receiving generally more precipitation (400–1200 mm) than western areas (0–400 mm). The highest seasonal rainfall, between 1000 mm and 1200 mm, occurs in the northeastern district of Sylhet.

## Monsoon season or Southwest Monsoon (June–September)

The monsoon season in Bangladesh is characterised by widespread cloud cover, heavy rainfall, and high humidity. During this season, occasional monsoon depressions and low-pressure systems originating from the Bay of Bengal enhance rainfall across the country. Over 70% of Bangladesh's total annual rainfall occurs during the monsoon season. Average rainfall during the reference period ranges from 1000 mm to 2800 mm, depending on the region (Figure 4.5b). The precipitation shows a distinct spatial pattern, namely a west-to-east gradient, with the highest rainfall amounts in the northeastern districts of Sylhet and Sunamganj (2600–2800 mm), and in the southeastern districts of Cox's Bazaar and Bandarban (2400–2600 mm). In contrast, the lowest amounts (1000–1200 mm) were

observed in the western districts of Rajshahi, Nawabganj, Meherpur, Chuadanga and Jhenaidha. Heavy to very heavy rainfall in the southeast can sometimes trigger landslides in hilly regions.

During this season, surface winds shift direction: they become southwesterly/southerly over the southern and central districts, and southeasterly over the country's northern districts. Wind speeds during this period tend to be light to moderate. The timing of monsoon onset and withdrawal varies from place to place and year to year. Typically, the Southwest Monsoon reaches southeastern Bangladesh in the first week of June and spreads across the entire country by the first half of June. It begins to withdraw from the northwestern parts of Bangladesh around 30th of September (Ahmed and Karmakar, 1993).

Despite frequent cloud cover and rainfall, the monsoon season is characterised by high temperatures as well. Because of the high humidity and cloud cover, average nighttime (minimum) temperatures range from 24 °C to 27 °C across the country, several degrees warmer than in any other season (Figure 4.4b). In terms of daily mean temperatures, the monsoon is the warmest season, with average values between 26 °C and 30 °C (Figure 4.2b). However, daily maximum temperatures are generally lower than in the pre-monsoon season, ranging from 29 °C to 34 °C (Figure 4.3b).

## Post-Monsoon season or Autumn (October–November)

The post-monsoon season serves as a transitional season between the monsoon and the winter season. The precipitation declines considerably during October and November, making the onset of the dry period across the country. However, this period is also associated with tropical cyclone activity in the Bay of Bengal. These systems typically move westward initially, then shift northwest, and sometimes re-curve toward the northeast, often impacting the coastal regions of Bangladesh. Some cyclones during this season may reach very severe intensity, accompanied by storm surges. On average, around 8% of the total annual precipitation occurs during this season in the reference period. Rainfall patterns show regional variations, with less rainfall in the western parts of the country (0–200 mm) and higher amounts in the east (200–400 mm) (Figure 4.5c).

Temperatures during the post-monsoon season are between the high temperatures of the pre-monsoon and monsoon seasons and the cooler conditions of winter. In the reference period, the average daily mean temperature ranged from 24 °C to 27 °C, with warmer conditions in the south and cooler temperatures in the north (Figure 4.2c). Daily maximum temperatures ranged from 29 °C to 32 °C, while minimum temperatures were between 19 °C and 23 °C (Figures 4.1–4.3 c).

## Winter Season or Northeast Monsoon (December–February)

The winter season in Bangladesh is characterized by mild temperatures, dry weather, and predominantly very light north to northwesterly winds. Skies are generally clear, though occasional cloud cover and fog can occur. During this season, average temperatures range from 18 °C to 22 °C (Figure 4.2d). As the ridge of sub-continental high pressure extends into

northwestern Bangladesh, temperatures begin to drop. When minimum temperatures fall below 10 °C, cold wave situations may develop. In the reference period, average daily minimum temperatures ranged from 11 °C to 17 °C, with cooler conditions in the north (Figure 4.4d). Daily maximum temperatures range from 25 °C to 28 °C (Figure 4.3.d). Winter is the driest season of the year, with only 2% of the total annual rainfall occurring during this season (Figure 4.5d).

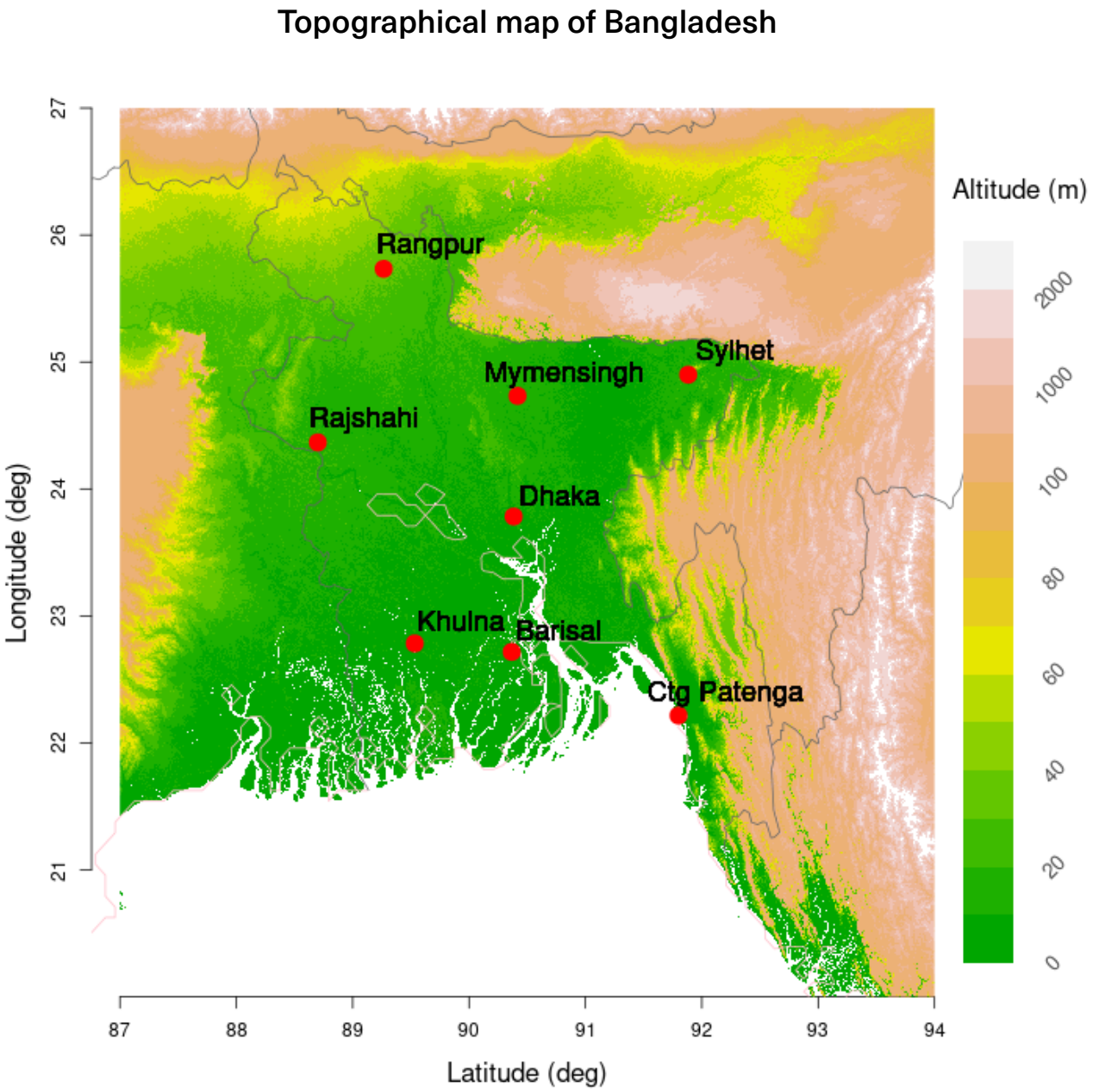


Figure 4.1 Topographical map of Bangladesh with the locations of eight division stations, based on altitude data from the NASA Shuttle Radar Topography Mission (SRTM) Global data set (SRTM, 2013).

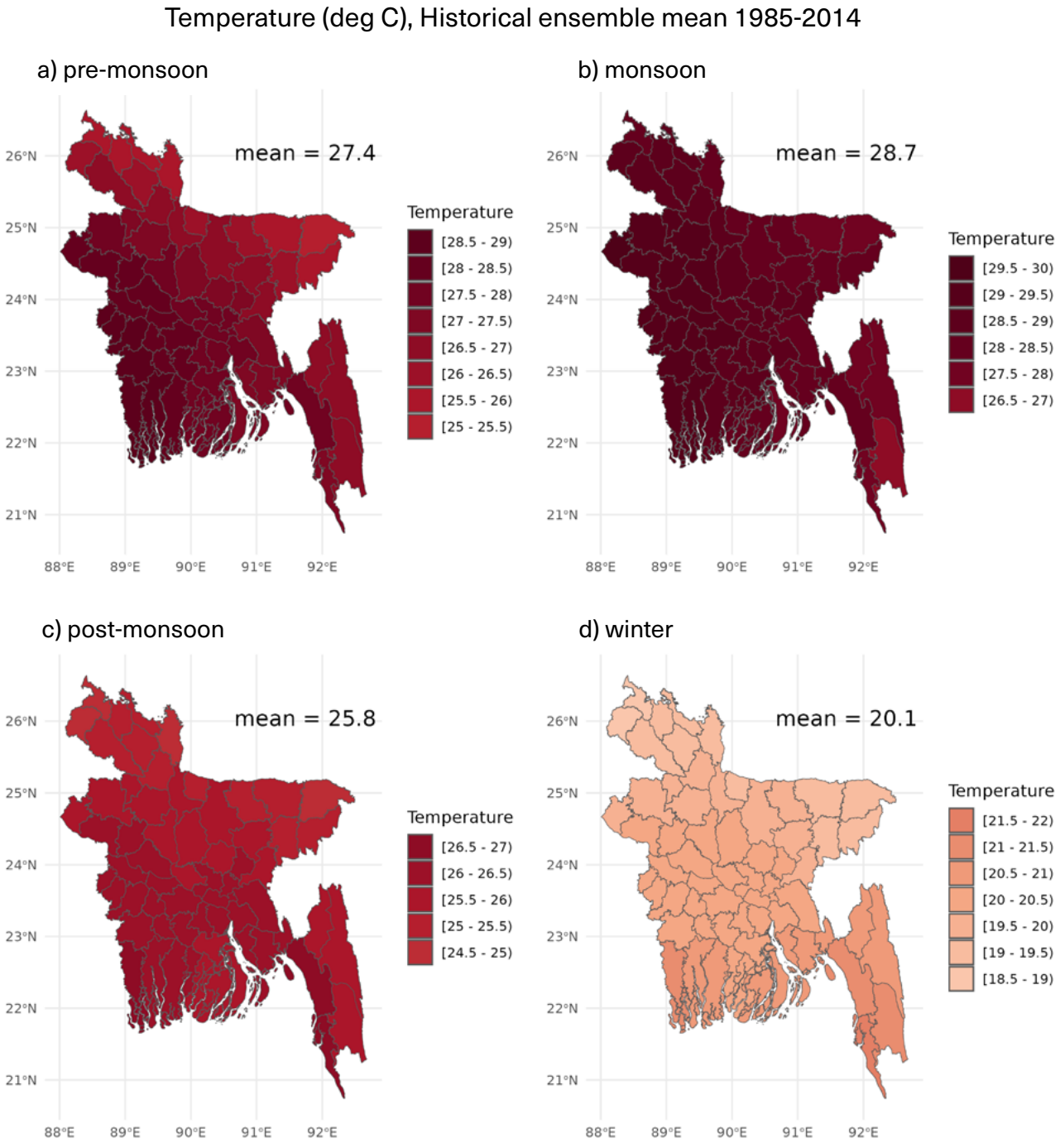


Figure 4.2 NEX-GDDP-CMIP6 ensemble mean of the daily mean temperature in Bangladesh in the reference period 1985–2014 for the a) pre-monsoon (March–May), b) monsoon (June–September), c) post-monsoon (October and November), and d) winter (December–February) seasons. The mean value of each map shows the country average.

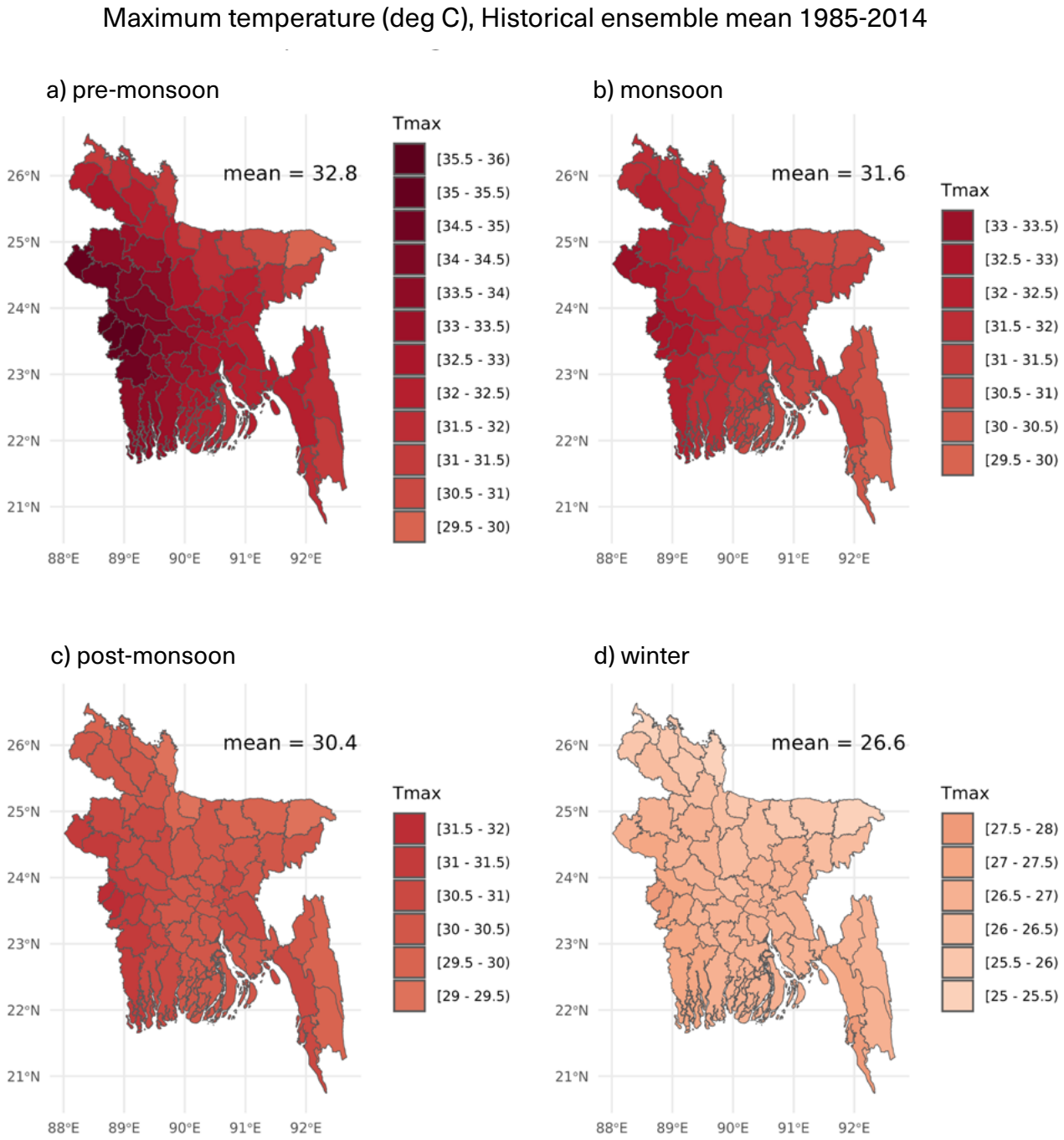


Figure 4.3 NEX-GDDP-CMIP6 ensemble mean of the daily maximum temperature in the reference period 1985–2014 for the pre-monsoon, monsoon, post-monsoon and winter seasons in Bangladesh. The mean value of each map shows the country average.

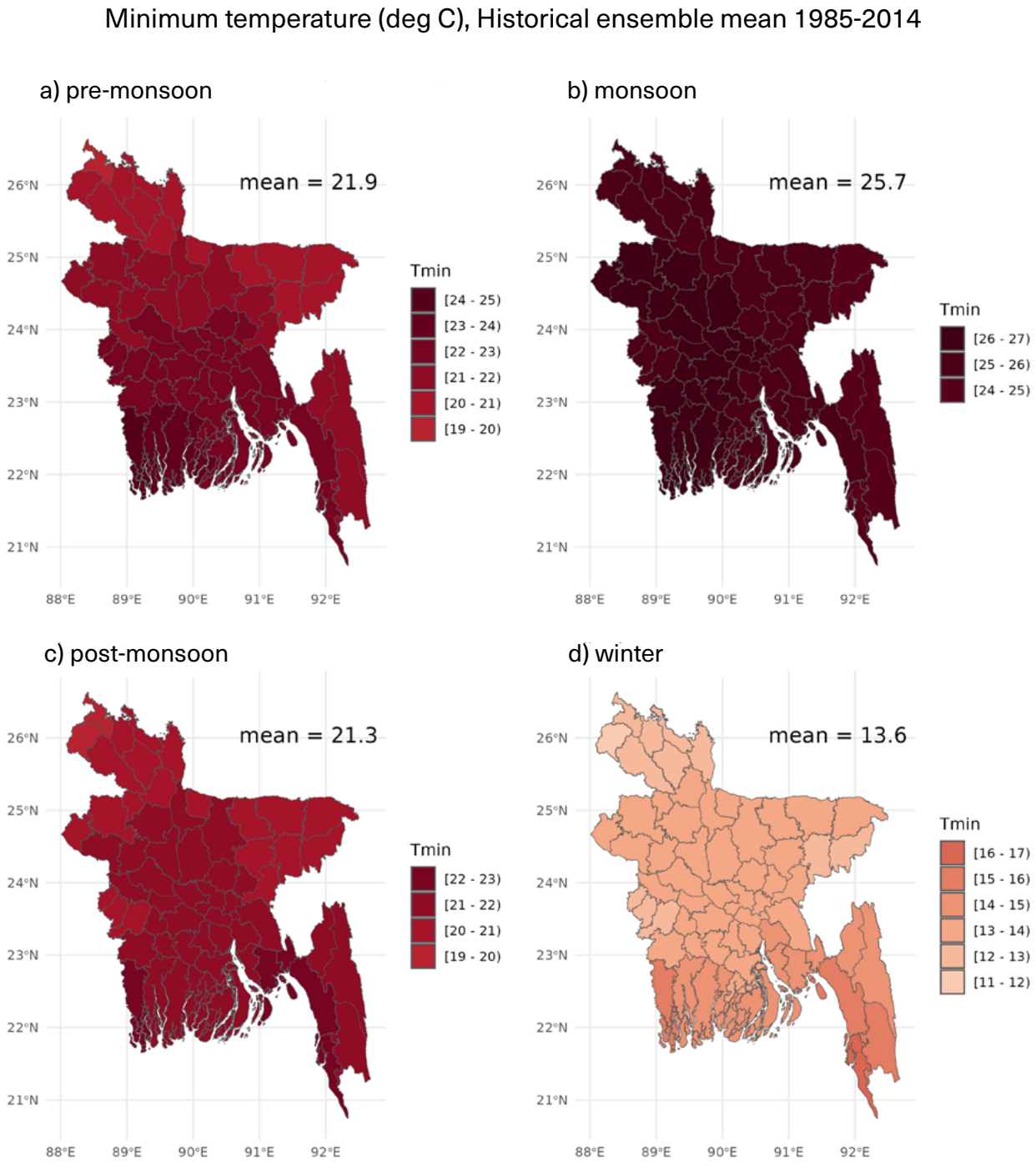


Figure 4.4 NEX-GDDP-CMIP6 ensemble mean of the daily minimum temperature in the reference period 1985–2014 for the pre-monsoon, monsoon, post-monsoon and winter seasons in Bangladesh. The mean value of each map shows the country average.

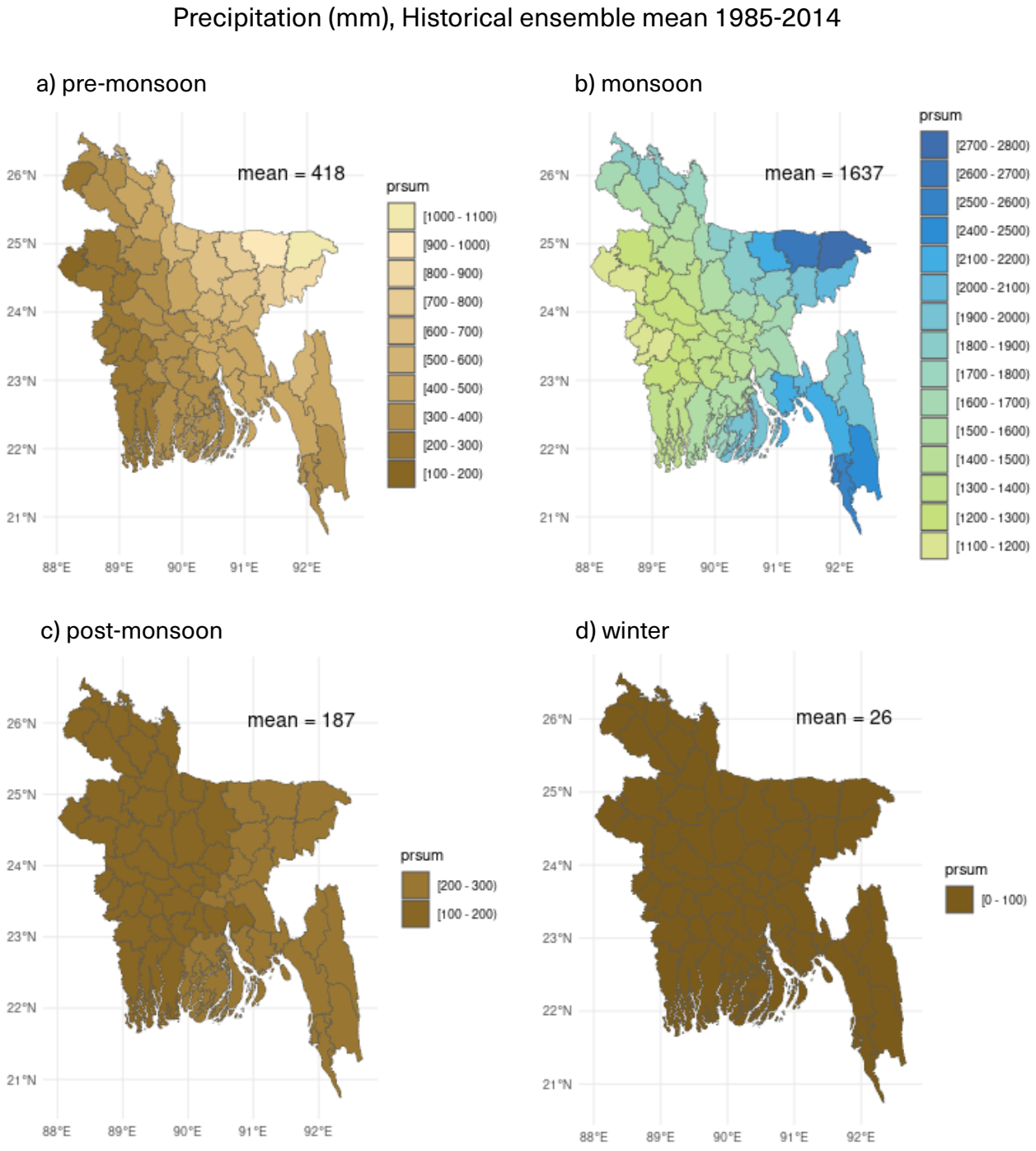


Figure 4.5 NEX-GDDP-CMIP6 ensemble mean of the average seasonal precipitation sum in the reference period 1985–2014 for the a) pre-monsoon b) monsoon c) post-monsoon and d) winter seasons. The mean value of each map shows the country average.

Photo: SK Hasan Ali/Shutterstock

5

# Future projections of temperature

## Daily mean temperature

The NEX-GDDP simulations project warming across all seasons, with an increase in the daily mean temperature of +1 °C to +2 °C by mid-century (2041–2070), and of +1.5 °C to +4.5 °C by the end of the century (2071–2100), depending on the season and region, under the high-emission scenario SSP3-7.0 (Figures 5.1 and 5.2). The weakest warming is projected during the monsoon season. By mid-century, the post-monsoon season shows the highest daily mean temperature increase of +1.8 °C. However, by the end of the century, the highest increase shifts to winter, with temperatures rising by up to +3.3 °C under SSP3-7.0. While the warming is relatively uniform across the country, slightly higher increases are projected in the eastern and northern regions across most seasons, scenarios and time horizons (maps showing results for other scenarios than SSP3-7.0 are presented in Appendix 2).

Projections under the low and medium emission scenarios initially resemble those of SSP3-7.0 in the mid-century but then diverge over time. Under the low emission scenario SSP1-2.6, the warming reaches +1 °C to +2 °C by mid-century, then levels off with little additional increase (Figures A2.1 and A2.4). The medium emission scenario SSP2-4.5 follows a similar early trajectory but ends up with a projected daily mean temperature increase of +1 °C to +4 °C by the end of the century (Figures A2.2 and A2.5). In contrast, the high-emission scenario SSP5-8.5 indicates a stronger warming already in the mid-century (+1.5 °C to +3 °C), with even more pronounced increases towards the end of the century, reaching +3 °C to +5 °C compared to the reference period (Figures A2.3 and A2.6).

The relationship between the various emission scenarios and their projected warming is illustrated in the time series of daily mean temperatures from eight district stations (Figure 5.3). These time series reveal that the projected future warming exceeds both the spread of the model ensemble and the year-to-year variations in observed temperature. All models (100%) project a temperature increase in the future, showing a very strong and consistent trend across all seasons. This means that the warming trend of the climate projections can easily be distinguished from the natural climate variability, underscoring the robustness of the results. Furthermore, the different temperature outcomes among emission scenarios by 2100 highlight the substantial influence of greenhouse gas emissions on the extent of future warming in Bangladesh.

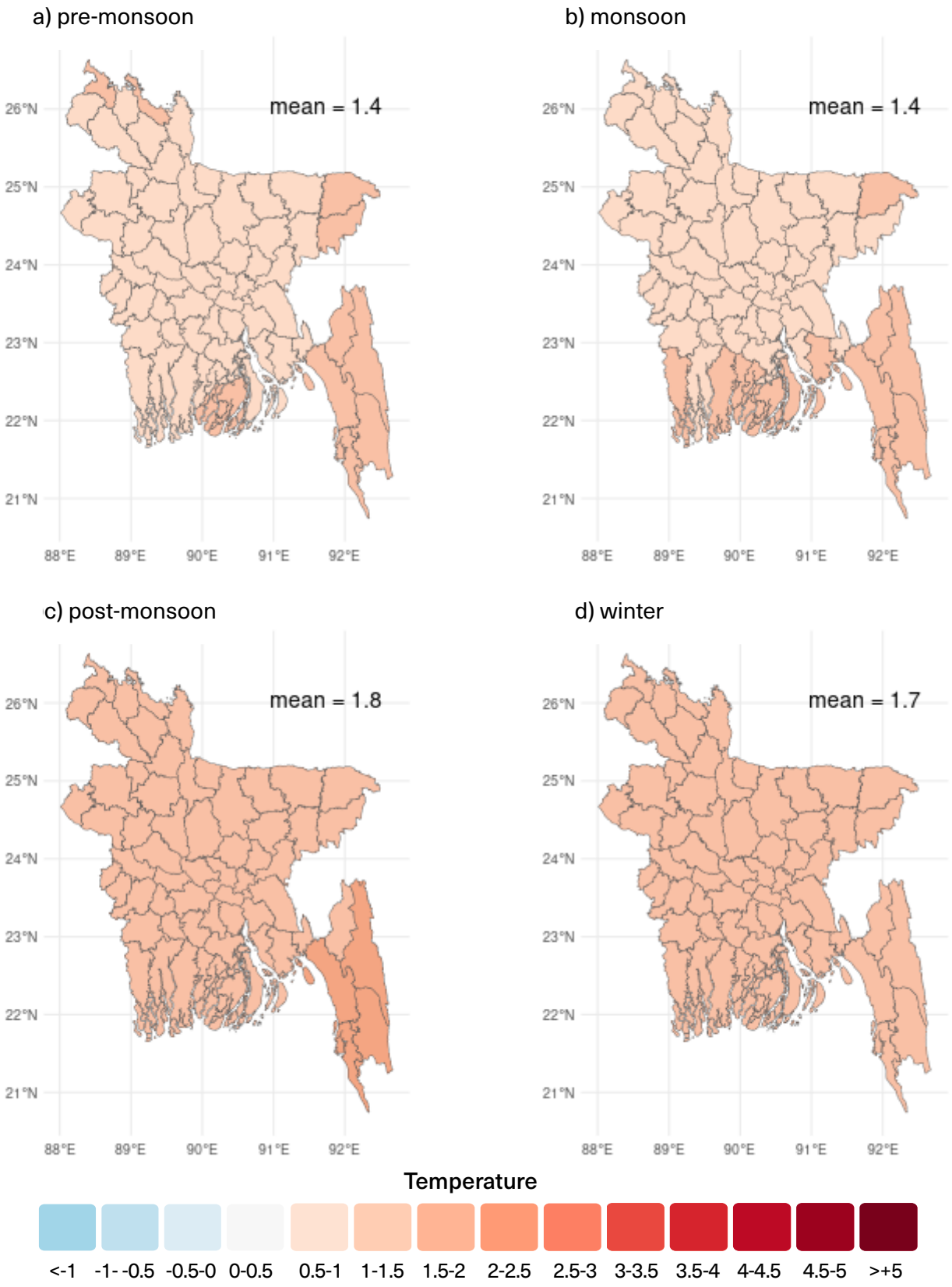


Figure 5.1 Changes in the daily mean temperature from the reference period (1985–2014) to mid-century (2041–2070) under emission scenario SSP3-7.0 as estimated by the NEX-GDDP-CMIP6 ensemble mean for the a) pre-monsoon, b) monsoon, c) post-monsoon, and d) winter seasons. The mean value of each map shows the country average.

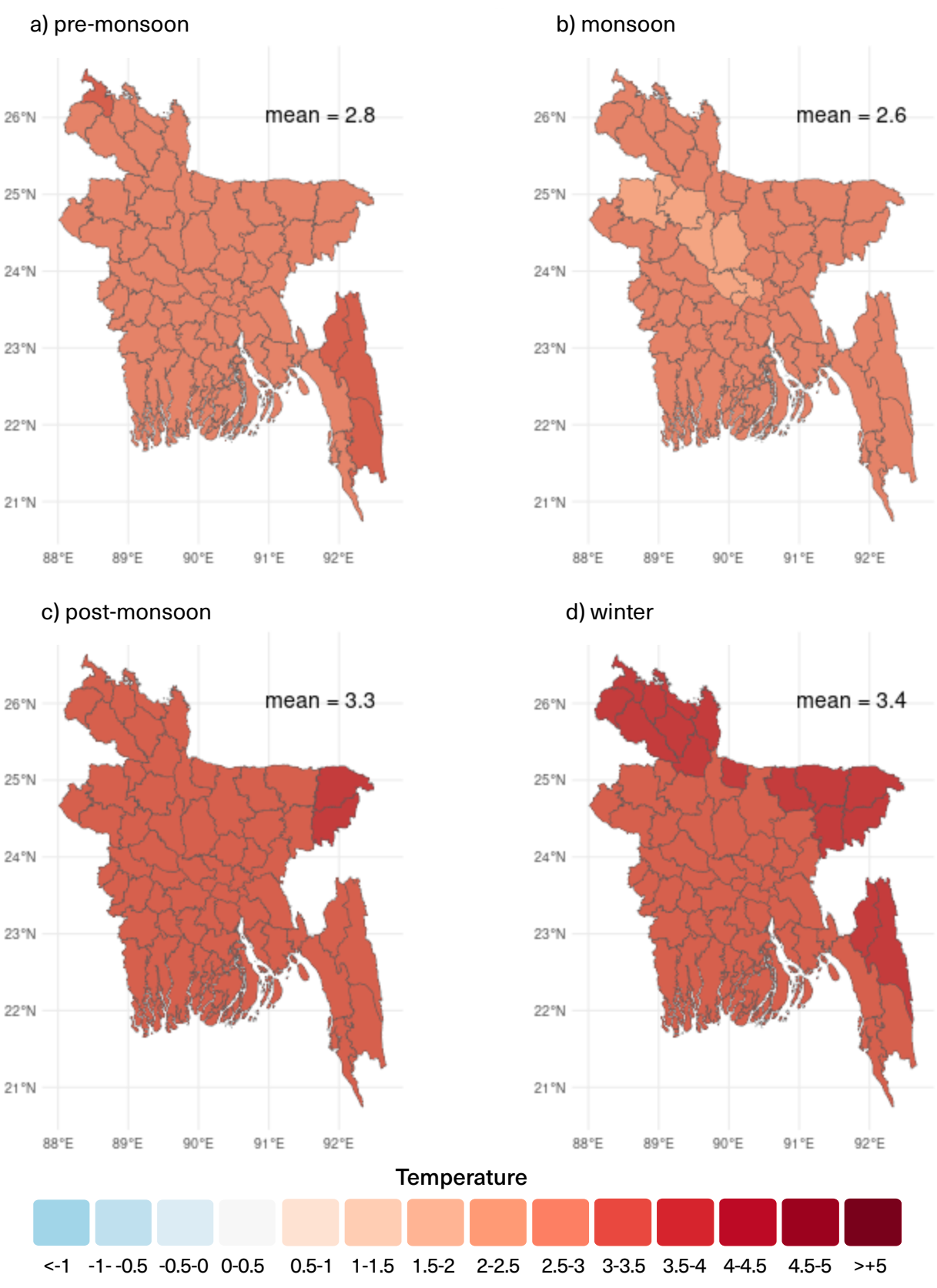


Figure 5.2 Changes in the daily mean temperature from the reference period (1985–2014) to the end of the century (2071–2100) under emission scenario SSP3-7.0 as estimated by the NEX-GDDP-CMIP6 ensemble mean for the pre-monsoon, monsoon, post-monsoon and winter seasons. The mean value of each map shows the country average.

## Annual mean temperature

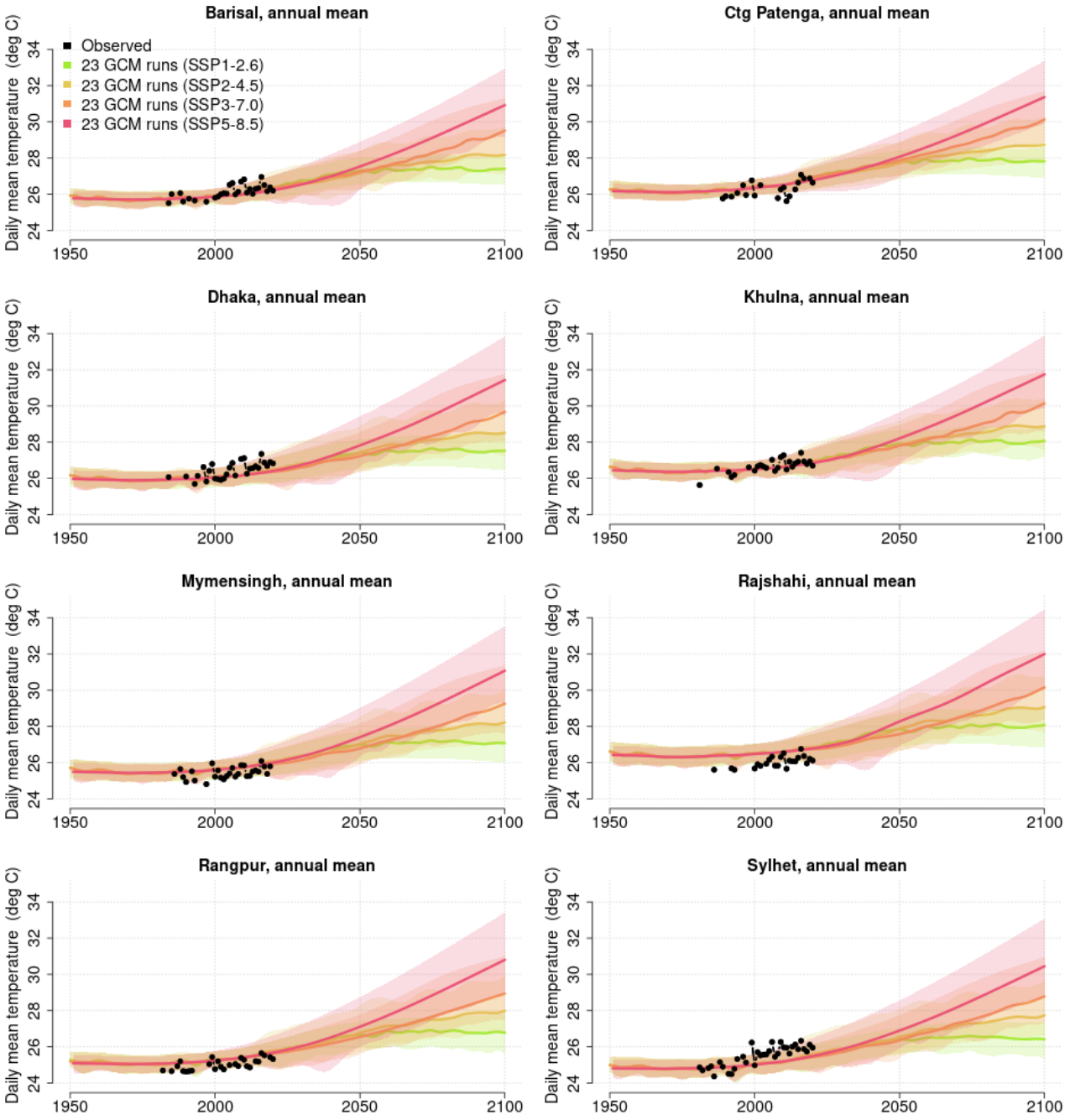


Figure 5.3 The annual mean temperature at eight division stations in Bangladesh, based on observations (black dots) and the NEX-GDDP-CMIP6 climate model ensemble mean (colored lines) and 5th to 95th percentile (envelopes) from the gridpoint nearest each station for emission scenarios SSP1-2.6, SSP2-4.5, SSP3-7.0, and SSP5-8.5 (see legend).

## Daily maximum temperature

The NEX-GDDP-CMIP6 ensemble simulations project a consistent warming trend in the daily maximum temperature across all seasons. Under the high-emission scenario SSP3-7.0, the daily maximum temperature is expected to increase by approximately +1.0 ℃ to +2.5 ℃ during the mid-century period (2041–2070), and by +1.5 ℃ to +4.0 ℃ by the end of the century (2071–2100), depending on the season and region (Figures 5.4 and 5.5).

During the mid-century, the strongest warming under SSP3-7.0 is projected to occur in the post-monsoon season with an average increase of +1.4 ℃ for the whole country, while the weakest warming is projected in the pre-monsoon season (+1.0 ℃ on average). By the end of the century, this pattern shifts: with the most significant warming projected during the winter season (+2.9 ℃ on average), and the least warming occurring in the pre-monsoon and monsoon seasons (+2.3 ℃ on average).

In the mid-century (2041–2070), both the low and medium emission scenarios project similar levels of warming as the high-emission scenario SSP3-7.0. However, their trajectories diverge significantly in the latter half of the century (as shown in Figures A2.7, A2.8, A2.10, and A2.11). The low-emission scenario SSP1-2.6 projects a temperature increase of approximately +1℃ to +2℃ by mid-century, followed by a stabilization, with minimal additional temperature rise beyond mid-century. In contrast, the medium emission scenario SSP2-4.5 follows a similar warming trend until mid-century, but continues to increase afterward. By the end of the century, this scenario projects a daily maximum temperature increase of +1℃ to +3℃ relative to the reference period. The high emission scenario SSP5-8.5 suggests a more pronounced warming trend already early on, with projected increases of +2℃ to +3℃ by mid-century (Figure A2.9). By the end of the century, this trajectory becomes even more extreme, with estimated temperature rises of +3℃ to +5℃ above historical levels (Figure A2.12). These projections highlight the critical influence of emission scenarios on long-term climate outcomes.

The projected increases in daily maximum temperatures (Figures 5.4 and 5.5) are lower than those for daily mean temperatures (Figures 5.1 and 5.2), indicating that nighttime temperatures are increasing faster than daytime temperatures.

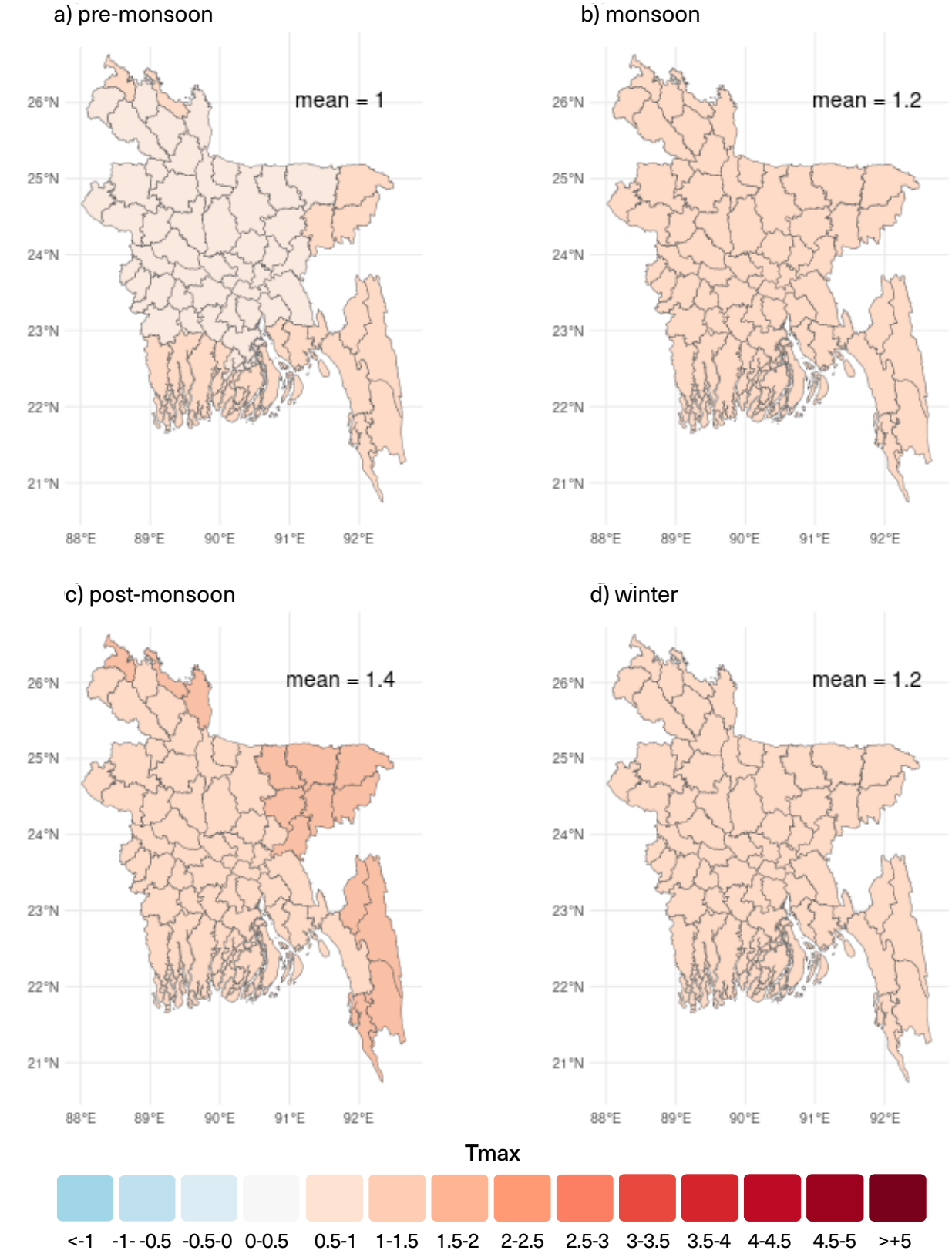


Figure 5.4 Changes in the daily maximum temperature from the reference period (1985–2014) to mid-century (2041–2070) under emission scenario SSP3-7.0, as estimated by the NEX-GDDP-CMIP6 ensemble mean for the a) pre-monsoon, b) monsoon, c) post-monsoon, and d) winter seasons. The mean value of each map shows the country average.

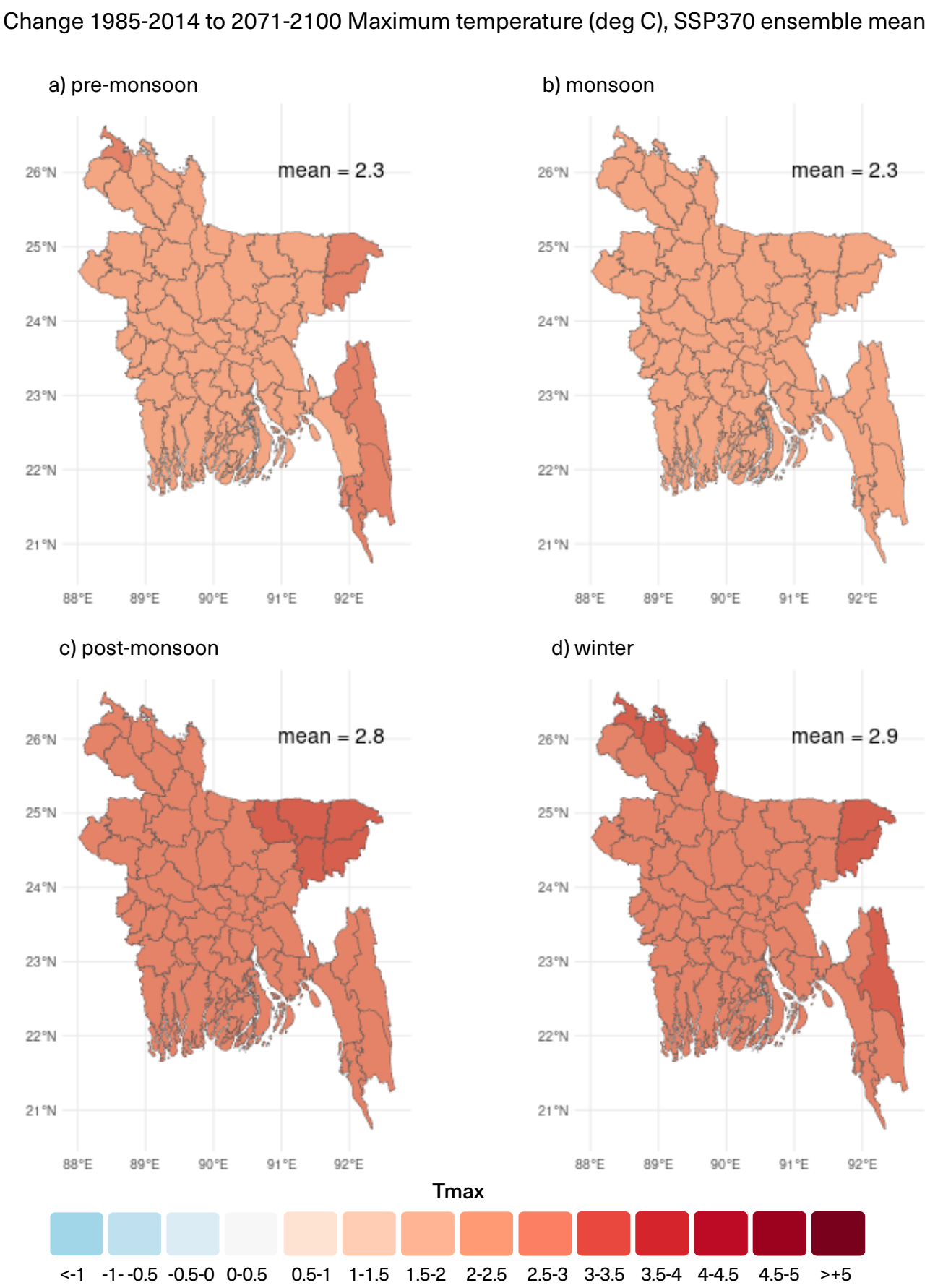


Figure 5.5 Changes in the daily maximum temperature from the reference period (1985–2014) to the end of the century (2071–2100) under emission scenario SSP3-7.0, as estimated by the NEX-GDDP-CMIP6 ensemble mean for the a) pre-monsoon, b) monsoon, c) post-monsoon, and d) winter seasons. The mean value of each map shows the country average.

## Daily minimum temperature

The daily minimum temperatures are projected to increase by approximately +2.0 °C to +3.0 °C during the mid-century period (2041–2070), rising further to +3.0 °C to +4.0 °C by the end of the century (2071–2100) under the high-emission scenario SSP3-7.0 (Figures 5.6 and 5.7). These increases are higher than those for daily maximum temperatures, indicating a stronger warming trend during nighttime, and thus on average a reduced diurnal temperature range.

The extent of warming varies depending on the season and region, as illustrated in Figures 5.6 and 5.7. During the mid-century period, the strongest warming is expected in the post-monsoon season, whereas the monsoon season shows the least warming. However, by the end of the century, this pattern shifts, with winter becoming the season to experience the most significant warming, while the monsoon season continues to exhibit the smallest minimum temperature increase. On average, the daily minimum temperature increases by about +2.0 °C in the post-monsoon season by mid-century. By the end of the century, the strongest warming is projected in winter, with a national average increase of +3.7 °C under SSP3-7.0.

Projections under the low- and medium-emission scenarios show slightly less intense warming in the mid-century compared to SSP3-7.0 (Figures A2.13 and A2.14). However, their long-term warming trajectories diverge significantly by the end of the century (as depicted in Figures A2.16 and A2.17). The low-emission scenario (SSP1-2.6) projects a modest increase of +1.0 °C to +2.0 °C by mid-century, followed by a plateau, indicating minimal additional warming beyond that point. This demonstrates the effectiveness of strong mitigation strategies. The medium-emission scenario (SSP2-4.5) shows a similar warming trend until mid-century but continues to warm thereafter, increasing by +2.0 °C to +3.0 °C relative to the historical baseline. The high-emission scenario SSP5-8.5, however, paints a much more severe picture, with daily minimum temperatures increasing by +2.0 °C to +3.0 °C by mid-century and escalating to +3.0 °C to +5.0 °C by the end of the century (Figures A2.15 and A2.18). Alarmingly, under SSP5-8.5 some regions, such as Rangpur and Rajshahi divisions, are expected to experience daily minimum temperature increases exceeding +5.0 °C above the historical baseline by 2100.

These projections emphasize the critical influence of different greenhouse gas emissions on regional climate outcomes. The findings clearly underscore the urgent need for global mitigation efforts, particularly for highly vulnerable countries like Bangladesh. Without significant reductions in emissions, the nation could face profound impacts across various key sectors, such as agriculture, public health, water resources, and climate-sensitive livelihoods. Proactive adaptation measures and robust policy frameworks are essential to address the long-term risks associated with rising temperatures.

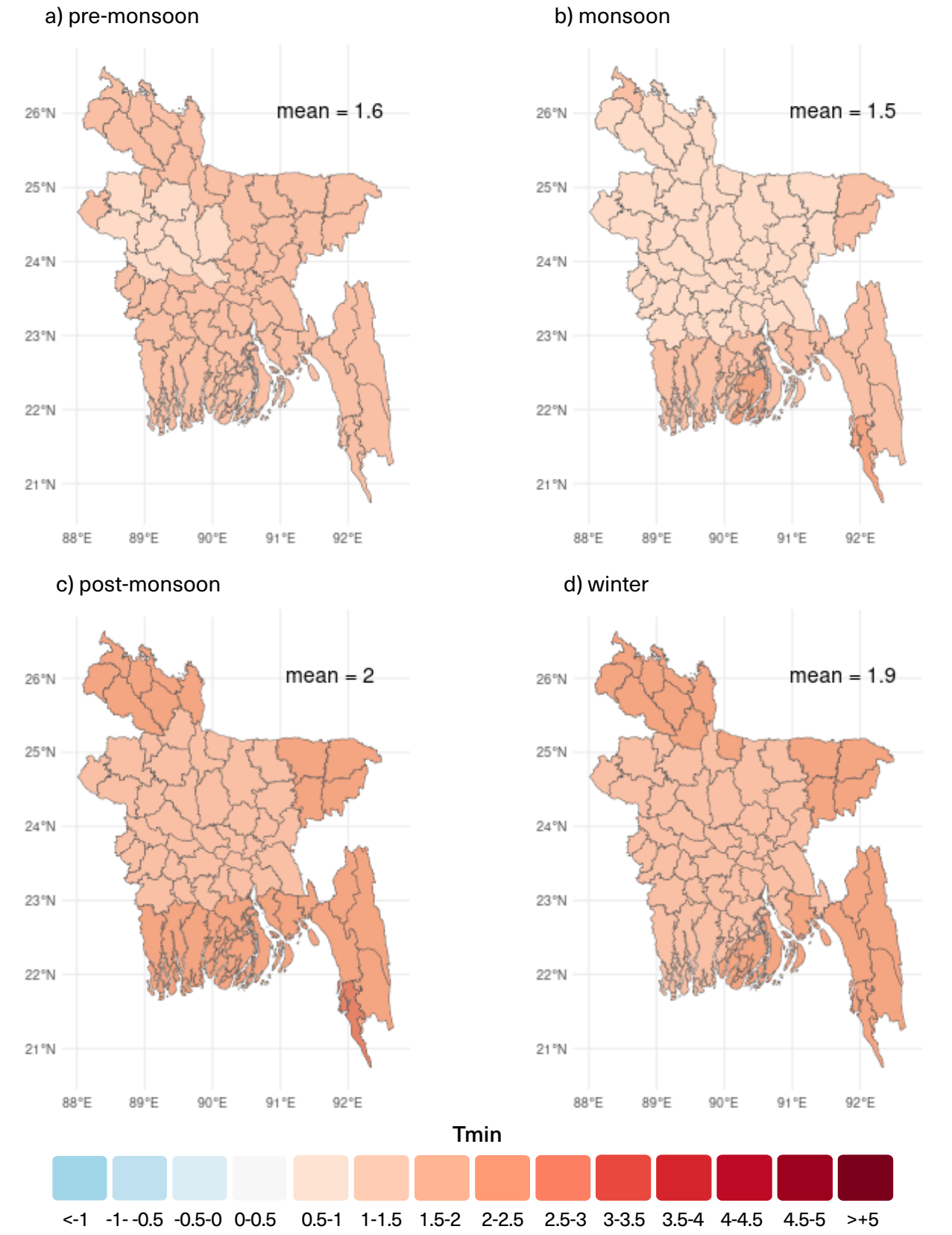


Figure 5.6 Changes in the daily minimum temperature from the reference period (1985–2014) to mid-century (2041–2070) under emission scenario SSP3-7.0, as estimated by the NEX-GDDP-CMIP6 ensemble mean for the a) pre-monsoon, b) monsoon, c) post-monsoon, and d) winter seasons. The mean value of each map shows the country average.

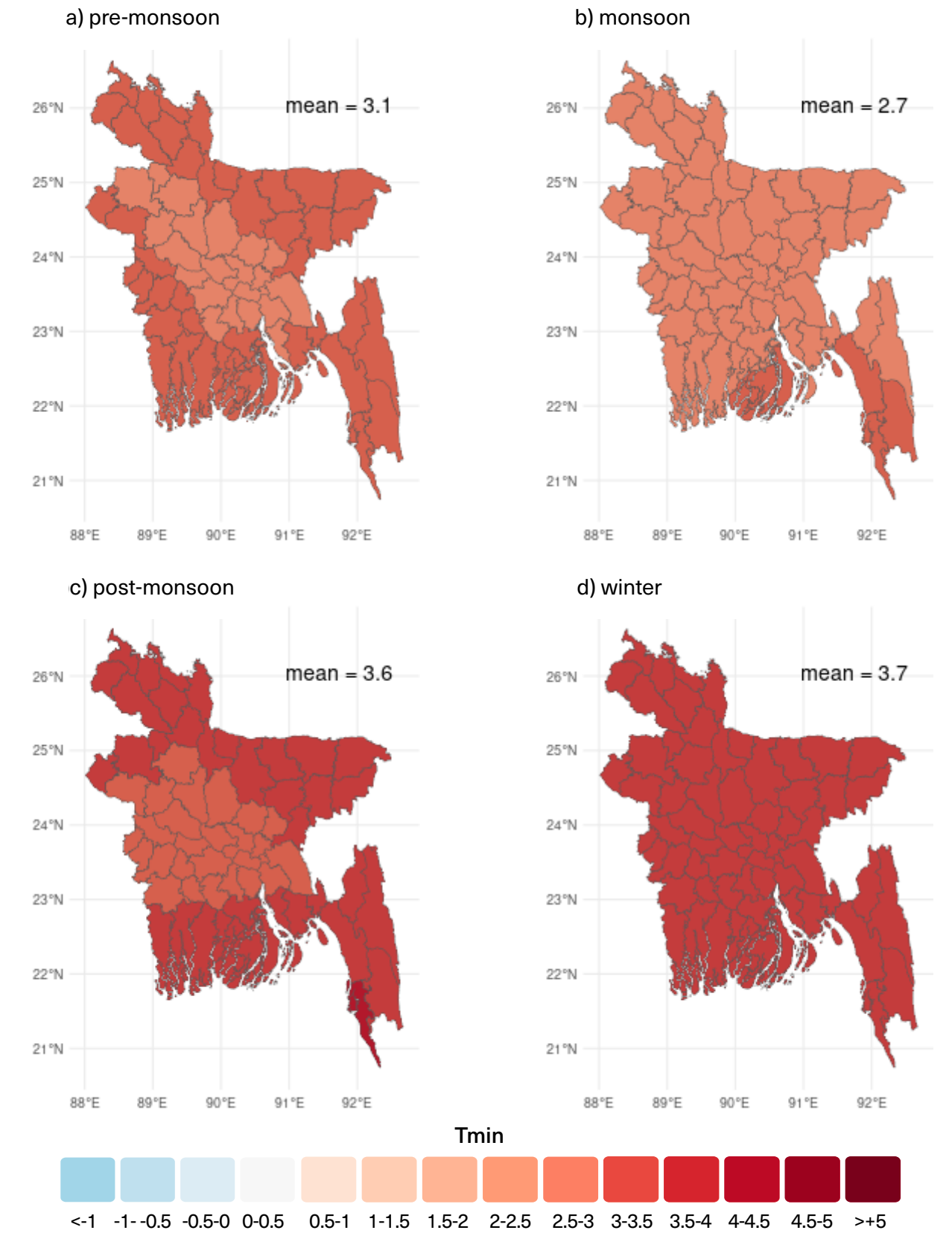


Figure 5.7 Changes in the daily minimum temperature from the reference period (1985–2014) to mid-century (2041–2070) under emission scenario SSP3-7.0, as estimated by the NEX-GDDP-CMIP6 ensemble mean for the a) pre-monsoon, b) monsoon, c) post-monsoon, and d) winter seasons. The mean value of each map shows the country average.

Photo: Rowshon21/Shutterstock

6

# Future projections of precipitation

Bangladesh experiences intense rainfall during the monsoon season, and future projections indicate a considerable increase in monsoonal precipitation under climate change (Figures 6.1 and 6.2). The seasonal precipitation under the high emission scenario SSP3-7.0 is projected to increase by approximately 15% relative to the reference period towards the end of the century. The largest increases are expected in the northeastern districts of Sylhet and Sunamganj, which already received the most precipitation in the reference period (Figure 4.5). By mid-century, the NEX-GDDP-CMIP6 ensemble mean under SSP3-7.0 suggests a regional increase of +200 to +250 mm in these areas, compared to a national average rise of +118 mm. This trend intensifies by the end of the century, with projected increases reaching +255 mm nationwide and +550 and +600 mm in Sylhet and Sunamganj.

Although the projected changes in the ensemble mean precipitation are notable, the year-to-year variability and the range within the model ensemble remain large (Figure 6.3). This means that, while the climate projections point to wetter monsoons in Bangladesh, the climate signal is still relatively weak when compared to natural variability. Nevertheless, the high-emission scenarios SSP3-7.0 and SSP5-8.5 both indicate a clear risk of substantially increased rainfall in the monsoon season, particularly in northeastern districts around Sylhet and Mymensingh. By the end of the century, 65% to 87% (15–20 out of 23 ensemble members, depending on the region) of the models project an increase in monsoon precipitation (Figure 6.4), indicating a relatively robust signal toward increasing rainfall. The model results thus suggest that, while the precipitation will continue to vary a lot from year to year in the future, high emissions of greenhouse gases elevate the risk of very intense monsoon precipitation.

The projections also show a tendency for increasing precipitation in the pre-monsoon and post-monsoon seasons by the end of the century. The pre-monsoon season is expected to experience the second-highest rainfall increases, with projected ensemble mean changes of +19 mm by mid-century and +75 mm by the end of the century (average for the whole country). For the post-monsoon season, increases are projected at +14 mm and +29 mm, respectively. These numbers may seem small compared to the projected changes in the monsoon season, but they represent seasonal increases of approximately 17–18% compared to the reference period.

Winter precipitation projections remain highly uncertain, with a roughly evenly split between models showing a precipitation increase and those showing a precipitation decrease, suggesting no robust trend during that period. Note, however, that winter is the season with the highest projected temperature increase towards the end of the century (see previous chapter). Thus increased evaporation will contribute to a reduction in the water budget, even if the changes in precipitation may be small.

Spatial patterns vary across regions. During the pre-monsoon season, the majority of the models (70–96% of the ensemble, depending on the region) exhibit increasing precipitation across central and northern Bangladesh, with ensemble mean increases ranging from +100 mm to +300 mm. On the other hand, the southern and coastal areas show less agreement among the models, and the projected ensemble mean change is small (0 to +50 mm). The post-monsoon projections show a weaker spatial pattern but still generally point toward increased precipitation across the country.

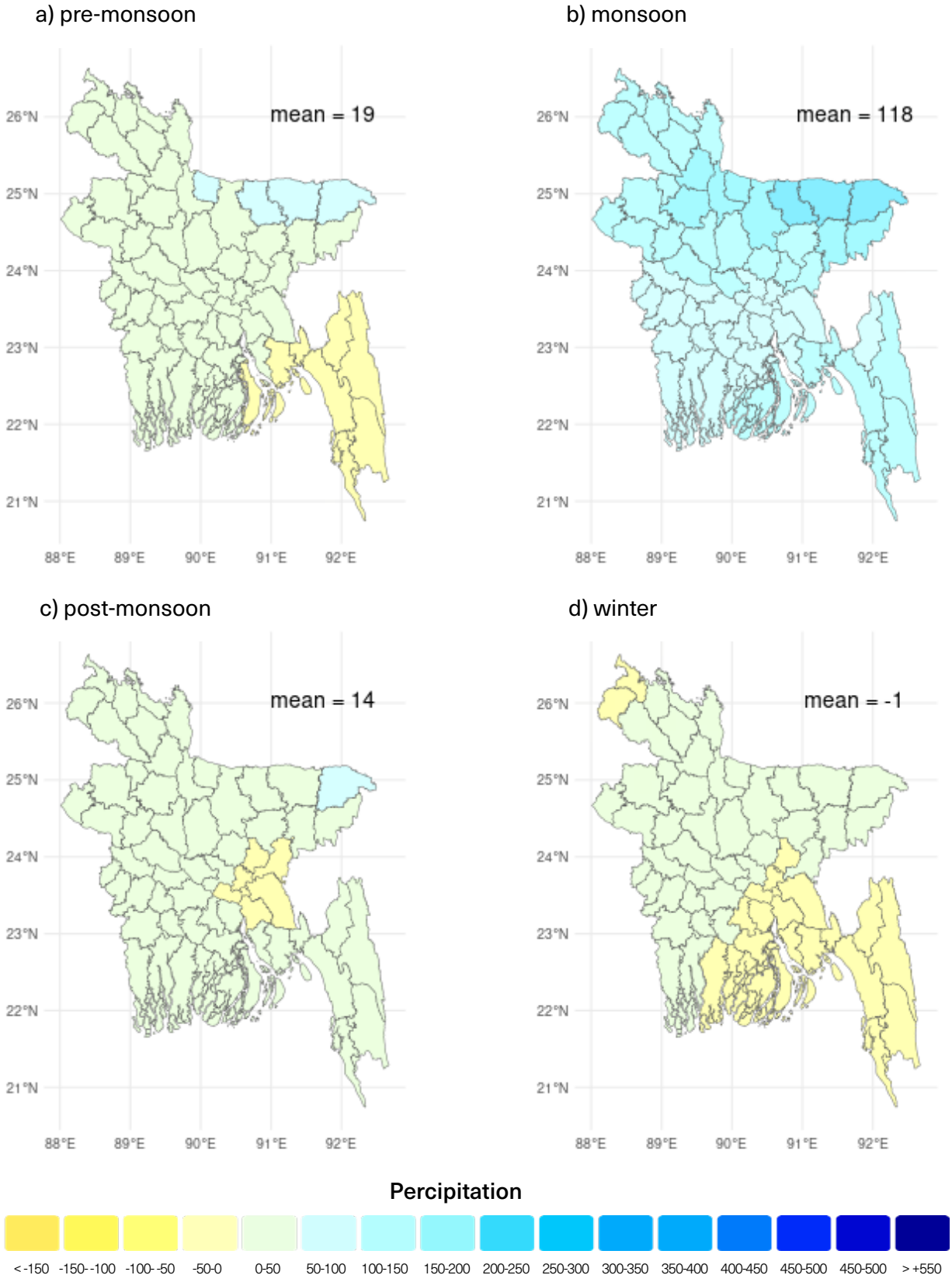


Figure 6.1 Changes in the average seasonal precipitation sum from the reference period (1985–2014) to mid-century (2041–2070) under emission scenario SSP3-7.0, as estimated by the NEX-GDDP-CMIP6 ensemble mean for the a) pre-monsoon, b) monsoon, c) post-monsoon, and d) winter seasons. The mean value of each map shows the country average.

The different emission scenarios show divergent precipitation trends in the latter half of the century, as illustrated in Figures A2.32 to A2.37. Under the low-emission scenario (SSP1-2.6), seasonal precipitation sums are projected to remain relatively stable. Both mid- and end-century projections indicate minimal change, with winter season rainfall being almost the same (+1 mm) and monsoon rainfall increasing by an average of +127 mm, showing little variation over time. The medium-emission scenario (SSP2-4.5) follows a similar trajectory to SSP1-2.6 until mid-century. However, it projects further increase thereafter. By the end of the century, average seasonal precipitation is expected to rise by +168 mm in the monsoon season, and around +30 mm in both the pre-monsoon and post-monsoon seasons, while projected changes are small in winter (+7 mm). The high-emission scenario (SSP5-8.5) projects more substantial changes. By mid-century, rainfall is expected to increase by +184 mm in the monsoon season, and by 2100, this scenario predicts a dramatic rise in monsoon precipitation, with increases exceeding +500 mm in the northeastern and southeastern regions. The highest precipitation levels are projected in the districts of Sylhet, Sunamganj, and Bandarban, indicating a more extreme trajectory under continued high emissions. SSP5-8.5 indicates increasing precipitation in the pre-monsoon (+90 mm) and post-monsoon seasons (+66 mm) as well, but little and inconsistent change in the winter.

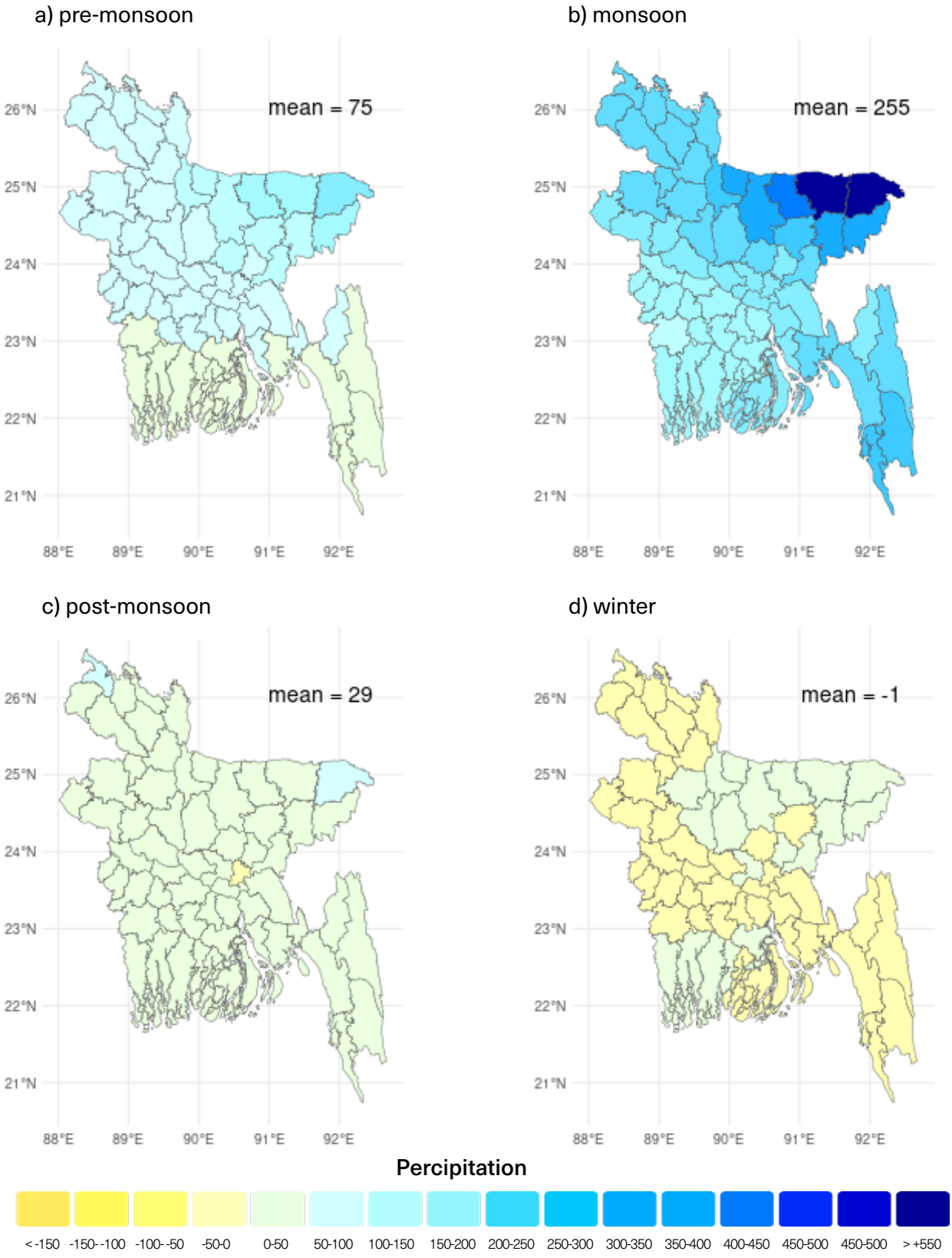


Figure 6.2 Changes in the average seasonal precipitation sum from the reference period (1985–2014) to the end of the century (2071–2100) under emission scenario SSP3-7.0, as estimated by the NEX-GDDP-CMIP6 ensemble mean for the a) pre-monsoon, b) monsoon, c) post-monsoon, and d) winter seasons. The mean value of each map shows the country average.

## Annual sum of precipitation

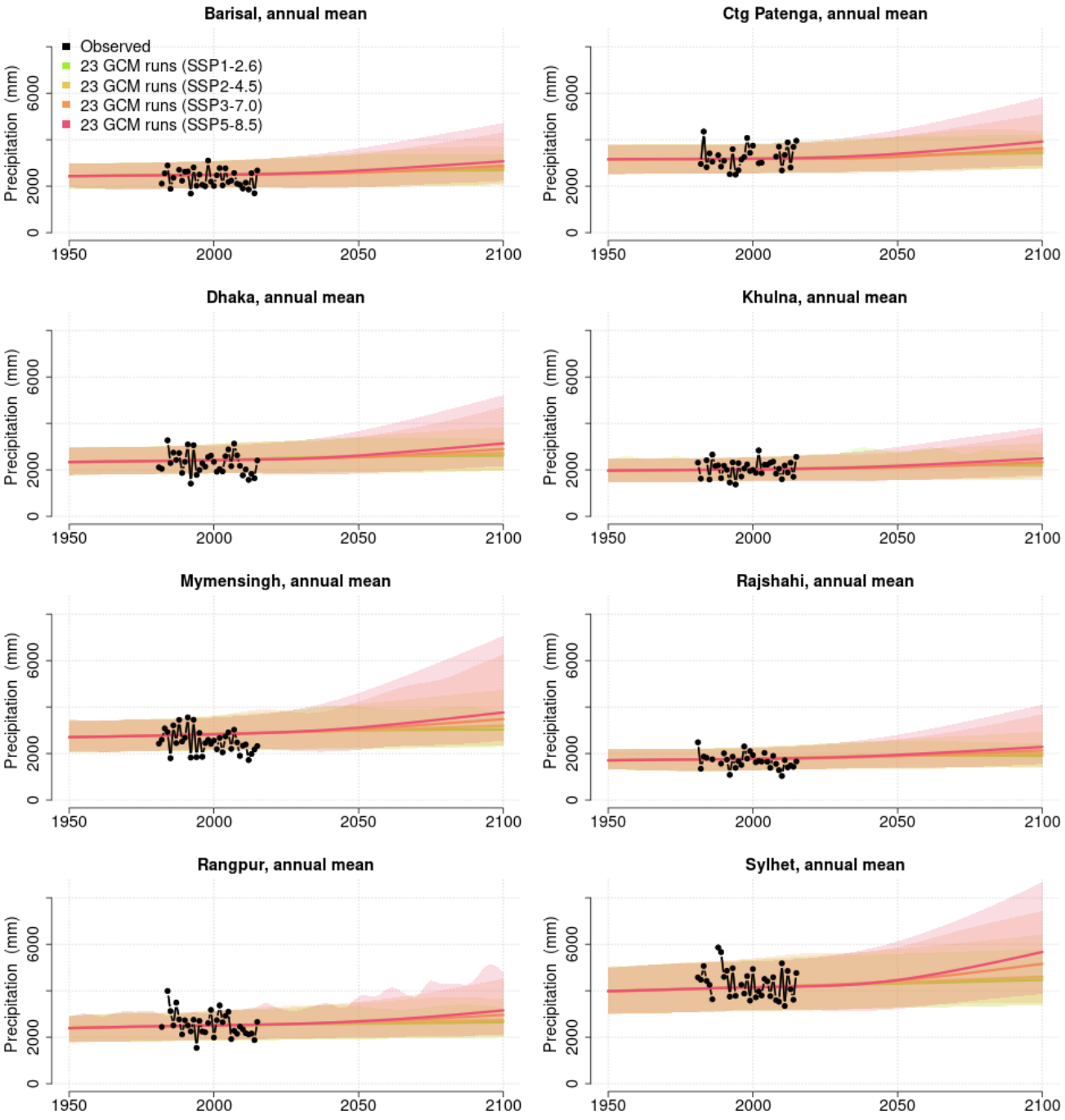


Figure 6.3 Annual sum of precipitation at eight divisions stations in Bangladesh, based on observations (black line) and the NEX-GDDP-CMIP6 climate model ensemble mean (colored lines) and 5th to 95th percentile (envelopes) from the gridpoint nearest each station for emission scenarios SSP1-2.6, SSP2-4.5, SSP3-7.0, and SSP5-8.5 (see legend).

Number of models with an increase from 1985-2014 to 2071-2100. Precipitation, SSP370

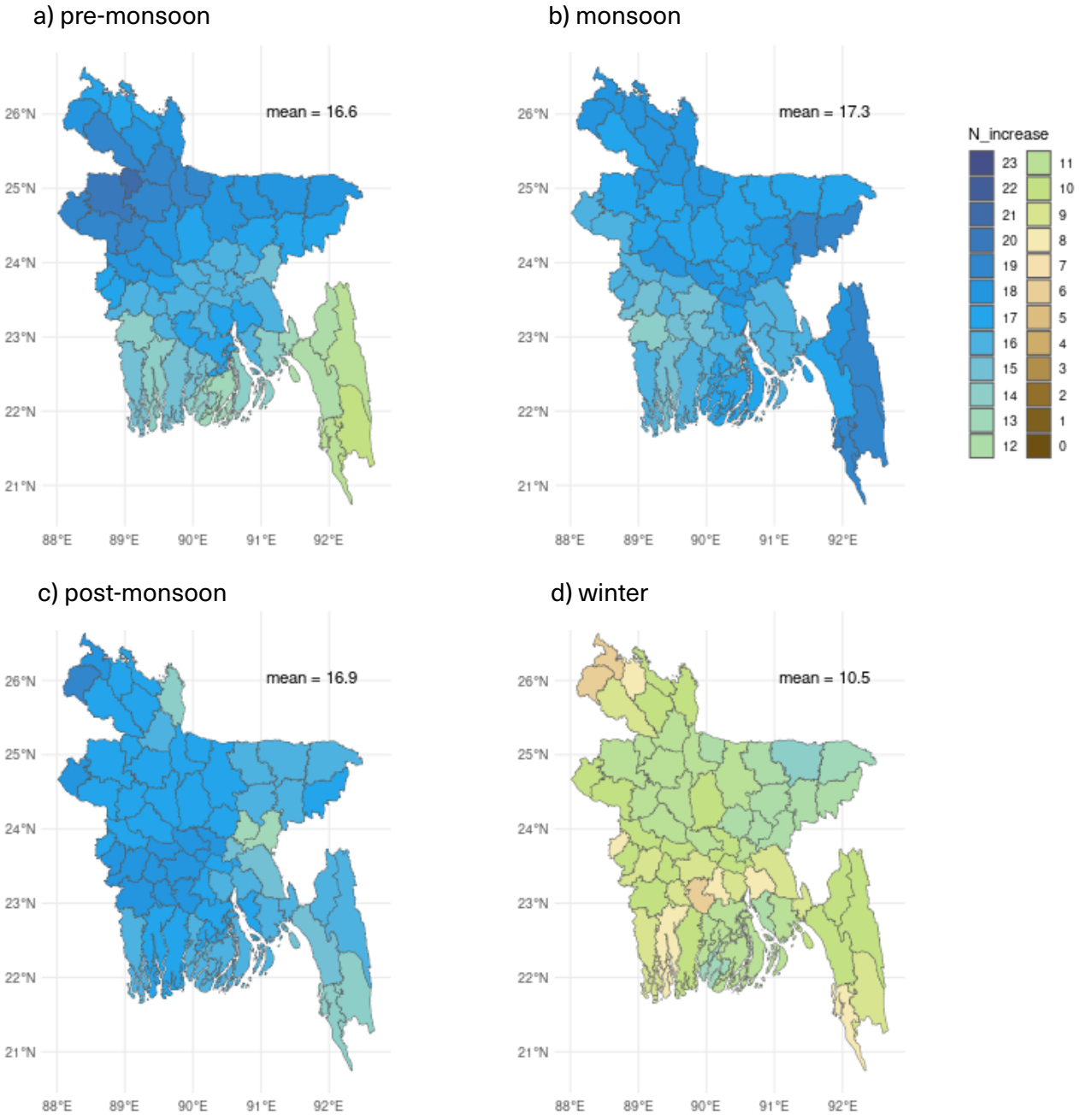


Figure 6.4 The number of models out of the 23 selected NEX-GDDP-CMIP6 ensemble members that show an increase in the seasonal precipitation sum from the reference period (1985–2014) to the end of the century (2071–2100), under emission scenario SSP3-7.0 for the a) pre-monsoon, b) monsoon, c) post-monsoon, and d) winter seasons. The mean value of each map shows the country average.

Photo: HM Shahidul Islam/Shutterstock

7

# Extreme events

## Extreme heat

One common approach for assessing temperature extremes and their potential detrimental impacts on human health and society is to track the number of hot days. In Bangladesh, a heatwave is officially declared when the daily maximum temperature exceeds 36 °C for three consecutive days. The Bangladesh Meteorological Department (BMD) further categorises heatwaves into three levels: mild (36–38 °C), moderate (38–40 °C), and severe (above 40 °C). Heatwaves cause stress on the human body, increasing the risk of cardiovascular events, heat strokes and respiratory complications (Ebi et al., 2021; Zhao et al., 2024). Over the past 40 years, both the frequency and intensity of heatwave-related deaths have risen, largely attributed to anthropogenic climate change (Vicedo-Cabrera et al., 2021). For simplicity in this report, and consistency with the report on detected climate changes (Rashid et al., 2024), an index calculating single day events has been used. We don't expect this simplification having any substantial effect on the climate change signal, even though the value changes.

During the reference period, heatwave conditions primarily occurred in the pre-monsoon season, with western districts such as Rajshahi and Khulna experiencing the highest numbers (Figure 7.1a). These areas recorded an average of 25–50 heatwave days (daily maximum temperature > 36 °C) per pre-monsoon season, while the rest of the country typically saw fewer than 25 days. Severe heatwave days, when daily maximum temperatures exceeded 40 °C, were less common, averaging only 2–6 days per season in the western districts and none in the rest of the country (Figure 7.2a).

Occasional mild heatwave conditions were also observed during the monsoon season in some western districts, averaging 5–10 days per season. However, severe heatwaves were extremely rare during this time of year.

The projections of daily maximum temperature indicate a substantial increase in the number of heatwave days across Bangladesh as a result of continued greenhouse gas emissions (Figures 7.3 and 7.4). Under the high emission scenario SSP3-7.0, the average number of pre-monsoon heatwave days is expected to more than triple from the reference period (1985–2014) to the end of the century (2071–2100). Days with severe heatwave conditions, which were few in the reference period, are projected to rise considerably. By the end of the century, the hottest western districts could experience as many as 15–25 days per season with a maximum temperature over 40 °C in the pre-monsoon season (Figure 7.6).

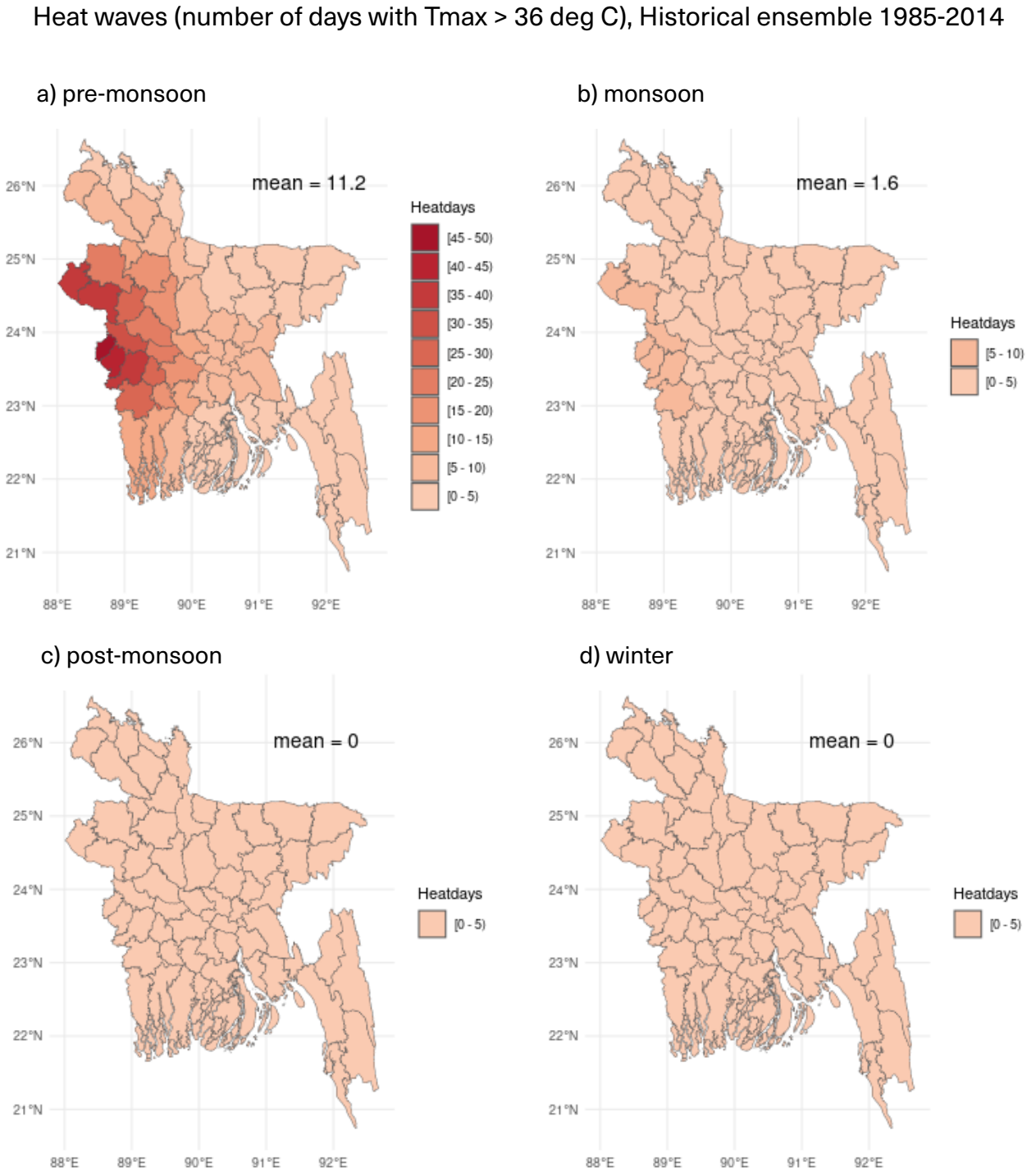


Figure 7.1 Number of heatwave days (daily maximum temperature > 36 ℃) for the four seasons in the reference period 1985–2014. The estimates are based on the NEX-GDDP-CMIP6 ensemble mean of the daily maximum temperature under emission scenario SSP3-7.0 for the a) pre-monsoon, b) monsoon, c) post-monsoon, and d) winter seasons. The mean value of each map shows the country average.

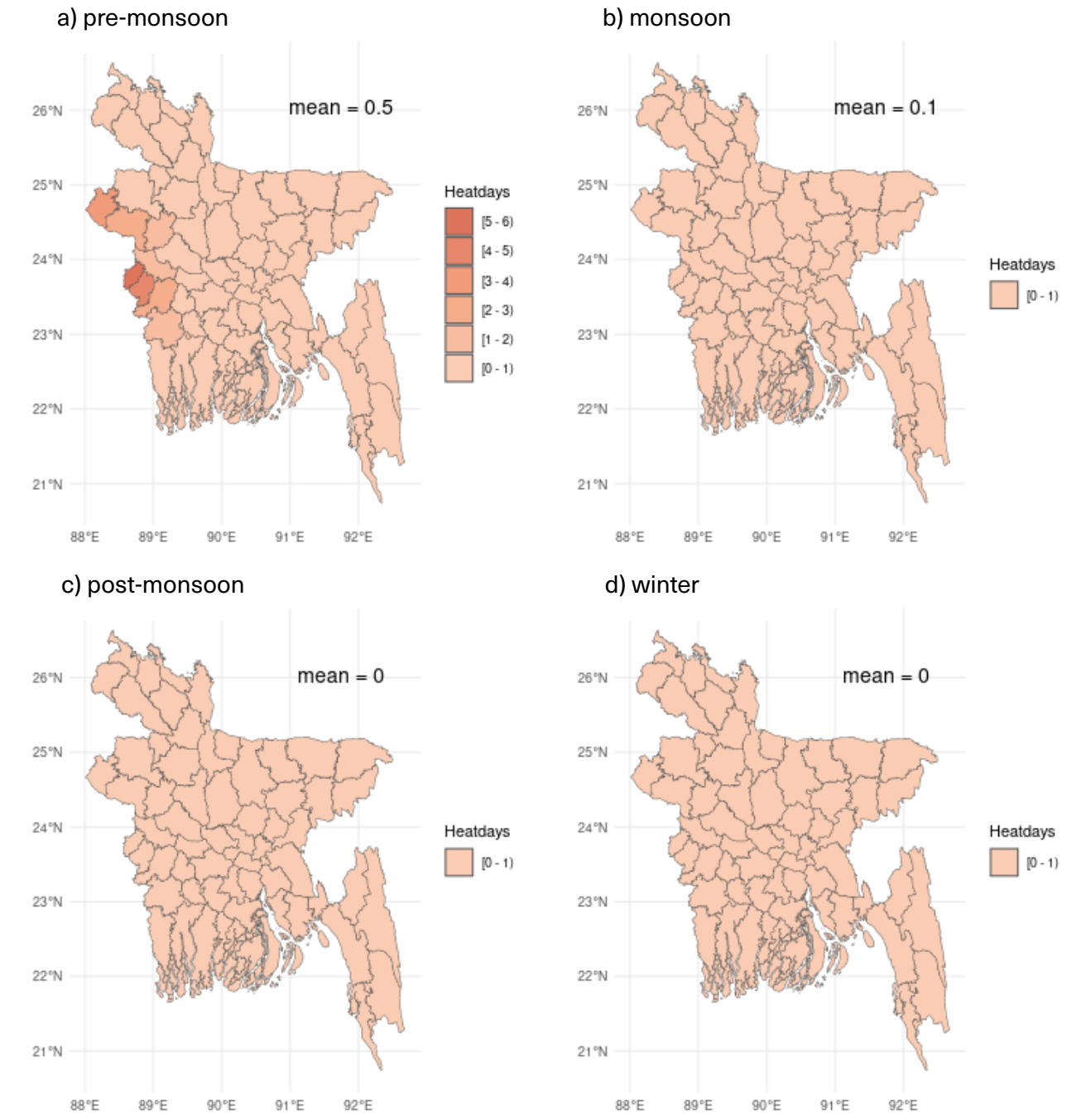


Figure 7.2 The number of severe heatwave days (daily maximum temperature > 40 ˚C) in the reference period, 1985–2014. The estimates are based on the NEX-GDDP-CMIP6 ensemble mean of the daily maximum temperature for the a) pre-monsoon, b) monsoon, c) post-monsoon, and d) winter seasons. The mean value of each map shows the country average.

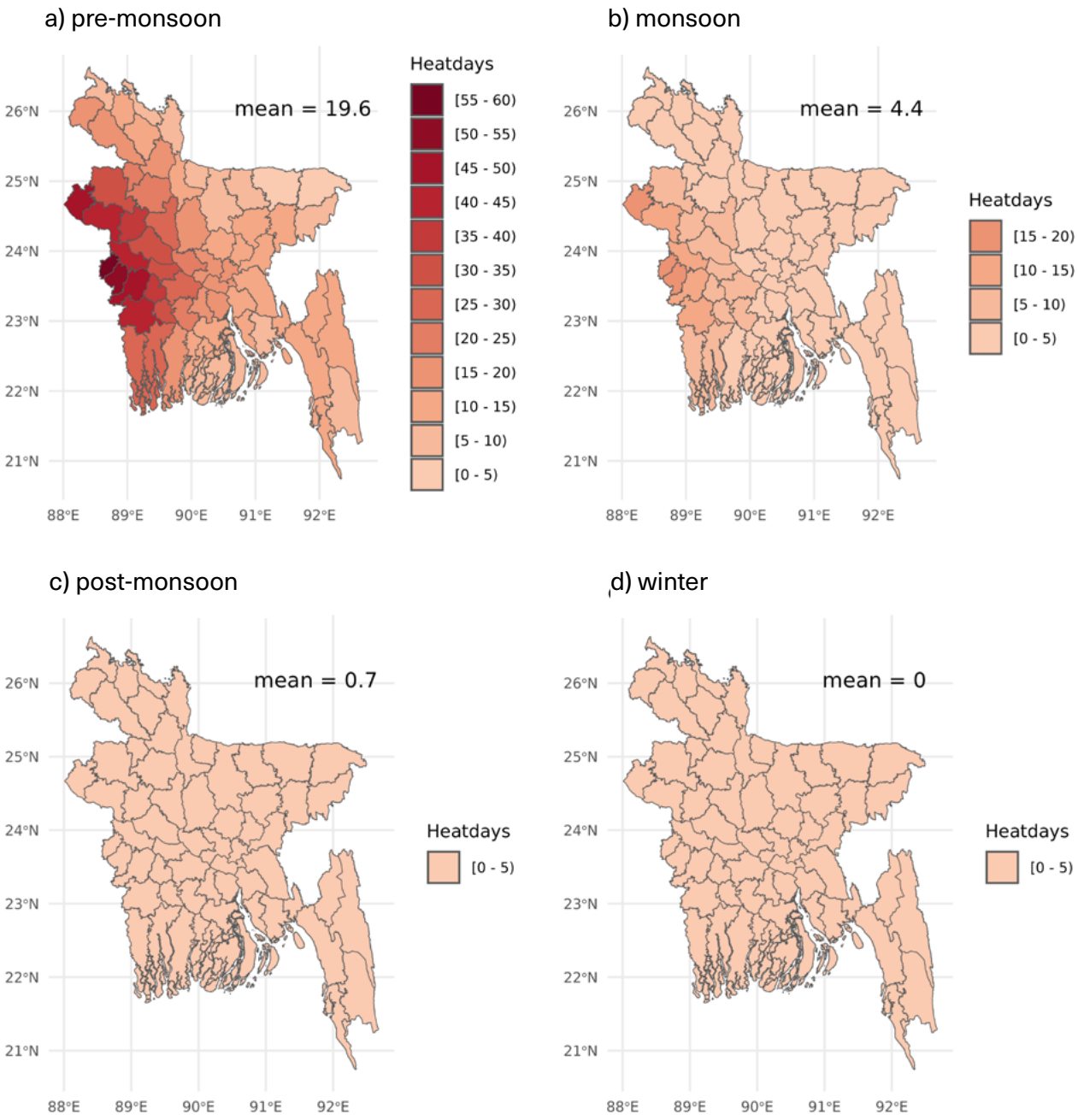


Figure 7.3 The number of heatwave days (daily maximum temperature > 36 ˚C) in the mid-century (2041–2070) assuming emission scenario SSP3-7.0. The estimates are based on the NEX-GDDP-CMIP6 ensemble mean of the daily maximum temperature for the a) pre-monsoon, b) monsoon, c) post-monsoon, and d) winter seasons. The mean value of each map shows the country average.

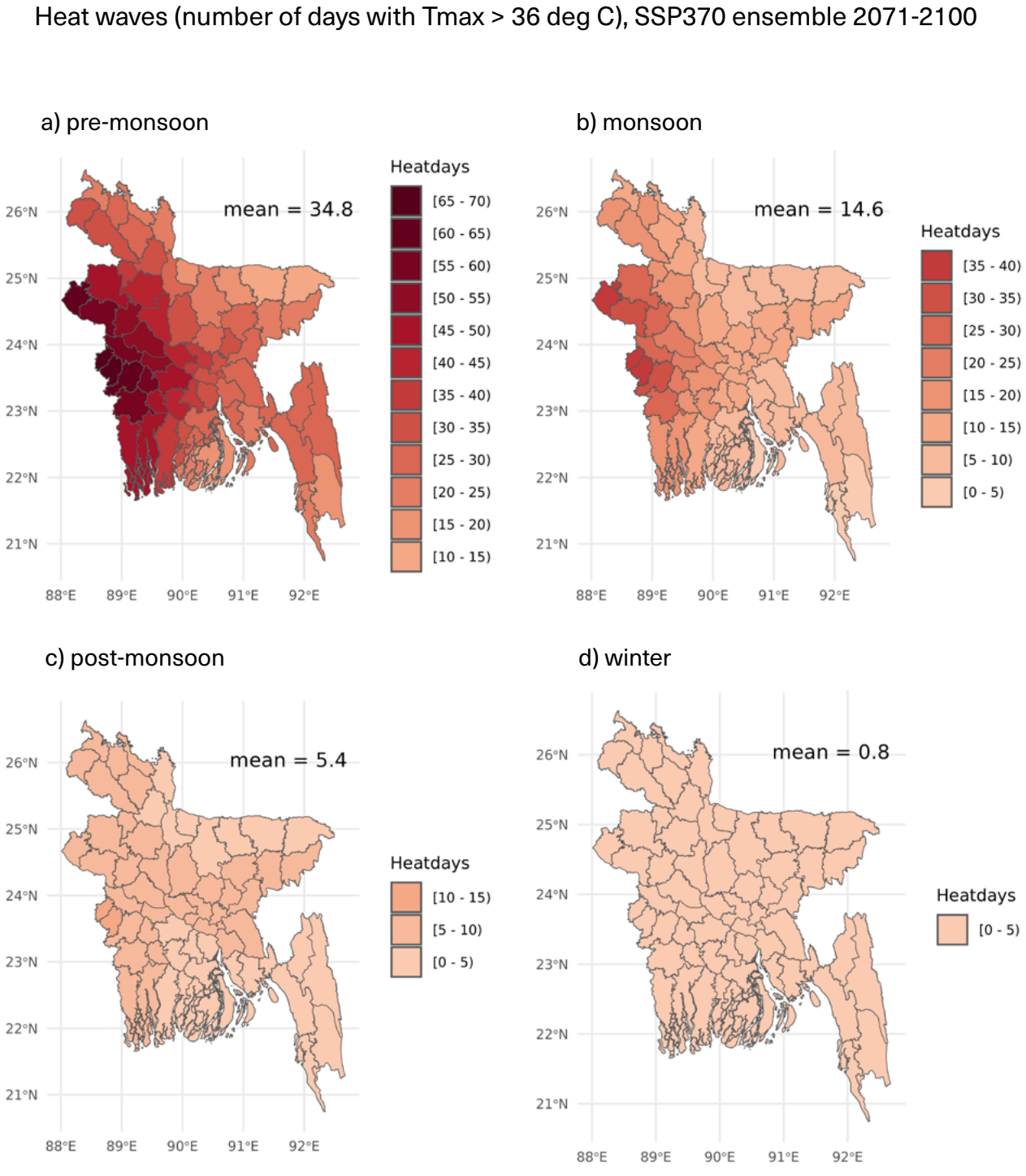


Figure 7.4 The number of heatwave days (daily maximum temperature > 36 ℃) at the end of the century (2071–2100) assuming SSP3-7.0. The estimates are based on the NEX-GDDP-CMIP6 ensemble mean of the daily maximum temperature for the a) pre-monsoon, b) monsoon, c) post-monsoon, and d) winter seasons. The mean value of each map shows the country average.

Severe heat waves (number of days with Tmax > 40 deg C), SSP370 ensemble 2041-2070

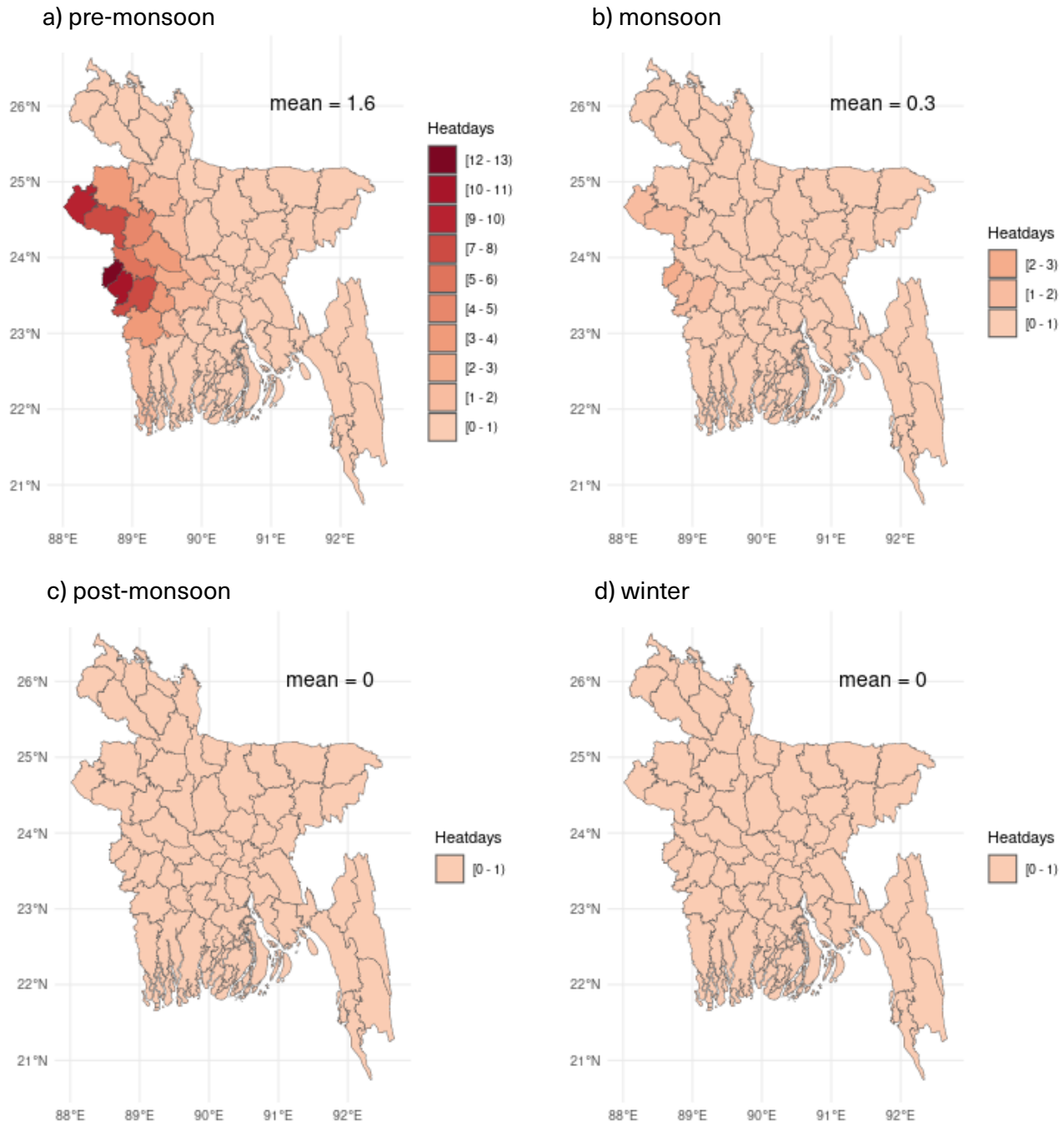


Figure 7.5 The number of severe heatwave days (daily maximum temperature > 40 ℃) in the mid-century (2041–2070) assuming SSP3-7.0. The estimates are based on the NEX-GDDP-CMIP6 ensemble mean of the daily maximum temperature for the a) pre-monsoon, b) monsoon, c) post-monsoon, and d) winter seasons. The mean value of each map shows the country average.

Severe heat waves (number of days with Tmax > 40 deg C), SSP370 ensemble 2071-2100

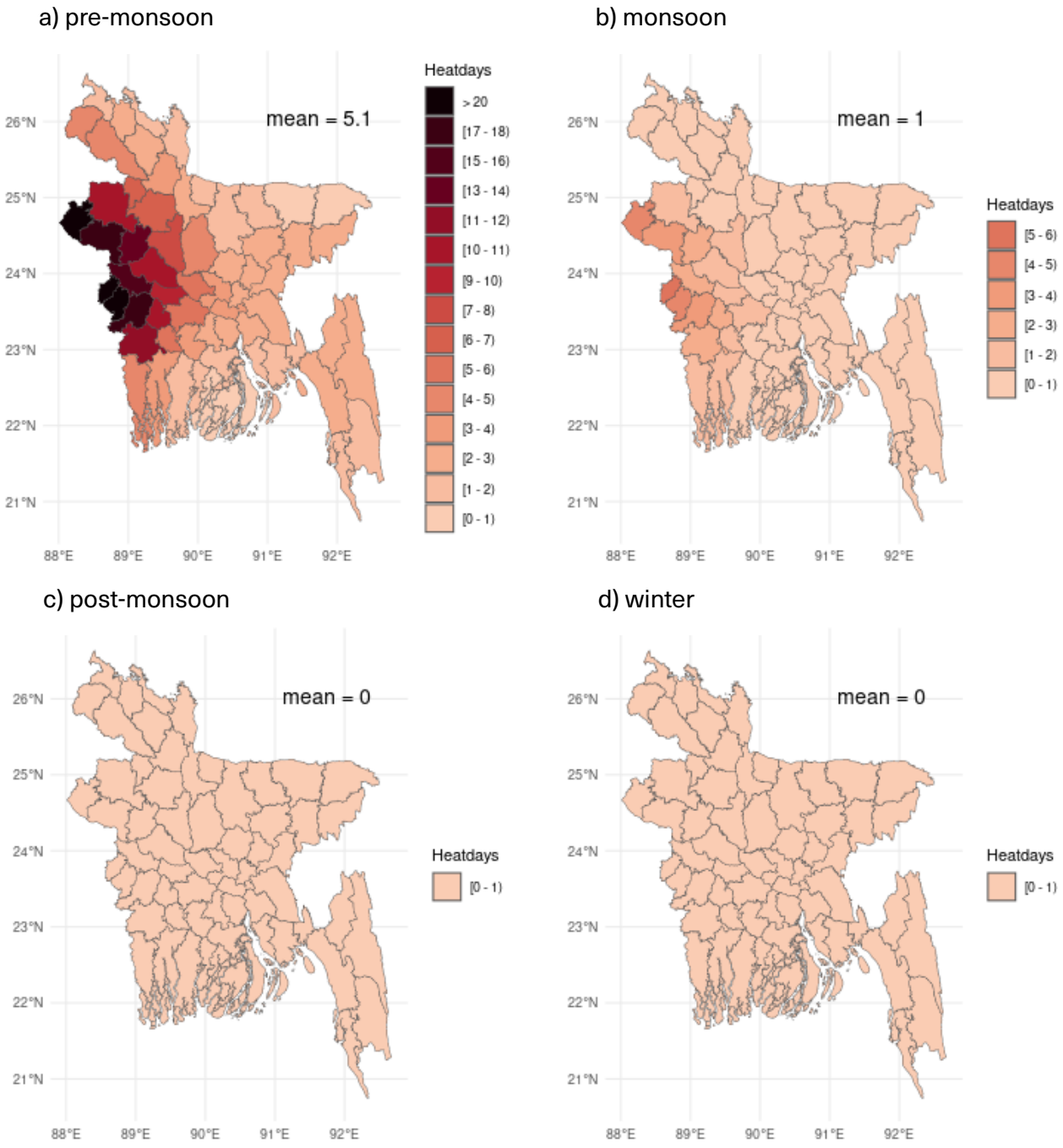


Figure 7.6 The number of severe heatwave days (daily maximum temperature > 40 ℃) at the end of the century (2071–2100) assuming SSP3-7.0. The estimates are based on the NEX-GDDP-CMIP6 ensemble mean of the daily maximum temperature for the a) pre-monsoon, b) monsoon, c) post-monsoon, and d) winter seasons. The mean value of each map shows the country average.

During the reference period, Dhaka experienced heatwaves primarily in the pre-monsoon months (March, April, and May), with a few instances extending into June. Beyond June, heatwaves were largely absent (Figure 7.7). However, future projections under different emission scenarios indicate a notable increase in both the frequency and intensity of heatwaves towards the end of the century. Even under the low-emission scenario (SSP1-2.6), the number of heatwaves is projected to be higher than in the reference period. The medium-emission scenario (SSP2-4.5) is expected to bring even more frequent events, with heatwaves expanding into additional months of the year. Under high to very high emission scenarios (SSP3-7.0 and SSP5-8.5), projections become significantly more alarming. Heatwaves are projected not only to intensify during the pre-monsoon season but also become more common during the monsoon and post-monsoon seasons. Alarmingly, some projections indicate heatwave events for the winter months — December, January, and February — reflecting a substantial shift in seasonal patterns and signaling increasingly challenging conditions for the capital, especially under the high to extreme emission scenarios (Figure 7.7).

Similar trends are evident across Bangladesh's seven remaining administrative divisions (Figures A2.25 to A2.31). Among them, Rangpur, Rajshahi, and Khulna are projected to be the most severely affected, with substantial increases in the number and duration of heatwaves under medium to very high emission scenarios (SSP2-4.5 to SSP5-8.5). While Barisal and Chattogram currently experience fewer heatwaves, likely due to moderating effects from ocean-land interactions, these regions are also expected to face significant increases in heatwave occurrences by century's end under high-emission scenarios. Sylhet and Mymensingh divisions, which presently are less prone to heatwaves due to high rainfall during the pre-monsoon and monsoon seasons, are likewise projected to experience more heatwaves in the future. Under SSP3-7.0 and SSP5-8.5, the number of heatwave days is projected to increase in both divisions, with Mymensingh expected to experience more intense events compared to Sylhet. In these extreme scenarios, the highest number of heatwave days in Mymensingh and Sylhet is projected to occur during the pre-monsoon and post-monsoon periods.

By the end of the century, Bangladesh is likely to face an escalating threat from heatwaves across all regions, with severity heavily dependent on emission scenarios. While some divisions are naturally already more vulnerable, even historically cooler or less-affected regions are projected to experience worsening conditions. These findings highlight the pressing need for urgent climate adaptation and mitigation strategies, particularly targeted heatwave preparedness and response efforts, to safeguard public health and societal well-being in a warming future.

## Heat waves in Dhaka

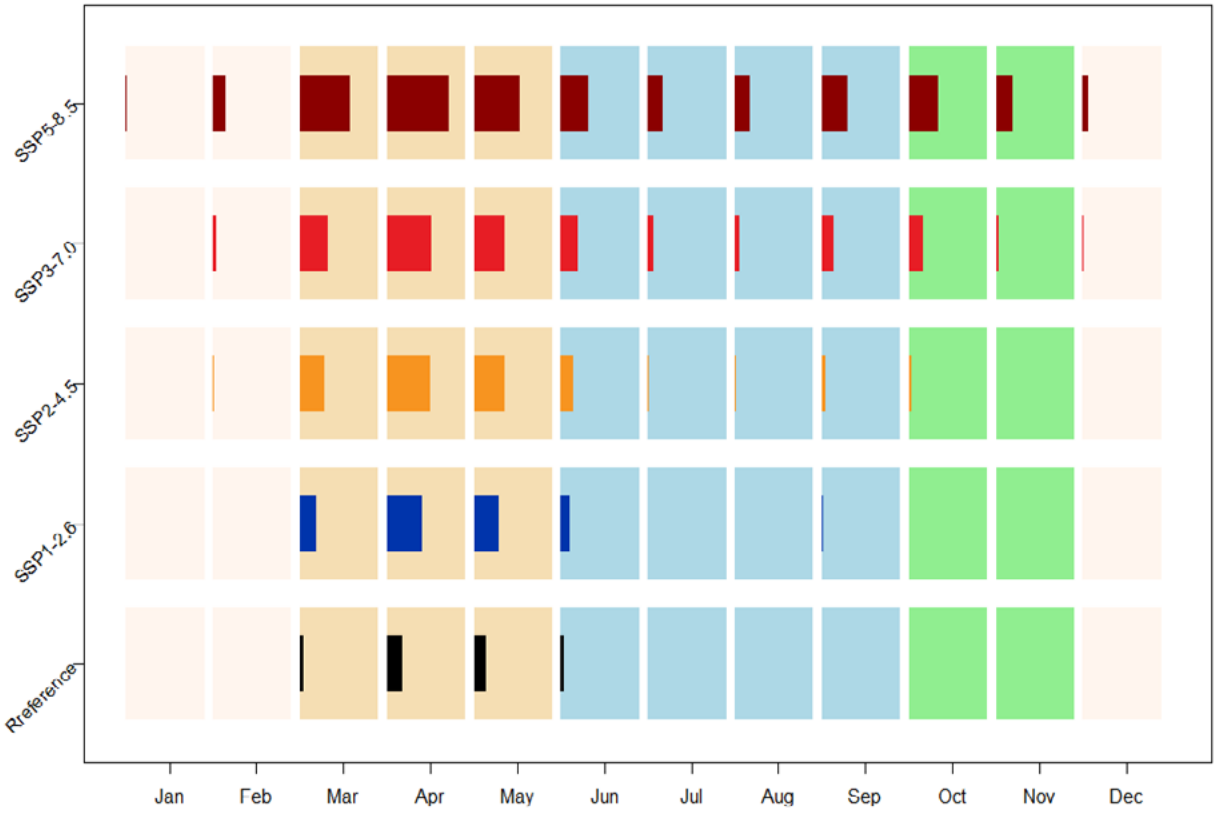


Figure 7.7 The number of heatwave days (daily maximum temperature > 36 ℃) in the end of the century (2071–2100) in Dhaka under different emission scenarios. The estimates are based on the NEX-GDDP-CMIP6 ensemble mean of the daily maximum temperature.

## Cold spells

In Bangladesh, a cold spell is declared when the daily minimum temperature falls below 10 ℃ for three or more consecutive days. The Bangladesh Meteorological Department classifies cold spells into three categories: mild (8–10 ℃), moderate (6–8 ℃), and severe (below 6 ℃). Temperatures this low occur only during the winter season, as illustrated in Figure 7.8. A simplified cold spell index is used here, counting single day cold spell conditions. The conclusions and climate signal would likely be similar if consecutive days were counted, although cold spells would be even more rare.

During the reference period, the country experienced an average of eight days with cold spell conditions (daily minimum temperature below 10 ℃) per winter. The western and northeastern parts experienced between 10 to 25 cold spell days per season, reflecting their generally colder winter climate. In contrast, the rest of the country experienced

relatively few cold spell days, typically ranging from 0 to 10 days per season. The highest number of cold spell days was recorded in the districts of Panchagarh, Thakurgaon, Moulvibazar, and Habiganj, highlighting these areas as particularly vulnerable during the colder months (see Figure 7.8). The regional variability of cold spells is influenced by geographic and climatic factors and highlights the importance of localized preparedness and early warning systems to mitigate the health and livelihood risks associated with cold spells in the most affected areas.

Looking ahead, climate projections from the NEX-GDDP-CMIP6 ensemble indicate a substantial decline in cold spell conditions by mid-century, with cold spell days becoming extremely rare by the end of the century. Under the high-emission scenario SSP3-7.0, the number of cold spell days is projected to drop to 0–8 days per season by mid-century (see Figure 7.9) and 0–4 days by the end of the century (Figure 7.10). Similar trends are observed across all emission scenarios. Under the low emission scenario SSP1-2.6, cold spell days decline to 0–10 days per winter, while under the very high-emission scenario SSP5-8.5, they nearly disappear, with only 0–2 days projected (Figures A2.38–A2.43).

These projections point to a notably warmer future winter climate in Bangladesh, where cold spells may no longer constitute a significant seasonal hazard, especially under high emission scenarios. While current cold-affected regions like Panchagarh and Thakurgaon remain vulnerable in the near term, the long-term trend suggests a diminishing threat, especially under high-emission scenarios.

These findings underscore the need to balance short-term cold spell preparedness with long-term adaptation strategies that account for greenhouse gas-induced warming. Strengthening cold spell early warning systems, improving healthcare response during cold spells, and adjusting agricultural calendars will be essential in the near term, particularly for vulnerable communities.

Cold spells (number of days with Tmin > 10 deg C), Historical ensemble mean 1985-2014

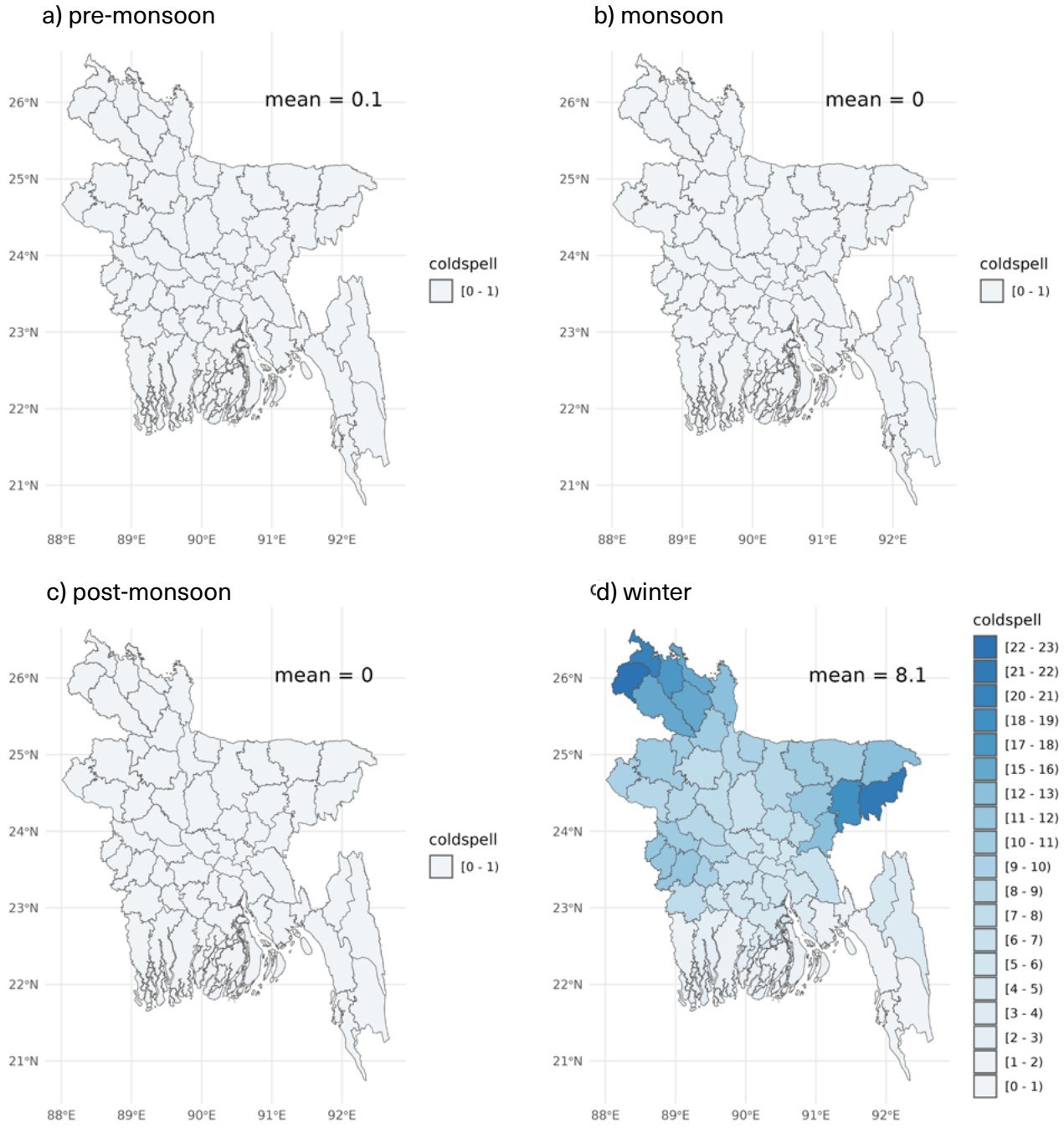


Figure 7.8 The number of cold spell days (daily minimum temperature < 10 ˚C) in the reference period, 1985–2014. The estimates are based on the NEX-GDDP-CMIP6 ensemble mean of the daily minimum temperature for the a) pre-monsoon, b) monsoon, c) post-monsoon, and d) winter seasons. The mean value of each map shows the country average.

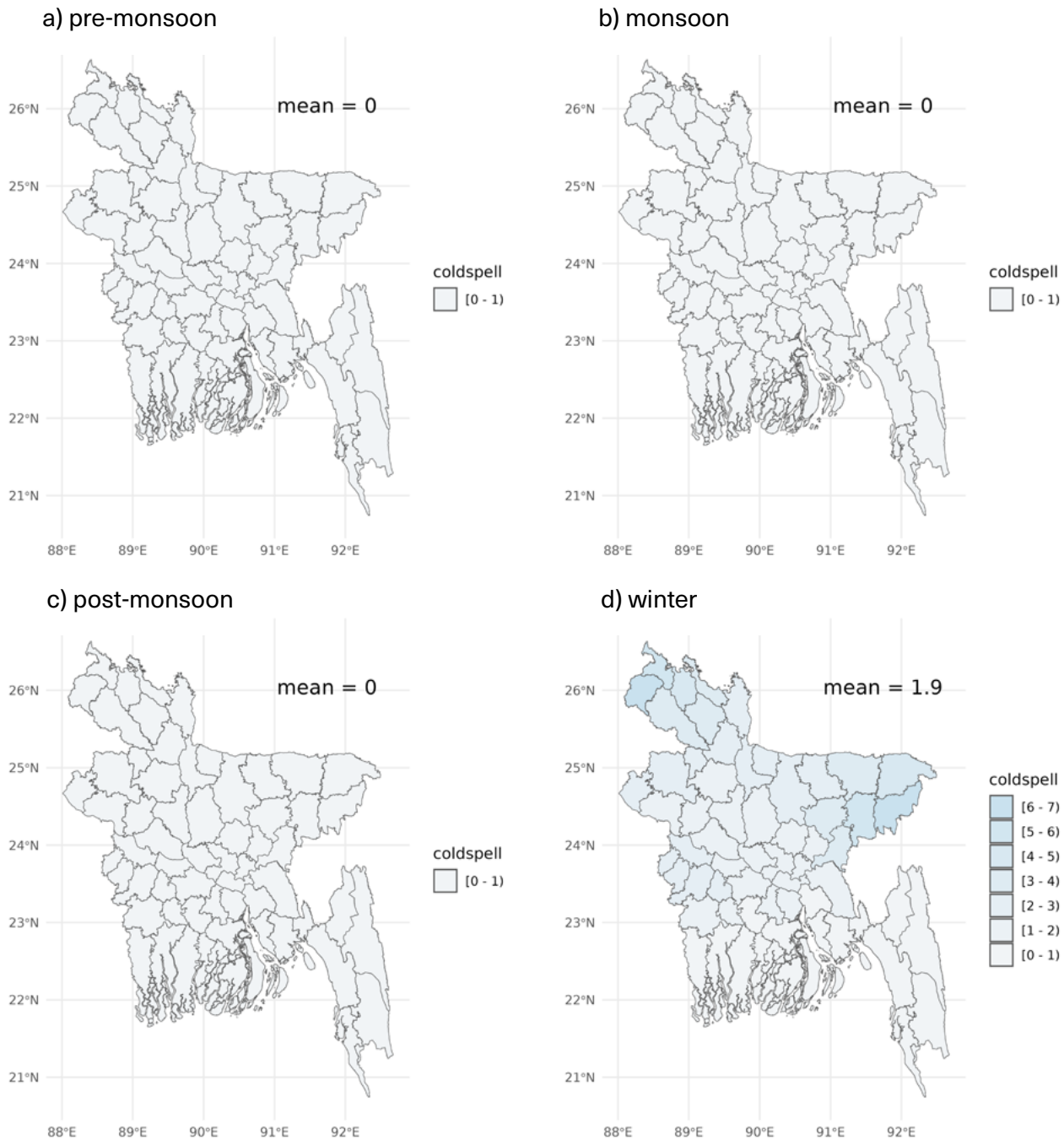


Figure 7.9 The number of cold spell days (daily minimum temperature < 10 ℃) in the mid-century (2041–2070) under SSP3-7.0. The estimates are based on the NEX-GDDP-CMIP6 ensemble mean of the daily minimum temperature for the a) pre-monsoon, b) monsoon, c) post-monsoon, and d) winter seasons. The mean value of each map shows the country average.

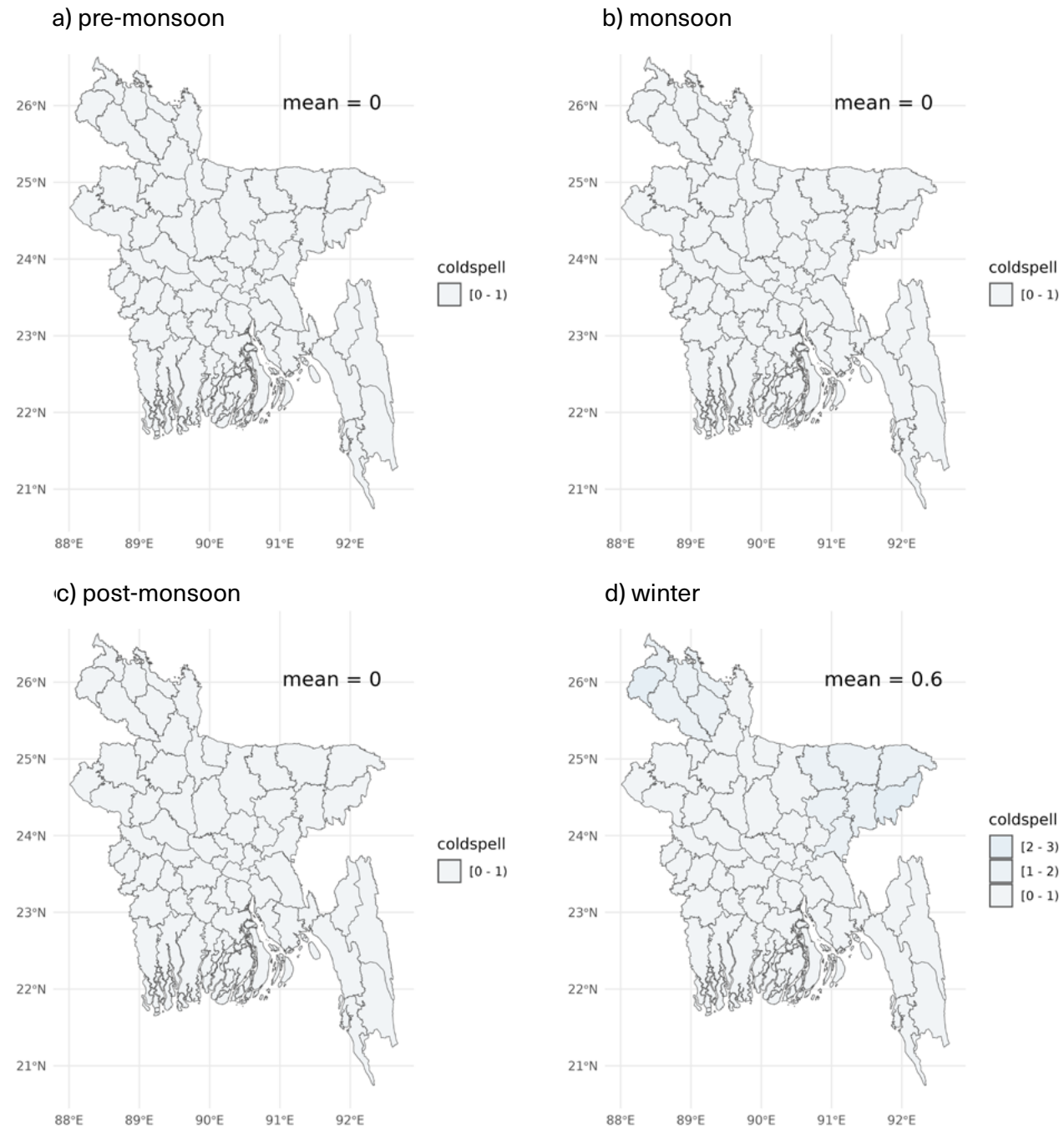


Figure 7.10 The number of cold spell days (daily minimum temperature < 10 ˚C) at the end of the century (2071–2100) under SSP3-7.0. The estimates are based on the NEX-GDDP-CMIP6 ensemble mean of the daily minimum temperature for the a) pre-monsoon, b) monsoon, c) post-monsoon, and d) winter seasons. The mean value of each map shows the country average.

Photo: Salvacampillo/Shutterstock

8

# Sea level rise

## Sea level in the Bay of Bengal and Bangladesh

The Indian Ocean, particularly the Bay of Bengal, has experienced noticeable changes in sea level along its coast in recent decades. These changes are primarily driven by global climate change, but regional processes such as ocean circulation shifts and land subsidence also play important roles. Changes in the level of the land surface, such as land subsidence, adds to the absolute sea level change of the ocean itself, resulting in the relative sea level change experienced at the coasts.

Global mean sea levels have been rising due to thermal expansion and the melting of glaciers and ice sheets. According to the IPCC Sixth Assessment Report (AR6; IPCC, 2021), global mean sea levels (GMSL) are projected to rise by 0.63 to 1.01 m (likely range; Fox-Kemper et al., 2021) by 2100 under the high-emission scenario (SSP5-8.5). Regional sea levels in the Bay of Bengal are expected to broadly follow these global trends, though they may be amplified by local factors. For comparison, under the low-emission scenario SSP1-1.9, GMSL is projected to rise by approximately 0.18 m, with a likely range of 0.15 to 0.23 m.

## Contributions to decadal and long-term changes in absolute sea level in the Bay of Bengal

In order to understand both regional absolute sea level changes and relative sea level changes at coastlines, knowledge of the contributions to sea level rise is key.

A major cause of global sea level rise is the ongoing melting of glaciers and the large ice sheets of Greenland and Antarctica. However, the resulting sea level change is not spatially uniform. As these massive ice sheets lose mass, their gravitational pull on nearby ocean water weakens, leading to a relative fall in sea level in surrounding areas, while distant regions experience a relative rise (see e.g., Tamisiea et al., 2001). This redistribution is most noticeable in the low latitudes, where the Bay of Bengal is located, resulting in an enhanced sea level rise in this region. Conversely, the melting of nearby glaciers tends to have a small mitigating effect on sea level rise in the Bay of Bengal, as the associated loss of mass locally reduces ocean water levels.

Another major contributor to sea level rise is thermal expansion of ocean waters, driven by rising global temperatures. As seawater warms, it expands, contributing to rising sea levels. Together with changes in salinity, the process is called steric sea level change. In tropical regions such as the Indian Ocean, temperature changes dominate this process. Uneven ocean warming and regional variations in ocean circulation cause these steric effects to vary geographically. The Indian Ocean has warmed significantly in recent decades, contributing to accelerated sea level rise due to thermal expansion (Roxy et al., 2020).

Changes in large-scale atmospheric circulation and wind patterns also affect regional sea levels. Events such as the Indian Ocean Dipole (IOD) and the El Niño–Southern Oscillation (ENSO) significantly alter wind patterns and ocean currents, redistributing heat and water across the basin. During positive IOD events, sea levels in the eastern Indian Ocean, including the Bay of Bengal, typically rise due to changes in wind patterns and ocean circulation (see, e.g., Aparna et al., 2012).

Monsoonal variability further contributes to these dynamics. Panickal (2017) found that the observed sea level rise in the North Indian Ocean was accompanied by a weakening of the summer monsoon in the last decades. This weakening has led to reduced upwelling off Arabia and Somalia, decreasing the southward heat transport and increasing heat storage in the northern Indian Ocean–thereby enhancing steric sea level rise.

An interesting but minor effect on the absolute sea level is the gravitational effect of terrestrial water redistribution, such as dam construction or groundwater extraction for consumption and irrigation. Similar to the effects of melting ice masses, significant changes in land water storage can shift mass and influence regional sea levels. Substantial groundwater depletion and surface water redistribution in South and West Asia (see e.g., Rodell et al., 2009) have led to a measurable reduction in sea level in the northernmost Indian Ocean.

## Vertical land motion in coastal Bangladesh

As oceans warm and expand, leading to rising absolute sea levels offshore, the sea level changes experienced on land, known as relative sea level changes, also depend on the vertical movement of the land surface. Relative sea level change is the result of absolute sea level rise minus vertical land movement (VLM).

On large spatial and geological time scales, VLM is influenced by glacial isostatic adjustment (GIA)—the slow rebound of the Earth's crust and mantle following the melting of massive ice sheets. While no major ice sheets covered the North Indian Ocean during recent ice ages, minor adjustments associated with global post-glacial processes produce minimal uplift in the region, estimated at 0.1 mm/yr (Sun & Riva, 2020).

Tectonic activity is another driver of VLM. The Indian Plate moves northeast at 5 cm/yr, while the Eurasian Plate moves northward at only 2 cm/yr, causing deformation at the plate boundary. Unlike many other delta systems where vertical land motion is driven primarily by sediment compaction, the Ganges–Brahmaputra Delta is strongly influenced by tectonic processes, generating VLM rates of up to 4 mm/year (Goodbred and Kuehl, 2000). Seismic activity such as earthquakes can also trigger abrupt vertical shifts in this tectonically active region.

Subsidence, the localised sinking of land surface or seafloor, is a critical issue in deltaic Bangladesh and it is influenced by both natural and human-induced factors. Subsidence-related vertical land motions are highly localised and variable, which makes it unsuitable for inclusion in global climate models and projections, nor does it make sense to compare rates here. Instead, site-specific studies are needed to assess local risks. The primary causes for subsidence include sediment compaction, groundwater extraction, and drainage of peatlands and wetlands. The Bengal Delta is formed from alluvial sediments deposited by the Ganges-Brahmaputra-Meghna river system. Over time, these sediments compact naturally, leading to gradual subsidence (Brown & Nicholls, 2015). Excessive pumping of groundwater, especially in urban areas like Dhaka, contributes to land subsidence as aquifers lose water and compact (Ouyang et al., 2024). Conversion of wetlands for agriculture and urban expansion results in oxidation and compaction of organic soils, contributing to land subsidence. This is especially relevant for the southwestern coastal regions and Haor wetlands in the northeast.

In addition, reduced sediment supply due to upstream dam construction and riverbank stabilization can reduce natural sediment deposition in coastal areas (e.g., Syvitski et al., 2009). However, in the tidal delta, monsoonal flooding and a high tidal range can re-deposit sediment onto the delta plain, effectively leading to sedimentation rates as high as ~5 cm/yr in some regions (Overeem et al., 2014).

## Projected sea level rise in the Bay of Bengal

In this summary we present projections for global and regional sea level rise by 2100 under the high-emission scenario (SSP5-8.5) with numbers for the so-called 'likely range' (66% likelihood), as presented in IPCC Sixth Assessment Report (AR6; Fox-Kemper et al., 2021). The numbers are differences between 2100 and the reference period 1995–2014.

Thermal expansion is projected to contribute 0.24–0.36 m to the global mean sea level (GMSL) rise, while global mean halosteric change is negligible (Gregory et al., 2019). For the ice-sheets, the projected contributions are assessed to be 0.09–0.18 m from the Greenland Ice Sheet, 0.03–0.34 m from the Antarctic Ice Sheet (AAIS), and 0.15–0.20 m from global glaciers. There is also a small contribution of 0.01–0.04 m from changes in land water storage to GMSL, but for this effect, the local patterns are more important.

As mentioned above, sea level rise is non-uniform due to ocean circulation and gravitational effects, so the numbers for the Bay of Bengal may be different. Fox-Kemper et al. (2021) provide maps of regional relative sea level projections for these contributions (their Figure 9.26). These maps show the median change instead of likely ranges. From these maps, the two ice sheets will contribute with some 10–12 cm each to sea level rise in the Bay of Bengal, as will the global glaciers. Ocean dynamics and thermal expansion will contribute around 30 cm to the Bay of Bengal. Projected halosteric changes are negligible and also have low model agreement (their Figure 9.12).

Due to strong groundwater depletion and surface water redistribution in South and West Asia (see e.g., Rodell et al., 2009) and the consequent gravitational effects, the contribution from land water storage is negative in the Gulf of Arabia and along the Indian coast, but zero at the coast of Bangladesh. Other small and negligible contributions are the gravitational, rotational, and deformational effects of global (water) mass redistribution, projected at a mere 2–5 cm lowering of the relative sea level in the region.

In summary, most projections of regional contributions, as well as their sum, lie within the likely range of the global projections, albeit somewhat on the low end of the likely range. Note that these maps of regional changes, as well as their calculations, are not exact. Understanding the relation between the different contributions and what they mean for sea level rise in the Bay of Bengal is important, but one can, for any practical purpose, such as adaptation, use the global projections.

In AR6, projections for contributions to global sea level rise for SSP5-8.5 are summed up to have a median value of 0.77 m and a likely range of 0.63 to 1.01 m. It is a matter of risk acceptance which part of the range is considered in adaptation. For instance, the median basically represents a 50/50 chance of flooding, provided the models are correct and

emissions follow the scenarios, while using the upper end of the likely range (66% range) would leave only a 17% chance of flooding.

The above analysis is limited to the sea level rise, and effects of this, by 2100, but there is no reason to expect the sea level rise to be limited to this century. One should consider the risk, especially for higher emission scenarios, of a continued sea level rise for the foreseeable future, i.e. for the coming centuries.

## Storm surges in the Bay of Bengal and flooding risk in Bangladesh

Storm surges occur when strong winds push seawater onto the land and low air pressure causes sea levels to rise. The Bay of Bengal is one of the most vulnerable regions in the world to the impacts of storm surges, which are here driven by tropical cyclones. These surges can cause catastrophic flooding, particularly in low-lying coastal areas such as Bangladesh. In rivers and on deltas, large amounts of rainfall in combination with a storm surge can create even higher water levels and flooding.

In the northern Indian Ocean, tropical cyclone intensities are only projected to increase by 4% (with a range of -4% to +10%) and frequencies are projected to decrease somewhat (Knutson et al., 2020). Since these projected changes are not only small but also highly uncertain, as a first-order approach it is purposeful to assume today's cyclone activity continues and to focus on their effects on top of the rising mean relative sea level. Higher sea levels will allow storm surges to reach further inland, flooding more areas than would be the case under current sea levels. Sea level rise also makes relatively weaker cyclones more devastating for coastal communities.

Khan et al. (2022) generated and analysed a storm surge database derived from a large ensemble of 3,600 statistically and physically consistent synthetic storm events and a high-resolution storm surge modelling system, and estimated extreme water levels as well as the extent of inundated areas of the Bengal Delta. The highest extreme water levels are shown to be most probable in the Meghna estuary and up the Meghna and Padma rivers, while most of the inundation during extreme events happens in the Sundarbans and the low-lying regions northwest of the Bhola Island (based on 50-year return levels; their Figure 5a). This area distribution is a smoothed pattern of statistical likelihood, and storm surges from single cyclones may behave differently. For instance, the Cyclone Sidr in 2007 gave the highest extreme water levels in the eastern Sundarbans instead of in the most probable regions (their Figure 3a). Note, however, that the inundated regions were not very different from what can be statistically expected, making the Sidr event an example of impacts to be expected.

A simple assessment of how these results would have looked with an added future sea level rise of 0.77 m can be done as follows: 1) Adding 0.77 m to the 50-year return levels estimated from Hiron Point and Chandpur records representing the mentioned most inundation-prone regions (Khan et al., 2022; their Figures 6b and f), gives surge levels associated with more than 300-years return periods for the Sundarbans and 250 years for the regions northwest of the Bhola Island; 2) Comparing inundation areas for 50- and 250-year return periods (Khan et al., 2022; their Figure 7d and g) shows that more than double the area, including most of the northern Barishal, would be inundated in a future 50-year event. (Note that inundation of the Sundarbans is not much different from 250-years and longer return periods.)

In this section only the added effect of mean sea level rise on storm surges has been considered. There are however studies that show potential increase in the frequency of devastating cyclones under future climate conditions (e.g., Emanuel, 2021).

## Chronic Sea Level Rise in Bangladesh

In 2024, the International Centre for Climate Change and Development (ICCCAD) published a scientific synthesis on “climate change impacts in Bangladesh” (Huq et al., 2024). The report indicates that chronic sea level rise will have several significant physical impacts on Bangladesh. Notably, the sea level in the coastal zone of Bangladesh is rising by 3.8 to 5.8 mm per year, which is faster than the global average of 2.1 mm per year. This rise is projected to cause permanent coastal inundation, with between 12% and 18% of Bangladesh's coastal area potentially submerged by the end of the century. This will have "devastating consequences for vital food crops".

Finally, the Sundarbans, the world’s largest mangrove forest located in southern Bangladesh, is particularly vulnerable to the physical impacts of chronic sea level rise. With a mean elevation of less than 1 meter above sea level, the mangroves are susceptible to inundation. Under a very high emissions scenario (RCP8.5), extreme sea level rise could flood 918 $km^2$ (23%) of the Sundarbans by 2100. Even under a medium-emission scenario (RCP4.5), around 40 $km^2$ (1%) could be flooded. The loss of the Sundarbans would not only impact local livelihoods and biodiversity but also reduce its vital role in shielding Bangladesh from cyclones (Sarker et al. 2020).

Photo: ATM Monemul Haque/Shutterstock

9

# Impacts

## Health Impacts from heat exposure

As climate change accelerates, Bangladesh faces significant challenges due to the anticipated warming throughout the 21st century. Rising levels of greenhouse gases are projected to increase both daytime and nighttime temperatures, with nighttime temperatures rising by several degrees and heatwaves increasing in frequency and intensity. The health implications of prolonged exposure to high temperatures are profound.

Heatwaves, particularly during the monsoon season when humidity is high, can significantly increase the risk of heat-related illnesses such as heat exhaustion and heatstroke (Romanello et al., 2024; Ebi et al., 2021; He et al., 2022). Heat exposure can impact the body immediately, causing heat exhaustion, heatstroke, and even death, and in the longer term, may lead to serious and chronic diseases of the cardiovascular and respiratory systems, as well as the kidneys (Flouris et al., 2024). Vulnerable populations, including the elderly, children, and individuals with pre-existing health conditions, are at heightened risk. People who lack access to clean water or protection from the sun and heat are also particularly exposed to danger during heatwaves. The combination of extreme heat and high humidity can strain the cardiovascular system and exacerbate respiratory conditions, leading to increased mortality rates and a burden on individuals as well as healthcare systems.

Stunting is a major health problem in Bangladesh, which is highly vulnerable to climate change and extreme heat. A recent study looked at how extreme heat in the first 1,000 days of life affects children's growth (Raza et al., 2025). The results show that even a 1% increase in extreme heat days raises the chance of stunting by 56%. The age of exposure matters. Children exposed to extreme heat in the first 0–23 months were more affected (67%) than those exposed before birth (28%). This shows how important the early years are for healthy growth and why interventions during this period are crucial, since catching up after 59 months is very difficult.

## Impact of heat on working conditions and economy

Outdoor work during heatwaves is associated with potentially serious health risks. For workers, who have to perform physical labour during heatwaves, the risk of overheating and heat related illness is exacerbated because physical activity increases the internal metabolic heat production, thus increasing the core temperature of the body (Lucas et al. 2014). Economic pressures, fear of job and wage loss, and pressure to meet deadlines, may cause workers to push beyond safe limits, becoming dehydrated and getting heat-related illnesses, which can be severe or even life-threatening (Flouris et al., 2024; Ioannou et al. 2023). Adaptation strategies such as adjusting work schedules, frequent hydration and breaks in cool environments, wearing ventilated clothing, and educating workers and employers about heat related illness, may reduce the morbidity and mortality among workers (Habibi et al. 2024).

Economically, the rise in temperatures can have detrimental effects on productivity and labor. High temperatures can lead to a decline in outdoor work capacity, particularly in sectors such as agriculture and construction, which are crucial to Bangladesh's economy (Romanello et al., 2024). Reduced labor efficiency can result in economic losses and affect the livelihoods of millions who depend on these industries. In short, carbon emissions come at a high cost, both in terms of increased morbidity and mortality and as personal, societal and economic loss (Bressler, 2021; Rennert et al., 2022).

## Air pollution and heat waves

As long spells of hot and dry conditions become more frequent, urban areas are expected to experience increasing issues with air pollution (Basak et al., 2023). During heatwaves, the air

is hot and stagnant: there is no rain to wash out the air pollution or wind to disperse it. This increases the lifetime and concentration of air pollution. Furthermore, high temperatures impact chemical reactions and increases the concentration of ground-level ozone which is harmful to humans. These findings point to the need for coordinated actions to reduce local air pollution as well as global carbon emissions.

## Dengue and malaria

Dengue and malaria are both tropical vector borne diseases. Malaria is caused by the single cell parasite of the genus plasmodium, which is spread by the mosquito Anopheles. The dengue virus is carried and spread by mosquitoes in the genus Aedes, which includes a number of mosquito species (Nature Education, 2014). Of these species, the primary vector of the dengue virus is the species Aedes aegypti.

There are clear connections between outbreaks of dengue and weather conditions, but there exists no universally accepted index for dengue risk. Universally recognized elements connected to dengue are: air temperature, rainfall and humidity. All indexes indicate that an increase in air temperature and humidity, alone or in combination, will result in increased risk of dengue. The connection with rainfall is more complex. An increased availability of standing water for breeding grounds increases the risk, while heavy rainfall may wash some of the larvae out of the region. A study for Dhaka is clear: “Maximum temperature, minimum temperature, humidity, and wind speed positively impact dengue incidence, while rainfall and sunshine hours have a significantly negative effect” (Hossain et al., 2023). These findings suggest that rising temperatures may increase the risk of dengue in Bangladesh. The lack of a standardised, locally calibrated dengue risk index hinders a quantification of future risk under changing climate conditions. One adaptive measure could be to establish a national, or regional, index for dengue, an index tailored to be used in both forecasting and climate analysis.

Bangladesh has had remarkable progress in protecting its people from malaria, significantly decreasing the number of infected and number of yearly deaths. The interplay of climate and malaria is very complex, one has to look at both the mosquito and the parasite's response to the changes. On an overall basis, increased temperature increases the mosquito and parasite burden, but there are thresholds. The optimum temperature for the development of the parasite is around 25 °C, while temperatures above 30 °C and below 15–18 °C halts the development. As for Dengue, there is an optimum rainfall where excess or too little will decrease the mosquito  burden. The last climate indicator with relevance is humidity, where higher humidity is related to longer lifespan of the mosquitos and possibly more rapid development of the parasites. Despite the remarkable progress in Bangladesh on the fight against malaria, climate change might increase the burden in Bangladesh, and a national, or regional, index might be a good adaptive measure.

## Cholera and other water borne diseases

The relationship between climate change and waterborne diseases in Bangladesh is a complex, systemic challenge that transcends sectors. Climate change may act as a foundational driver,

altering the nation's physical and biological landscape in ways that create an ideal environment for pathogens like vibrio cholerae to thrive. The dual threats of slow-onset salinization and sudden-onset flooding converge with pre-existing public health vulnerabilities, creating a perfect storm for epidemics. This is further amplified by the silent crisis of climate-induced migration, which funnels vulnerable populations into urban centers.

Looking at Cholera as an example of possible future changes, a study by Kruger et.al (2022) shows a dramatic picture where the hotspots, that are concentrated to coastal areas, are shown to spread out throughout the country. There is also a connection between Cholera and heat waves, especially in the cities. E.g. the Dhaka metropolitan area has more than 20 million people, and the population is rising, especially with poor people moving in from the villages. The increase in population may push the need for clean water past the supply, and some might end up drinking contaminated water. This risk is increased during heat waves due to more water consumption and that the build up towards heat waves might include almost ideal conditions for vibrio cholerae.

A linked challenge with this is the impact of severe weather and connected flooding. A severe weather incident, with flooding may, and will, interfere with the supply of clean drinking water, and may result in large areas without clean sources of water. In the past this has proven to be a problem, e.g. within days of the cyclone Aila in 2009 where about 10000 people were infected with water borne diseases like diarrhea and dysentery (Wikipedia: Cyclon Aila).

The examples of water borne diseases shows the necessity of a two pronged adaptation strategy. There is a need for long term adaptation to decrease the spread of e.g. cholera and ensure everybody has access to clean water on a daily basis, at the same time the need of preparedness for when the cyclone and flooding strikes to quickly establish access to clean water and prevent an outbreak.

## Food security: impacts on agriculture, livestock and fisheries

The agricultural sector in Bangladesh, a cornerstone of the nation's economy, is particularly vulnerable to the impacts of rising temperatures. Heatwaves can disrupt crop yields and affect food security (Sikder and Xiaoying, 2014; Hossain et al., 2016). High temperatures can lead to increased evapotranspiration, reducing soil moisture and affecting the growth of staple crops such as rice and wheat. These conditions can also exacerbate pest infestations and diseases, further threatening agricultural productivity. The resulting strain on food resources could lead to higher prices and increased poverty, impacting the most vulnerable communities.

Climate change also poses risks to livestock (NAP of Bangladesh 2023-2030). Extreme heat increases the risk of heatstroke and outbreaks of disease and may result in mass death among animals. Even more moderate increases in temperature may reduce the production in milk, egg and meat. Risks associated with cold spells, such as diseases and reduced food intake, are expected to be reduced as a result of increasing temperatures. Flooding and extreme precipitation can put livestock at direct and indirect risk, for example through reduced availability of fodder and clean water. Rising sea levels pose a threat to agricultural production by salinity intrusion and flooding. The salinization of farmland is already evident, with a 27% increase in salt-affected coastal areas since the 1970s, which has consequences for crops and livelihoods. The inundation of coastal areas threatens food security for a large

portion of the population, especially the 37% engaged in agriculture (Huq et al. 2024). Furthermore, increasingly saline waters are projected to disrupt fisheries, which are a critical source of protein for impoverished coastal communities (Huq et al. 2024). The mangroves of the Sundarbans, which are habitats and breeding grounds for fish, are also threatened by damage from cyclones.

The salinization also affects freshwater resources, as saline water can infiltrate groundwater and surface water, impacting drinking water supplies. The contamination of drinking water supplies by saline intrusion poses a significant health risk, potentially leading to increases in cardiovascular disease, hypertension, and waterborne diseases. Poor water quality also poses difficulties for the menstrual health and hygiene of women and adolescent girls in coastal regions.

Adaptation measures such as growing salt- and heat-tolerant crops, using integrated farming strategies e.g. combining agriculture and aquaculture, and learning climate-smart practices such as crop rotations, may counteract some of the negative impacts of climate change (Akhter et al. 2025).

## Forests and forestry

Through the process of photosynthesis, trees absorb and store carbon dioxide from the atmosphere (Miah et al. 2011). They are a natural carbon sink and as such critical to mitigating global warming. Bangladesh has committed to reducing greenhouse gas emissions from deforestation and enhancing the carbon absorption capacity through reforestation, and has taken significant steps to achieve this under the REDD+ Strategy (2016–2030) (Bangladesh Forest Department, 2016). The strategy aims to address deforestation while promoting sustainable forest management and afforestation initiatives. Despite these efforts, reforestation and planting in some areas—such as coastal mangrove afforestation—have been counteracted by deforestation in other regions, particularly in the Chattogram Hill Tracts and peri-urban areas, where agriculture, urbanization, and illegal logging remain significant drivers (Mamnun and Hossen, 2020; Global Forest Watch, 2023). Effective governance will be key to counteract the ecological, financial and socioeconomic pressures that drive deforestation (Nadiruzzaman et al. 2025).

Forests in Bangladesh play a critical role in supporting human livelihoods and protecting communities from natural disasters. They provide essential ecosystem services, such as fuelwood, timber, and food production, which are vital for rural communities' income and subsistence, and indirect but equally important benefits like water purification, soil fertility and crop pollination (Islam et al. 2017, Ahammad et al. 2019). Forest ecosystems, such as the Sundarbans mangroves, act as natural barriers against tropical cyclones and storm surges, reducing the devastating impacts of these extreme weather events on coastal populations (Sarker et al. 2020; Parvin et al. 2023). Similarly, forests in hilly areas, such as the Chattogram Hill Tracts, help prevent soil erosion and landslides, which are becoming more frequent due to deforestation and erratic rainfall patterns exacerbated by climate change (Kafy et al. 2017; Nadiruzzaman et al. 2025). Protecting and restoring these forests is thus essential not only for mitigating climate change but also for safeguarding human lives and livelihoods.

## Displacement and damage from sea level rise and storm surges

As previously discussed, chronic sea level rise is causing permanent coastal inundation, increased salinity, and threats to freshwater resources and the Sundarbans (Huq et al. 2024). Storm surges, exacerbated by rising sea levels, also lead to widespread flooding and increased salinity. These physical changes have significant cascading impacts on the population. Regarding chronic sea level rise, the projected rise in southern Bangladesh could displace around 0.9 million people by 2050, forcing them to leave their homes.

Storm surge flooding events, which are intensified by sea level rise, pose immediate and severe threats to the population. Huq et al. (2024) notes that during Cyclone Amphan in 2020, storm surges flooded areas located up to 15 km inland after damaging coastal embankments, forcing 500,000 families from their homes. Projections indicate that if a similar cyclone occurred in 2100 with the projected sea level rise, the number of people exposed to the storm surge could be 50–80% higher than in 2020, unless global temperature rise is limited to 2 °C. These events not only cause immediate displacement and loss of homes but also increase the salinity of soil and water, making recovery and continued habitation more difficult for coastal communities.

The average annual loss due to climate-related disasters in Bangladesh is estimated at around $3 billion, or 1–2% of GDP, with much higher figures in individual years, indicating a significant economic burden on the population. In 2019 alone, 4.1 million people were displaced because of climate disasters. Overall, both chronic sea level rise and storm surges present compounding threats to the lives, livelihoods, health, and displacement of the population in Bangladesh.

## Adaptation and Resilience Efforts

Bangladesh is recognized as a global leader in adaptation and resilience, having decades of experience in supporting communities. A significant success is the Cyclone Preparedness Programme (CPP), which has dramatically reduced cyclone-related deaths from six digits to double digits through early warning systems, community engagement, and the construction of 4,530 cyclone shelters by 2022.

Coastal polders, protecting around 25% of the coastal zone, are crucial for adapting to tidal floods and salinity intrusion, with ongoing projects upgrading these embankments and directly protecting over 670,000 people. Innovative climate-smart agricultural practices like saline-tolerant rice, gher farming, and floating agriculture are helping to safeguard food security.

Bangladesh has also developed numerous national adaptation policies and plans since being one of the first least developed countries to create a National Adaptation Programme of Action in 2005. These include the Bangladesh Delta Plan 2100 (GED 2018), the Mujib Climate Prosperity Plan (MEFCC 2022), and the National Adaptation Plan of Bangladesh 2023–2050 (MEFCC 2023), increasingly recognizing the importance of locally led adaptation. The

government is already investing significantly in climate adaptation, spending approximately 6–7% of its annual budget, with about 75% from domestic sources. This proactive approach, combined with successes in disaster preparedness and adaptation planning, offers reasons for optimism despite the significant challenges.

Bangladesh needs to move beyond policy-making and ensure system-wide, cross-sectoral action to align with the WHO Global Action Plan on Climate Change and Health (Faruqui et al. 2025). A key priority is making the national health infrastructure climate-resilient. Although a few pilot projects exist, they are limited and fragmented. Since hospitals and health centers are frontline responders during climate emergencies, they need strong infrastructure standards to withstand extreme weather and provide uninterrupted care. By addressing this gap, Bangladesh can set a global example by turning the WHO vision into practical, scalable solutions that protect both health systems and vulnerable populations.

These ambitious local adaptation measures could reduce the damage of climate change, but as Bangladesh's contribution to greenhouse gas emissions is small, in total and per capita (Ritchie et al. 2023, IEA 2025), the country cannot solve the climate crisis alone. Immediate and efficient international efforts to phase out fossil fuels and limit global warming are essential to reduce the potential harm on communities in Bangladesh and elsewhere. The projections of climate change presented and discussed in this report highlight that different emission scenarios can lead to vastly different climate futures. In other words, the future is not set in stone and much can still be done to steer clear of the worst outcomes of anthropogenic climate change. Even though the future climate development isn't set, there is a strong need for continued focus on climate adaptation in Bangladesh no matter which future scenario that turns out to be most representative

Photo: Md Rafayat Haque Khan/Shutterstock

# Acknowledgements

This report has been produced under the project SAREPTA which is financed by NORAD. Furthermore, the authors wish to acknowledge the support from Bangladesh Meteorological Department and Norwegian Meteorological Institute and the colleagues who work there. A special thanks is forwarded to the reviewers, Professor Dr. Sheikh Mohammad Sayem of the Bangladesh Agricultural University (BAU), Dr. Farjana Jahan at HSPSD, icddr, b, and Mr. Niaz Md. Farhat Rahman, Principal Scientific Officer at Bangladesh Rice Research Institute (BRRI), who have helped to ensure the quaity of the report. Similar thanks are extended to the colleagues at Norwegian Meteorological Institute for quality assurance through review. We also wish to express our gratitude to Mai-Linn Finstad Svehagen at Norwegian Meteorological Institute for design and typesetting. The frontpage photo of Dhaka is taken by Lumenite/Shutterstock.

We extend our sincere gratitude to the German Federal Foreign Office (GFFO), Save the Children Bangladesh, and RIMES for their invaluable support in the publication and dissemination of the Future Climate Projection Report for Bangladesh.

# References


Acharya, N., Faniriantsoa, R., Rashid, B., Sultana, R., Montes, C., Dinku, T. & Hassan, S. (2020), "Developing High-Resolution Gridded Rainfall and Temperature Data for Bangladesh: The ENACTS-BMD Dataset". Preprints, 2020120468. https://doi.org/10.20944/preprints202012.0468.v1.

Ahmed. R. & Karmakar. S. (1993), "Arrival and withdrawal dates of the summer monsoon in Bangladesh." International Journal of Climatology 13(7):727 – 740, DOI : 10.1002 / joc.3370130703.

Ahammad, R., Stacey, N., Sunderland, T.C.H. (2019) Use and perceived importance of forest ecosystem services in rural livelihoods of Chittagong Hill Tracts, Bangladesh, Ecosystem Services, 35, pp. 87-98, ISSN 2212-0416, https://doi.org/10.1016/j.ecoser.2018.11.009

Akhter, J., Muhammad Ramzan Ali, Foezullah Talukder, Sheikh Mohammad Sayem (2025)
Agricultural adaptation actions to address climate change in the coastal region of Bangladesh: A systematic review, Climate Services, 39, 100599, ISSN 2405-8807, https://doi.org/10.1016/j.cliser.2025.100599.

Aparna, S. G., J. P. McCreary, D. Shankar, & P. N. Vinayachandran, (2012), "Signatures of Indian Ocean Dipole and El Niño–Southern Oscillation events in sea level variations in the Bay of Bengal", J. Geophys. Res., 117, C10012, doi:10.1029/2012JC008055.

Bangladesh Forest Department. (2016). Bangladesh REDD+ Strategy 2016–2030. Retrieved from http://www.bforest.gov.bd

Basak, P., Dey, S., & Elahi, K. M. (2023). Air pollution in urban Bangladesh from climate change and public health perspectives. Climate Change and Human Health Scenarios. Global Perspectives on Health Geography . https://doi.org/10.1007/978-3-031-38878-1_9

(PDF) Sustainable Urban Development: Where Bangladesh Stands?. Available from: https://www.researchgate.net/publication/394846059_Sustainable_Urban_Development_Where_Bangladesh_Stands [accessed Sep 16 2025].

Benestad, R. E., D. Chen, & I. Hanssen-Bauer, (2008), "Empirical-statistical downscaling". World Scientific Publishing Company.

Benestad, R. E., Mezghani, A., Lutz, J., Dobler, A., Parding, K. M., & Landgren, O. A. (2023), "Various ways of using empirical orthogonal functions for climate model evaluation", Geoscientific Model Development, 16(10), 2899–2913. https://doi.org/10.5194/gmd-16-2899-2023

Bressler, R. D. (2021), "The mortality cost of carbon. Nature Commu-nications", 12(1), 1–12. https://doi.org/10.1038/s41467-021-24487-w.

Brown, S. & Nicholls, R. J. (2015), "Subsidence and human influences in mega deltas: The case of the Ganges–Brahmaputra–Meghna". Science of The Total Environment, 527–528, 362–374. https://doi.org/10.1016/j.scitotenv.2015.04.124.

Clarke, B., Otto, F., Stuart-Smith, R., & Harrington, L. (2022), "Extreme weather impacts of climate change: an attribution perspective. Environmental Research: Climate", 1(1), 012001. https://doi.org/10.1088/2752-5295/ac6e7d

Costello, A., M. Abbas, A. Allen, et al. (2009), "Managing the Health Effects of Climate Change: Lancet and University College London Institute for Global Health Commission." Lancet 373, no. 9676: 1693–1733.

Emanuel, K. (2021), "Tropical cyclone risk in Bangladesh", MAUSAM, 72, 27–34, https://doi.org/10.54302/mausam.v72i1.122.

Ebi, K. L., Capon, A., Berry, H. L., Broderick, C., de Dear, R., Havenith, G., Honda, Y., Kovats, R. S., Ma, W., Malik, A., McGregor, G. R., Nybo, L., Sari Kovats, R., & van Aalst, M. K. (2021), "Hot weather and heat extremes: health risks". The Lancet, 398(10301), 698–708. https://doi.org/10.1016/S0140-6736(21)01208-3

Eyring, V., Bony, S., Meehl, G. A., Senior, C. A., Stevens, B., Stouffer, R. J., & Taylor, K. E. (2016), "Overview of the Coupled Model Intercomparison Project Phase 6 (CMIP6) experimental design and organization", Geosci. Model Dev., 9, 1937–1958, https://doi.org/10.5194/gmd-9-1937-2016.

Fahad, M.G., Islam, A.S., Nazari, R., Hasan, M.A., Islam, G.M.T., & Bala, S.K. (2017), "Regional changes of precipitation and temperature over Bangladesh using bias corrected multi-model ensemble projections considering high emission pathways." International Journal of Climatology, 38(4), 1634-1648. doi:10.1002/joc.5284.

Faruqui, W. A., Nagabhatla, N., & Haghebaert, G. (2025). Unpacking climate change and health nexus in Bangladesh: 10 points on how the country can prepare to implement and support the WHO's global action plan on climate change and health (2025) (UNU-CRIS Working Paper No. 16). United Nations University Institute on Comparative Regional Integration Studies. https://cris.unu.edu

Field, C., Barros, V., Stocker, T. F., Qin, D., Dokken, D. J., Ebi, K. L., Mastrandrea, M. D., Mach, K. J., Plattner, G.-K., Allen, S. K., Tignor,230M., and Midgley, P. M., eds. (2012), "Managing the Risks of Extreme Events and Disasters to Advance Climate Change Adaptation. A Special Report of Working Groups I and II of the Intergovernmental Panel on Climate Change", Cambridge University Press, Cambridge, UK, and New York, NY, USA.

Flouris, A., Azzi, M., Graczyk, H., Nafradi, B., and Scott, N., eds. 2024. Heat at Work: Implications for Safety and Health. A Global Review of the Science, Policy and Practice. ILO

Fox-Kemper, B., Hewitt, H. T., Xiao, C., Adalgeirsdottir, G., Drijfhout, S. S., Edwards, T. L., et al. (2021), "Ocean, cryosphere and sea level change. In V. Masson-Delmotte, P. Zhai, A. Pirani, S. L. Connors, C. Péan, S. Berger, et al. (Eds.), Climate change 2021: The physical science basis. Contribution of Working Group 1 to the Sixth Assessment Report of the Intergovernmental Panel on Climate Change. Cambridge University Press.

GED (2018), The Bangladesh delta plan 2100. General Economics Division (GED), Planning Commission, Government of the People's Republic of Bangladesh. https://oldweb.lged.gov.bd/UploadedDocument/UnitPublication/1/756/BDP%202100%20Abridged%20Version%20English.pdf

Giorgi, F. & Gutowski, W. J., (2015), "Regional Dynamical Downscaling and the Cordex Initiative". Annual Review of Environment and Resources, Vol. 40, pp. 467-490, 2015, Available at SSRN: https://ssrn.com/abstract=2688529 or http://dx.doi.org/10.1146/annurev-environ-102014-021217

Global Forest Watch (2023). Bangladesh – Forest Monitoring Overview. Retrieved from https://www.globalforestwatch.org

Goodbred, S. L. & S. A. Kuehl, (2000), "The significance of large sediment supply, active tectonism and eustasy on margin sequence development: Late Quaternary stratigraphy and evolution of the Ganges-Brahmaputra delta". Sedimentary Geology, 133, doi:10.1016/S0037-0738(00)00041-5.

Gregory, J. M., Andrews, T., Ceppi, P., Mauritsen, T., & Webb, M. J. (2019), "How accurately can the climate sensitivity to $CO_2$ be estimated from historical climate change"? Climate Dynamics. https://doi.org/10.1007/s00382-019-04991-y

Habibi, P., Razmjouei, J., Moradi, A. et al. (2024) Climate change and heat stress resilient outdoor workers: findings from systematic literature review. BMC Public Health 24, 1711. https://doi.org/10.1186/s12889-024-19212-3

He, Cheng, et al. "The effects of night-time warming on mortality burden under future climate change scenarios: a modelling study." The Lancet Planetary Health 6.8 (2022): e648-e657.

Hossain S, Islam MM, Hasan MA, Chowdhury PB, Easty IA, Tusar MK, Rashid MB, Bashar K. Association of climate factors with dengue incidence in Bangladesh, Dhaka City: A count regression approach. Heliyon. 2023 May 5;9(5):e16053. https://doi.org/10.1016/j.heliyon.2023.e16053

IEA (2025), International Energy Agency (IEA) estimates of CO2 emissions from fuel combustion in the energy sector in 2022, Country profile for Bangladesh https://www.iea.org/countries/bangladesh/emissions [online resource, last accessed on June 24, 2025]

Ioannou, L. G., Foster, J., Morris, N. B., Piil, J. F., Havenith, G., Mekjavic, I. B., ... Flouris, A. D. (2022). Occupational heat strain in outdoor workers: A comprehensive review and meta-analysis. Temperature, 9(1), 67–102. https://doi.org/10.1080/23328940.2022.2030634

Islam, M.M., Hossain, M.M. (2017). Community Dependency on the Ecosystem Services from the Sundarbans Mangrove Wetland in Bangladesh. In: Prusty, B., Chandra, R., Azeez, P. (eds) Wetland Science . Springer, New Delhi. https://doi.org/10.1007/978-81-322-3715-0_16

Jihan, M.A.T.; Popy, S.; Kayes, S.; Rasul, G.; Maowa, A.S.; Rahman, M.M. (2025), "Climate change scenario in Bangladesh: historical data analysis and future projection based on CMIP6 model". Sci Rep 15, 7856. https://doi.org/10.1038/s41598-024-81250-z

Hersbach, H., Bell, B., Berrisford, P., Hirahara, S., Horányi, A., Muñoz-Sabater, J., Nicolas, J., Peubey, C., Radu, R., Schepers, D., Simmons, A., Soci, C., Abdalla, S., Abellan, X., Balsamo, G., Bechtold, P., Biavati, G., Bidlot, J., Bonavita, M., ... Thépaut, J.-N. (2020), "The ERA5 global reanalysis. Quarterly Journal of the Royal Meteorological Society", 146(730), 1999–2049. https://doi.org/10.1002/qj.3803

Hewitson, B.C., Daron, J., Crane, R.G. et al. (2014), "Interrogating empirical-statistical downscaling". Climatic Change 122, 539–554. https://doi.org/10.1007/s10584-013-1021-z

Hossain, B.M.S., &M. A. Noor, (2016). "Impact of climate change on agriculture and food security in Bangladesh." International Journal of Multidisciplinary Education and Research 1.8 (2016): 05-11.

Hoque, M.Z., Cui, S., Xu, L.; Islam, I., & Tang, J. (2019), Ding, S. Assessing Agricultural Livelihood Vulnerability to Climate Change in Coastal Bangladesh. Int. J. Environ. Res. Public Health 2019, 16, 4552. https://doi.org/10.3390/ijerph16224552

Hostetler, S.W., Bartlein, P.J., and Alder, J.R. (2018), "Atmospheric and surface climate associated with 1986–2013 wildfires in North America." Journal of Geophysical Research. Bio-geosciences, v. 123, no. 5, p. 1588–1609, https://doi.org/10.1029/2017JG004195.

Huq, S., Khan, M., Islam, A.S. & Mirza, A. B. (2024). Climate change impacts in Bangladesh: What climate change means for a country and its people. International Centre for Climate Change and

Development (ICCCAD) report. https://www.icccad.net/wp-content/uploads/2024/02/Bangladesh_Final_Covers_26-Jan-2024_ONLINE_compressed.pdf

IPCC, (2019), "Summary for policymakers. Climate change and land: an IPCC special report on climate change, desertification, land degradation, sustainable land management, food security, and greenhouse gas fluxes in terrestrial ecosystems PR Shukla, J Skea, E Calvo Buendia, V Masson-Delmotte, H-O Pörtner et al.3–36 Rep., Intergov. Panel Clim. Change Geneva: https://www.ipcc.ch/site/assets/uploads/sites/4/2020/02/SPM_Updated-Jan20.pdf

IPCC, (2021), "Climate Change 2021: The Physical Science Basis. Contribution of Working Group I to the Sixth Assessment Report of the Intergovernmental Panel on Climate Change" [Masson-Delmotte, V., P. Zhai, A. Pirani, S.L. Connors, C. Péan, S. Berger, N. Caud, Y. Chen, L. Goldfarb, M.I. Gomis, M. Huang, K. Leitzell, E. Lonnoy, J.B.R. Matthews, T.K. Maycock, T. Waterfield, O. Yelekçi, R. Yu, and B. Zhou (eds.)]. Cambridge University Press, Cambridge, United Kingdom and New York, NY, USA, In press, doi:10.1017/9781009157896.

Kafy, A. A., Rahman, M. S., & Ferdous, L. (2017). Exploring the association of land cover change and landslides in the Chittagong hill tracts (CHT): A remote sensing perspective. In Proceedings of the International Conference on Disaster Risk Management, Dhaka, Bangladesh (Vol. 23).

Khan, M. J. U., Durand, F., Emanuel, K., Krien, Y., Testut, L., and Islam, A. K. M. S. (2022), "Storm surge hazard over Bengal delta: a probabilistic–deterministic modelling approach", Nat. Hazards Earth Syst. Sci., 22, 2359–2379, https://doi.org/10.5194/nhess-22-2359-2022.

Khanom T., (2016), "Effect of salinity on food security in the context of interior coast of Bangladesh. Ocean and Coastal Management", 130: 205–212. https://doi.org/10.1016/j

Khatun, Mossammat Ayesha., Rashid, Md. Bazlur and Hygen, Olav. Hans, (2016), "Climate of Bangladesh", MET report, no. 08/2016, ISSN 2387-4201, Climate, Norwegian Meteorological Institute. http://www.bmd.gov.bd/p/Climate-Report/.

Knutson, T.R. et al., (2020), "Tropical Cyclones and Climate Change Assessment: Part II: Projected Response to Anthropogenic Warming". Bulletin of the American Meteorological Society, 101(3), E303–E322, doi:10.1175/bams-d-18-0194.1.

Sophia E Kruger, Paul A Lorah, Kenichi W Okamoto (2022), "Mapping climate change's impact on cholera infection risk in Bangladesh" PLOS Glob Public Health. 2022 Oct 14;2(10):e0000711. doi: 10.1371/journal.pgph.0000711

Labeurthre, David and Reffet, Anatole and Schrapffer, Anthony, (2024), "An Overview of Statistical Downscaling Methods: Techniques, Applications, and Advances". https://ssrn.com/abstract=5046442 or http://dx.doi.org/10.2139/ssrn.5046442

Lucas, R. A., Epstein, Y., & Kjellstrom, T. (2014). Excessive occupational heat exposure: a significant ergonomic challenge and health risk for current and future workers. Extreme physiology & medicine, 3(1), 14.

Mamnun, M., & Hossen, S. (2020). Spatio-temporal analysis of land cover changes in the evergreen and semi-evergreen rainforests: A case study in Chittagong Hill Tracts, Bangladesh. International Journal of Forestry, Ecology and Environment, 2(2), 87-99.

Mezghani, A., Dobler, A., Benestead, R. E., Haugen, J. E. and Parding, K. M. (2019), "Subsampling Impact on the Climate Change Signal over Poland Based on Simulations from Statistical and Dynamical Downscaling." Journal of Applied Meteorology and Climatology, 58, 1061-1078.

Miah, D., Shin, M.Y., Koike, M. (2011). Carbon Sequestration in the Forests of Bangladesh. In: Forests to Climate Change Mitigation. Environmental Science and Engineering(). Springer, Berlin, Heidelberg. https://doi.org/10.1007/978-3-642-13253-7_5

Mohammed Khaled, Islam A. K. M. Saiful, Islam G. M. Tarekul, Alfieri Lorenzo, Khan Md. Jamal Uddin, Bala Sujit Kumar and Das Mohan Kumar. (2018), "Future Floods in Bangladesh under 1.5°C, 2°C, and 4°C Global Warming Scenarios." J. Hydrol. Eng., 23(12), DOI: 10.1061/(ASCE)HE.1943-5584.0001705.

MEFCC (2022), Mujib Climate Prosperity Plan 2022 - 2041. Ministry of Environment, Forest and Climate Change (MEFCC), Government of the People's Republic of Bangladesh https://bangladeshbiosafety.org/wp-content/uploads/2024/07/Mujib-Climate-Prosperity-Plan-2022-2041.pdf

MEFCC (2023), National Adaptation Plan of Bangladesh 2023-2050. Ministry of Environment, Forest and Climate Change (MEFCC), Government of the People's Republic of Bangladesh https://bangladeshbiosafety.org/bangladesh-doc/national-adaptation-plan-bangladesh-2023-english/

Murphy, J. (2000), "Predictions of climate change over Europe using statistical and dynamical downscaling techniques". Int. J. Climatol., 20: 489-501. https://doi.org/10.1002/(SICI)1097-0088(200004)20:5

NAP (2023-2030) National Adaptation Plan of Bangladesh https://faolex.fao.org/docs/pdf/BGD214817.pdf

Nature Education, (2014), Dengue Transmission, accessed 2025-04-28 https://www.nature.com/scitable/topicpage/dengue-transmission-22399758/

Nadiruzzaman, M., Shewly, H. J., Rashid, M. B., Mukul, S. A., & Dutta, O. (2025). Beyond Climate Reductionism: Environmental Risks and Ecological Entanglements in the Chittagong Hill Tracts of Bangladesh. Earth, 6(3), 63. https://doi.org/10.3390/earth6030063

NOAA (2025). https://www.noaa.gov/news/2024-was-worlds-warmest-year-on-record.
Nordhaus, W.D., (2017), "Revisiting the social cost of carbon. Proceedings of the National" Academy of Sciences 114, 1518–1523.

Ouyang, L., Zhao, Z., Zhou, D., Cao, J., Qin, J., Cao, Y., & He, Y. (2024), "Study on the Relationship between Groundwater and Land Subsidence in Bangladesh Combining GRACE and InSAR". Remote Sensing, 16(19), 3715. https://doi.org/10.3390/rs16193715.

Overeem, I., K. Rogers, P. Passalacqua, A. Canestrelli, S. Cohen, and K. Matin. (2014), "Sedimentation Patterns in the Ganges-Brahmaputra Delta System". Search and Discovery Article #50994. https://www.searchanddiscovery.com/documents/2014/50994overeem/ndx_overeem.pdf

Panickal, S., Jadhav, J., Raghavan, K., Narayanasetti, S., Griffies, S. (2017), "Multidecadal Weakening of Indian Summer Monsoon Circulation Induces an Increasing Northern Indian Ocean Sea Level: Sea Level Rise in the North Indian Ocean". Geophysical Research Letters. 44. doi:10.1002/2017GL074706.

Parvin, S., Md. Hashmi Sakib, Md. Latiful Islam, Christopher L. Brown, Md. Saiful Islam, Yahia Mahmud. (2023). Coastal aquaculture in Bangladesh: Sundarbans's role against climate change, Marine Pollution Bulletin, 194 (B), 115431, ISSN 0025-326X, https://doi.org/10.1016/j.marpolbul.2023.115431.

Raza WA, Misha F, Hossain SS, Gulshan J, Rashid B, Sayem SM, Aranya SG, Chaudhery D. (2025). "Extreme heat exposure in the first 1000 days: implications for childhood stunting in Bangladesh". Public Health. 241:83–8. https://doi.org/10.1016/j.puhe.2025.02.002.

(PDF) Call to action: recognize and prevent the effects of extreme heat on early childhood development and health. Available from: https://www.researchgate.net/publication/394932365_Call_to_action_recognize_and_prevent_the_effects_of_extreme_heat_on_early_childhood_development_and_health [accessed Sep 12 2025].

Rashid, Md. B., Sultana, A., Hassan, S. M. Q., Kuya, E., Parding, K., and Hygen, H. O. (2024), "Changing climate of Bangladesh", MET report, no. 04/2024, ISSN 2387-4201, Climate, Norwegian Meteorological Institute. DOI: 10.13140/RG.2.2.15681.94561

Rennert, K., Errickson, F., Prest, B.C. et al. Comprehensive evidence implies a higher social cost of CO2. Nature 610, 687–692 (2022). https://doi.org/10.1038/s41586-022-05224-9

Ritchie, H., Rosado, P., and Roser, M. (2023) Data Page: Per capita $CO_2$ emissions, part of the following publication: $CO_2$ and Greenhouse Gas Emissions. Data adapted from Global Carbon Project, Various sources. Retrieved from https://ourworldindata.org/grapher/co-emissions-per-capita [online resource, last accessed June 24, 2025]

Rodell, M., Velicogna, I., Famiglietti, J. (2009), "Satellite Based Estimates of Groundwater Depletion in India". Nature. 460. 999-1002. 10.1038/nature08238.

Romanello, Marina, et al. "The 2024 report of the Lancet Countdown on health and climate change: facing record-breaking threats from delayed action." The Lancet 404.10465 (2024): 1847-1896.

Roxy, M.K. et al. (2020), "Indian Ocean Warming". In: Krishnan, R., Sanjay, J., Gnanaseelan, C., Mujumdar, M., Kulkarni, A., Chakraborty, S. (eds) Assessment of Climate Change over the Indian Region. Springer, Singapore. https://doi.org/10.1007/978-981-15-4327-2_10

Sarker, A. R., Nobi, M. N., Roskaft, E., Chivers, D. J., & Suza, M. (2020). Value of the storm-protection function of Sundarban mangroves in Bangladesh. Journal of Sustainable Development, 13(3), 128-137.

Schmidli, J., C. M. Goodess, C. Frei, M. R. Haylock, Y. Hundecha, J. Ribalaygua, and T. Schmith (2007), "Statistical and dynamical downscaling of precipitation: An evaluation and comparison of scenarios for the European Alps", J. Geophys. Res., 112, D04105, doi:10.1029/2005JD007026.

SRTM (2013), NASA Shuttle Radar Topography Mission (SRTM) Global. Distributed by OpenTopography. https://doi.org/10.5069/G9445JDF. Accessed 2025-06-25

Sikder, Rajesh, and Jian Xiaoying. "Climate change impact and agriculture of Bangladesh." Journal of Environment and Earth Science 4.1 (2014): 35-40.

Sun, Y., & Riva, R. E. M. (2020), "A global semi-empirical glacial isostatic adjustment (GIA) model based on Gravity Recovery and Climate Experiment (GRACE) data". Earth System Dynamics, 11 (1), 129-137. https://doi.org/10.5194/esd-11-129-2020.

Syvitski, J., Kettner, A., Overeem, I. et al. (2009), "Sinking deltas due to human activities". Nature Geosci 2, 681–686. https://doi.org/10.1038/ngeo629.

Tamisiea, M. E., Mitrovica, J. X., Davis, J. L., & Milne, G. A. (2001), "Global geoid and sea level changes due to present-day ice mass fluctuations". Journal of Geophysical Research: Solid Earth, 106(B12), 30,849–30,863. https://doi.org/10.1029/2000JB000011

Thrasher, B., Wang, W., Michaelis, A. Melton, F., Lee, T., & Nemani, R. (2022), "NASA Global Daily Downscaled Projections, CMIP6". Sci Data 9, 262 (2022). https://doi.org/10.1038/s41597-022-01393-4

Uddin, Kamal Md. (2017), "Climate Change and Global Environmental Politics: North-South Divide", Environmental Policy and Law, Volume 47, Issue 3-4, 2017 https://journals.sagepub.com/doi/epdf/10.3233/EPL-170022

Vicedo-Cabrera, A. M., Scovronick, N., Sera, F., Guo, Y., Huber, V., Schleussner, C.-F., Mitchell, D., Tong, S., Coelho, M. S. Z. S., Salvo, D., Madureira, J., Paunescu, A. C., Holobaca, I. H., Acquaotta, F., Hashizume, M., Honda, Y., Garca, S. D., Kim, H., Tobias, A., ... Gasparrini, A. (2021), "The burden of heat-related mortality attributable to recent human-induced climate change". Nature Climate Change, 11(6), 492–500. https://doi.org/10.1038/s41558-021-01058-x

Wkipedia: Cyclon Aila, https://en.wikipedia.org/wiki/Cyclone_Aila (read 16.09.2025)

Wood, A. W., Maurer, E. P., Kumar, A. & Lettenmaier, D. P. Long-range experimental hydrologic forecasting for the eastern United States. J. of Geophysical Research-Atmospheres 107 (2002).

Wood, A. W., Leung, L. R., Sridhar, V. & Lettenmaier, D. P. Hydrologic implications of dynamical and statistical approaches to downscaling climate model outputs. Climatic Change 62, 189–216 (2004).

Zhao, X., Li, Y., Wang, S., & Chen, J. (2024), "Explainable El Niño predictability from climate mode interactions". Journal of Climate Dynamics, 62(4), 1234–1250. https://doi.org/10.1007/s00382-023-06543-2

Zorita, E. & von Storch, H., (1999), "The analog method as a simple statistical downscaling technique: comparison with more complicated methods." Journal of Climate 12(8), 2474-2489.

# Appendix 1: Methods and data

## CMIP6-NEX-GDDP downscaled climate model data

The analysis in this report was based on the NASA Earth Exchange Global Daily Downscaled Projections (NEX-GDDP-CMIP6) (Thrasher et al., 2022). The ensemble consists of 35 model simulations (Table A1) from the Coupled Model Intercomparison Project Phase 6 (CMIP6) (Eyring et al., 2016), which were downscaled to a higher spatial resolution using a daily version of the monthly bias correction/spatial disaggregation (BCSD) method (Wood et al., 2002; 2004). The downscaling procedure interpolated the GCM data to a common 0.25 x 0.25 degree spatial resolution grid and bias-corrected the data to more closely resemble observational data, while retaining extreme events. For temperature, monthly large-scale trends were extracted prior to downscaling and subsequently added back.

| GCM | ripf | grid | Tasmax | Tasmin | Tas | Pr |
|---|---|---|---|---|---|---|
| **ACCESS-CM2** | r1i1p1f1 | gn | all | all | all | all |
| **ACCESS-ESM1-5** | r1i1p1f1 | gn | all | all | all | all |
| **BCC-CSM2-MR** | r1i1p1f1 | gn | all | all | all | all |
| **CanESM5** | r1i1p1f1 | gn | all | all | all | all |
| CESM2 | r4i1p1f1 | gn | none | none | all | all |
| CESM2-WACCM | r3i1p1f1 | gn | none | none | some | some |
| CMCC-CM2-SR5 | r1i1p1f1 | gn | some | some | all | all |
| **CMCC-ESM2** | r1i1p1f1 | gn | all | all | all | all |
| **CNRM-CM6-1** | r1i1p1f2 | gr | all | all | all | all |
| **CNRM-ESM2-1** | r1i1p1f2 | gr | all | all | all | all |
| **EC-Earth3** | r1i1p1f1 | gr | all | all | all | all |
| **EC-Earth3-Veg-LR** | r1i1p1f1 | gr | all | all | all | all |
| FGOALS-g3 | r3i1p1f1 | gn | all | all | all | all |
| GFDL-CM4 | r1i1p1f1 | gr1 | some | some | some | some |
| GFDL-CM4 | r1i1p1f1 | gr2 | some | some | some | some |
| **GFDL-ESM4** | r1i1p1f1 | gr1 | all | all | all | all |
| **GISS-E2-1-G** | r1i1p1f2 | gn | all | all | all | all |
| HadGEM3-GC31-LL | r1i1p1f3 | gn | some | some | some | some |
| HadGEM3-GC31-MM | r1i1p1f3 | gn | some | some | some | some |
| IITM-ESM | r1i1p1f1 | gn | none | none | all | all |
| **INM-CM4-8** | r1i1p1f1 | gr1 | all | all | all | all |
| **INM-CM5-0** | r1i1p1f1 | gr1 | all | all | all | all |
| **IPSL-CM6A-LR** | r1i1p1f1 | gr | all | all | all | all |
| KACE-1-0-G | r1i1p1f1 | gr | all | all | all | all |
| KIOST-ESM | r1i1p1f1 | gr1 | some | some | some | some |
| **MIROC-ES2L** | r1i1p1f2 | gn | all | all | all | all |
| **MIROC6** | r1i1p1f1 | gn | all | all | all | all |
| **MPI-ESM1-2-HR** | r1i1p1f1 | gn | all | all | all | all |
| **MPI-ESM1-2-LR** | r1i1p1f1 | gn | all | all | all | all |
| **MRI-ESM2-0** | r1i1p1f1 | gn | all | all | all | all |
| NESM3 | r1i1p1f1 | gn | some | some | some | some |
| **NorESM2-LM** | r1i1p1f1 | gn | all | all | all | all |
| **NorESM2-MM** | r1i1p1f1 | gn | all | all | all | all |
| **TaiESM1** | r1i1p1f1 | gn | all | all | all | all |
| **UKESM1-0-LL** | r1i1p1f2 | gn | all | all | all | all |

*Table A1.1 The availability of climate models of the NEX-GDDP-CMIP6 ensemble for different climatological variables (Tasmax, Tasmin, and Tas are the daily maximum, minimum, and mean air temperature, Pr is the daily precipitation sum). For each model and variable, the table shows if data are available for all, some or none of the emission scenarios (historical, SSP1-2.6, SSP2-4.5, SSP3-7.0, and SSP5-8.5). Background colors show the same information (green = all, yellow = some, red = none). The table includes model name (GCM), variant id (ripf = realization, initialization, physics and forcing), and spatial grid (gn means output on the model's native grid; gr, gr1 and gr2 indicates that the output has been regridded) of each model simulation. Three models that were found to have a deviating seasonal cycle of precipitation or temperature compared to observations are marked with red font. The 23 models that were used in the climate analyses presented in the report are marked with bold font.*

## Validation of the NEX-GDDP-CMIP6 data

To ensure that the NEX-GDDP-CMIP6 data set provides credible projections of anthropogenic climate change for South Asia and Bangladesh, we validated the downscaled climate data against observations for the historical period. Out of the 35 models in the CMIP6-NEX-GDDP ensemble, we used 23 in our analyses (marked in bold font in Table A1.1). Three were excluded due to discrepancies between the observed and modeled seasonal cycles of precipitation or temperature, and another ten because they did not provide data for all relevant emission scenarios and climate variables. The details of the validation are described below.

## Reference data

As a reference for precipitation, we used the ENACTS-BMD data set (Acharya et al., 2020) which provides gridded observational data for Bangladesh on a 0.05 x 0.05 degree spatial resolution for the period 1981–2021. The data set is produced by combining satellite imagery and station observations. A comparison of the mean ENACTS-BMD precipitation to station-based observations from Bangladesh showed a strong agreement between the two data sets.

For the temperature, we used ERA5 (Hersbach et al., 2020) as a reference. ERA5 is a global reanalysis product that provides comprehensive data for the atmosphere, land, and ocean based on assimilation of a range of observational sources (e.g. station observations, satellite records, radar-gauge composites). The ERA5 data have a spatial resolution of 0.25 x 0.25 degrees and are available back to 1950.

For the validation of NEX-GDDP-CMIP6, we focused on the period 1981–2014. The reference period was chosen because the ENACTS-BMD data set starts in 1981, and the historical period of the CMIP6 models extends to 2014, after which the emission scenarios start.

## Validation method

As opposed to weather prediction models, climate models are not expected to reproduce or predict the weather conditions day-by-day or year-by-year. Each model simulation represents one of many possible developments. Direct comparison of historical observations and model data for the same time steps is therefore not a relevant measure of model quality. Instead, statistical properties (e.g., spatial patterns, seasonal cycles, or inter-annual variability) of model output and observations for a historical reference period can be compared to each other.

We evaluated the climate models using a method developed by Benestad et al. (2023), in which a common Empirical Orthogonal Analysis (common EOF) is applied to model data and observations concurrently. The common EOF procedure identifies a set of spatial patterns that are present in both the model and observational data sets. It also outputs a set of eigenvalues that represent the relative importance of each pattern and Principal Components (PCs) that describe their variation in time (the mean seasonal cycle) associated with each spatial pattern and for each data set. The first mode explains most of the variance of the data, and each following mode carries less weight and is typically related to smaller scale variability. To use the common EOF method for validation, the PCs associated with the observations are compared to the PCs of the models.

## Results of the validation

The first leading common EOF mode of the precipitation seasonal cycle explains almost 97% of the variance of the combined data set ENACTS-BMD and NEX-GDDP-CMIP6 (Figure A1.1, upper right panel). The spatial pattern EOF1 (Figure A1.1, upper left panel) is characterized by high precipitation in the northeast and southeast, and lower precipitation in the west, which is in line with the average precipitation pattern in Bangladesh in the monsoon season. The first Principal Component (PC1) associated with the observations shows a clear seasonal cycle, with the highest values in the monsoon season, most notably in June and July, and lowest precipitation in winter (Figure A1.1, lower panel). The models show a similar PC1 seasonal cycle, but with slightly higher values in the later months of the monsoon season (August and September). One model, KACE-1-0-G, diverges notably from the observations and other models in several months.

The second precipitation mode explains only 2% of the variance (Figure A1.2, upper right panel). The spatial pattern, EOF2 (Figure A1.2, upper left panel), has a maximum in the south-east of Bangladesh. The PC2 seasonal cycle displays a minimum in the pre-monsoon season (May) and a maximum in the monsoon season (July or August), associated with both the observations and models (Figure A1.2, lower panel). This common EOF mode can be seen as an adjustment of the spatial precipitation pattern, which is different in May compared to July and August, especially in the southeast. There is a slight difference in timing between the observations and models, but there is overall good agreement. Again, KACE-1-0-G stands out as different compared to observations and other models.

Looking at the three leading common EOF modes, KACE-1-0-G is consistently an outlier (Figure A1.3). In the third EOF mode (not shown), NorESM2-LM also has a diverging seasonal cycle, with a strangely high value in November, but since this mode explains only 0.6% of the variance, this is assumed not to be as serious. On the basis of the common EOF analysis of precipitation, KACE-1-0-G is excluded from the NEX-GDDP-CMIP6 ensemble used in this report.

For temperature, the first leading common EOF mode, which explains 98% of the variance (Figure A1.4, upper right panel), has a spatial pattern characterized by a northwest to southeast gradient (Figure A1.4, upper left panel). The principal component shows a seasonal cycle with negative values in the winter season and positive values from April to September (Figure A1.4, lower panel). The second mode explains only 1.6% of the total variance (Figure A1.5, upper right panel). EOF2 looks like a northeast to southwest dipole (Figure A1.5, upper left panel) and PC2 describes a seasonal cycle with two peaks, in April and November (Figure A1.5, lower panel). For both of these common EOF modes, as well as the third, the PCs associated with ERA5 and the PCs connected to the NEX-GDDP-CMIP6 models are very similar (Figure A1.6). Two models, FGOALS-g3 and CMCC-CM2-SR5, show stronger discrepancies compared to ERA5 than the rest of the NEX-GDDP-CMIP6 ensemble. These models are also excluded from further analysis.

## Influence of ensemble selection on the climate change signal

In addition to the three models identified as outliers in the validation described above, another 9 models were excluded from analyses due to missing data for some variables and scenarios (Table A1). The advantage of having a consistent ensemble is that it ensures that the estimated difference between two time periods or scenarios is due to changes in the projected climate, and not related to changes in model composition. However, there is a risk that reducing the ensemble size also results in a failure to represent natural climate variability and the range of possible outcomes of climate change. Selecting a small subsample of models may also skew the climate change signal, giving a stronger or weaker ensemble mean warming depending on the models selected (Mezghani et al., 2019). To evaluate the impact of ensemble selection, we compare the full NEX-GDDP-CMIP6 ensemble to the subset used for analyses.

The mean temperature and precipitation in Bangladesh changes very little in both the historical period (1985–2014) and in the end future (2071–2100) as a result of the ensemble selection (Figure A1.7). Comparing the full NEX-GDDP-CMIP6 ensemble of 35 models to the reduced ensemble of 23 models used in analyses, there was a small difference in the ensemble mean value in all seasons, for both precipitation and temperature. The ensemble maximum of the temperature in the historical period was reduced when excluding the models that were excluded after the validation, but otherwise, the results were not strongly affected. The ensemble mean was not skewed in any direction and the ensemble quantiles still covered most of the range. This suggests that the subset of models used in this report represents the range of possible changes of the climate sufficiently well.

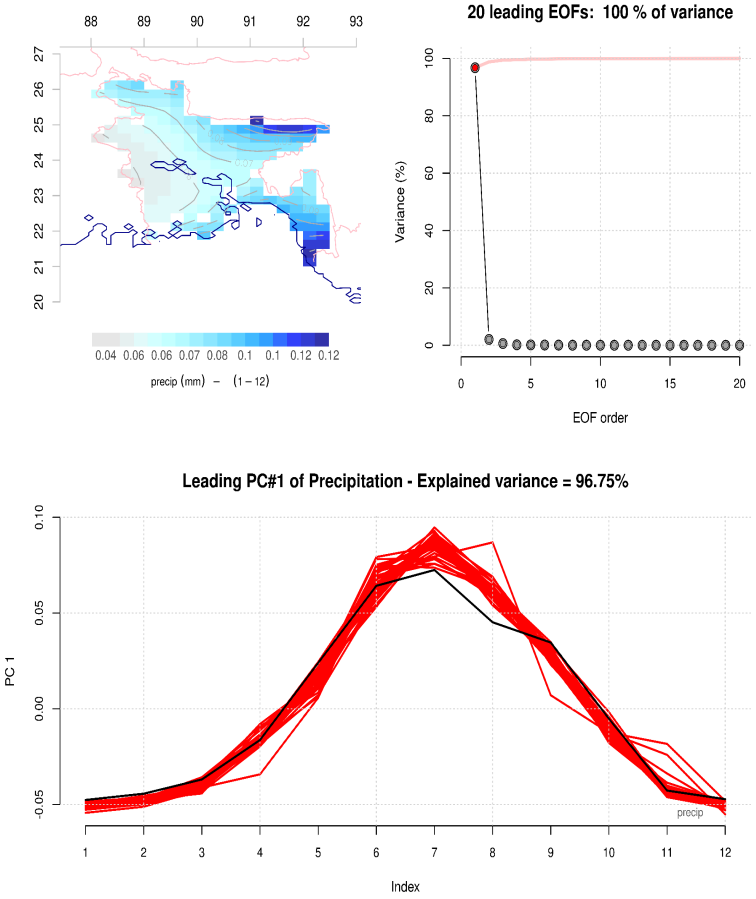


*Figure A1.1 Key results from the common EOF analysis of the seasonal mean precipitation cycle of the NEX-GDDP-CMIP6 ensemble (climate model data) and ENACTS-BMD (gridded observations) in the period 1981–2014. The figure shows a map of the spatial pattern associated with the first leading EOF mode (EOF1, top left panel), a plot displaying the total variance explained by each mode (top right panel), and the first Principal Component (PC1, bottom panel) which describes the seasonal cycle connected to EOF1 for the observations (black line) and the NEX-GDDP-CMIP6 models (red lines). The first mode explains almost 97% of the variance of the seasonal mean precipitation cycle.*

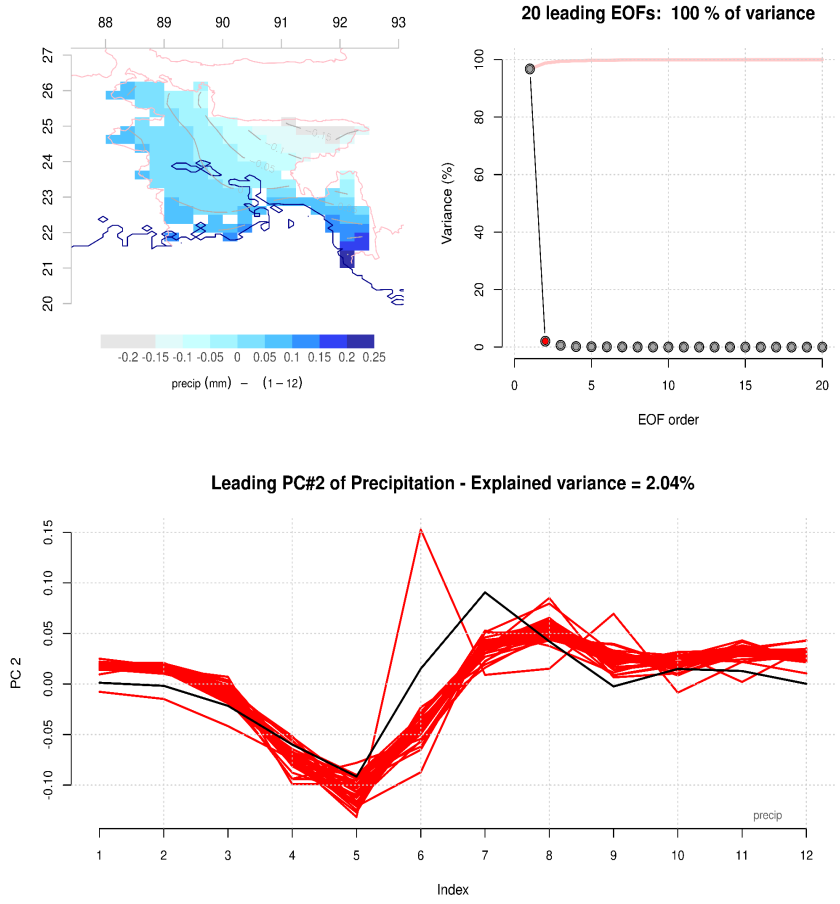


*Figure A1.2 Key results from the common EOF analysis of the seasonal mean precipitation cycle of the NEX-GDDP-CMIP6 ensemble (climate model data) and ENACTS-BMD (gridded observations) in the period 1981–2014. The figure shows results for the second leading EOF mode (EOF2). Details as in Figure A1.1.*

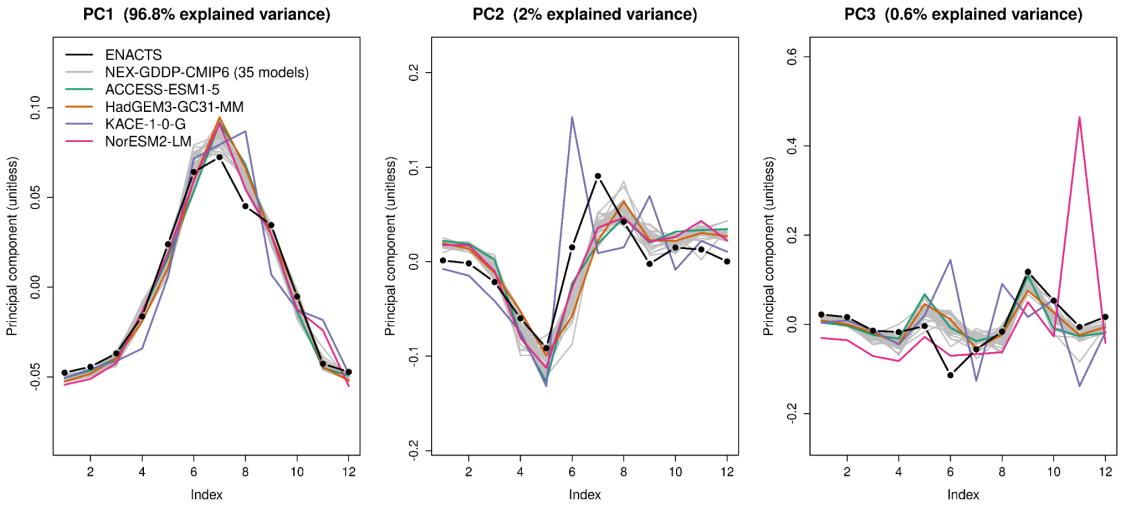


*Figure A1.3 The first three principal components (PCs) obtained from common EOF analysis of the seasonal mean precipitation cycle in the period 1981–2014 (more details in Figure A1.1). The black line in each panel shows the PC associated with the assimilated gridded observations (ENACTS-BMD), grey lines represent the PCs of the NEX-GDDP-CMIP6 climate model ensemble, and the colored lines highlight the models that have the largest deviation from the observational PCs.*

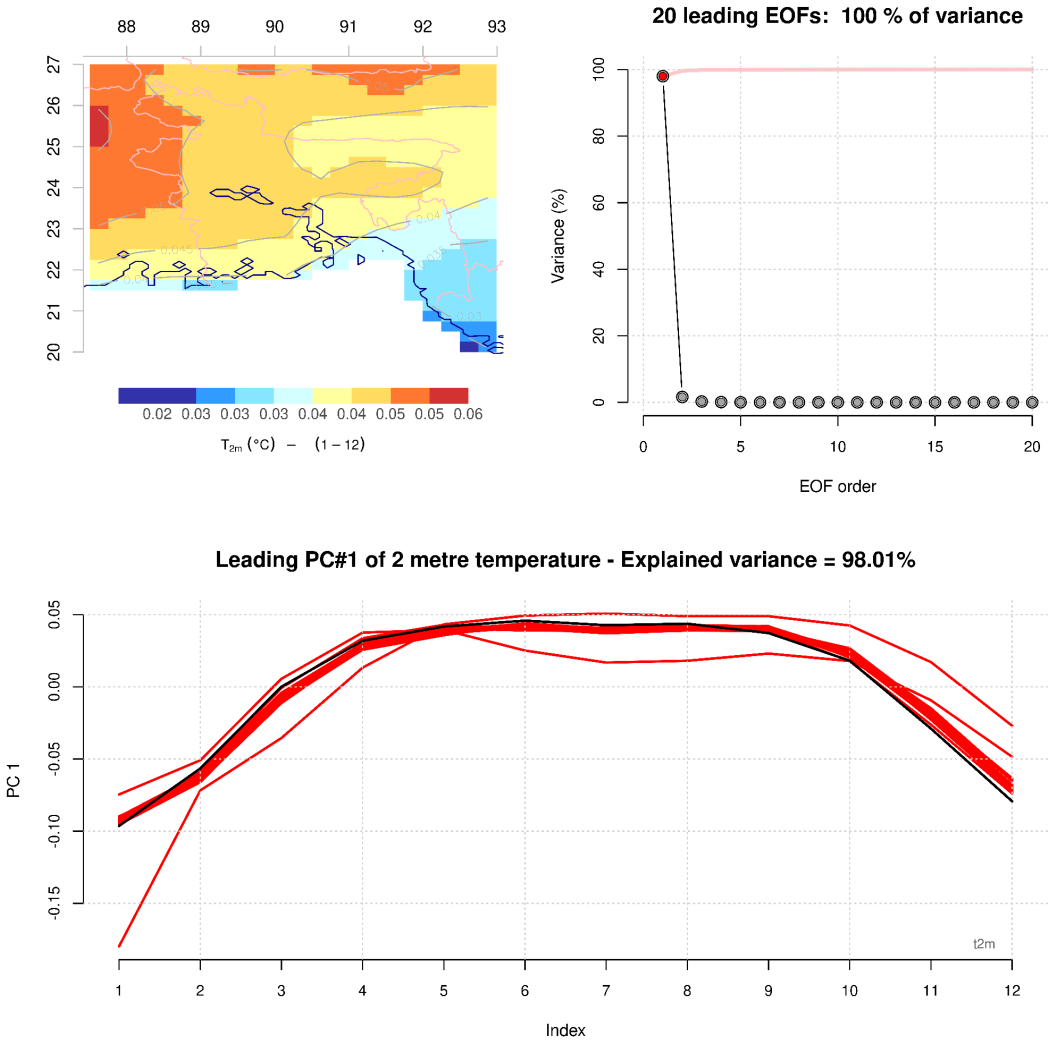


*Figure A1.4 Key results from the common EOF analysis of the seasonal mean temperature cycle of the NEX-GDDP-CMIP6 ensemble (climate model data) and the ERA5 reanalysis data set (assimilated observations) in the period 1981–2014. The figure shows results for the first leading mode of variability, which explains 98% of the variance of the collected temperature data. Details as in Figure A1.1.*

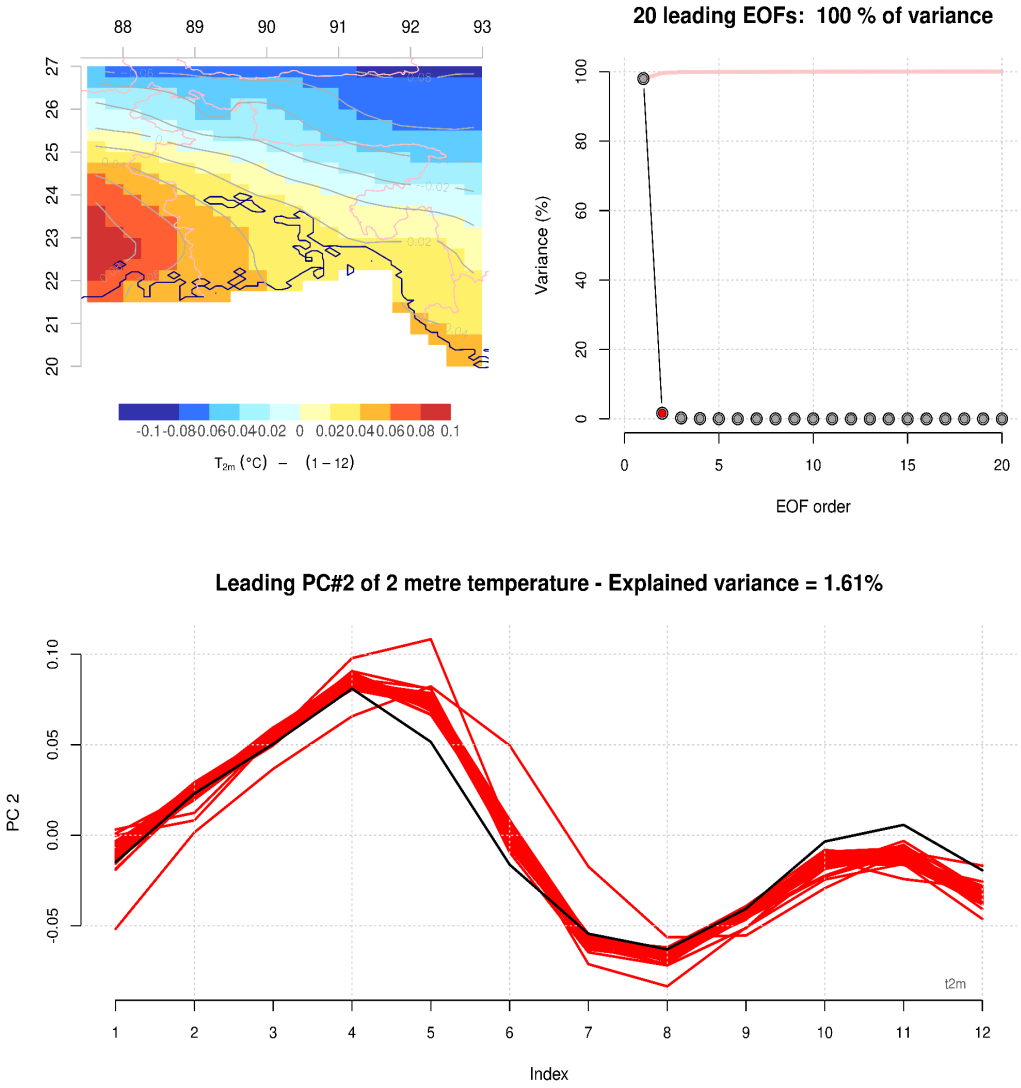


*Figure A1.5 Key results from the common EOF analysis of the seasonal mean temperature cycle of the NEX-GDDP-CMIP6 ensemble (climate model data) and the ERA5 reanalysis data set (assimilated observations) in the period 1981–2014. The figure shows results for the second leading mode of variability, which explains 1.6% of the variance of the collected temperature data. Details as in Figure A1.1.*

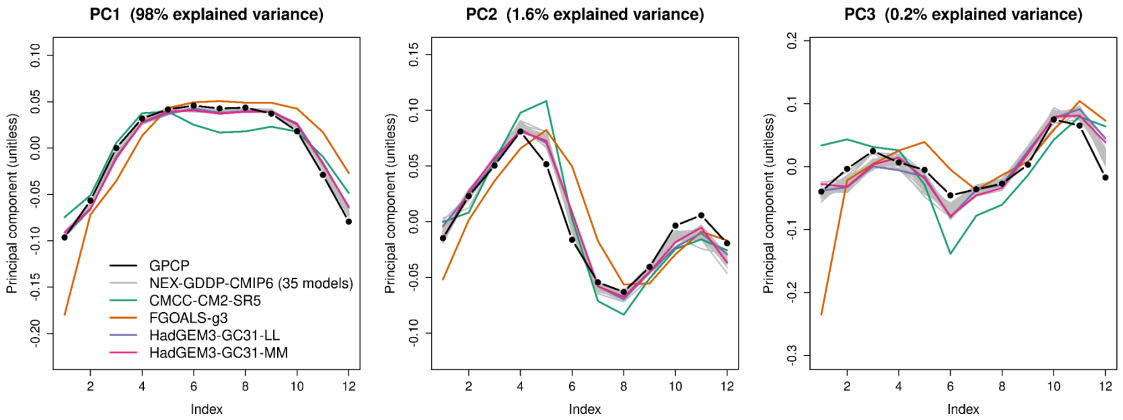


*Figure A1.6 The first three principal components (PCs) obtained from common EOF analysis of the seasonal mean temperature cycle. The black line in each panel shows the PC associated with the assimilated observations (ERA5 reanalysis), grey lines represent the PCs of the NEX-GDDP-CMIP6 climate model ensemble, and the colored lines highlight the models that have the largest deviation from the observational PCs.*

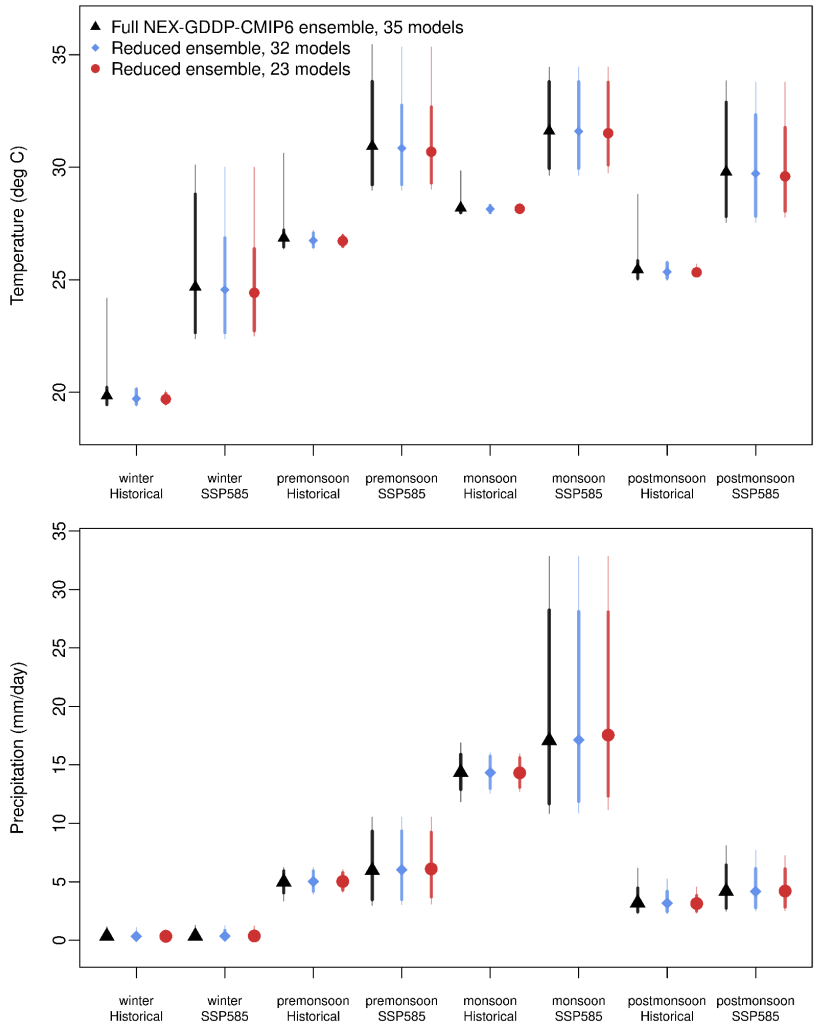


*Figure A1.7 Influence of model selection on a) mean temperature and b) precipitation in Bangladesh. Symbols show the ensemble mean, thick lines the 5th to 95th percentiles, and thin lines the ensemble minimum and maximum. Black markers represent the full NEX-GDDP-CMIP6 ensemble, blue shows results without KACE-1-0-G, CMCC-CM2-SR5, and FGOALS-g3, and red represents an ensemble which also excludes models that have unavailable data for some scenarios and variables. Results are displayed for all seasons, for the historical period (1985–2014) and future (2071–2100) under emission scenario SSP5-8.5.*

## Seasonal cycle of Bangladesh: NEX-GDDP-CMIP6 vs surface based observations

Surface based measurements of precipitation and temperature have been carried out at stations in Bangladesh for a long time. Data since 1948 is available at BMD, with an increase in the number of observational stations since 1970. Operation of the measurement stations as well as gathering, distribution, and quality control of the data is managed by the Bangladesh Meteorological Department (BMD). Recent tests of homogeneity have shown that the data are of consistently good quality from around 1981 (Rashid et al., 2024).

Comparing the seasonal cycle of the NEX-GDDP-CMIP6 ensemble in the historical reference period 1985–2014 (presented in Chapter 4, Figures 4.2–4.5) with corresponding maps based on surface-based observations (Figures A1.8–A1.11) shows that the model data have the same spatio-temporal variations as the observed climatology. The seasonal mean precipitation and

temperature based on observations and models closely resemble each other, both in terms of the average values for the whole country and the spatial distribution. The NEX-GDDP-CMIP6 data set is bias-corrected and has been tuned to local observations, so any other results would be surprising. Nevertheless, it is an important result as it confirms that the NEX-GDDP-CMIP6 provides a realistic picture of the present-day climate.

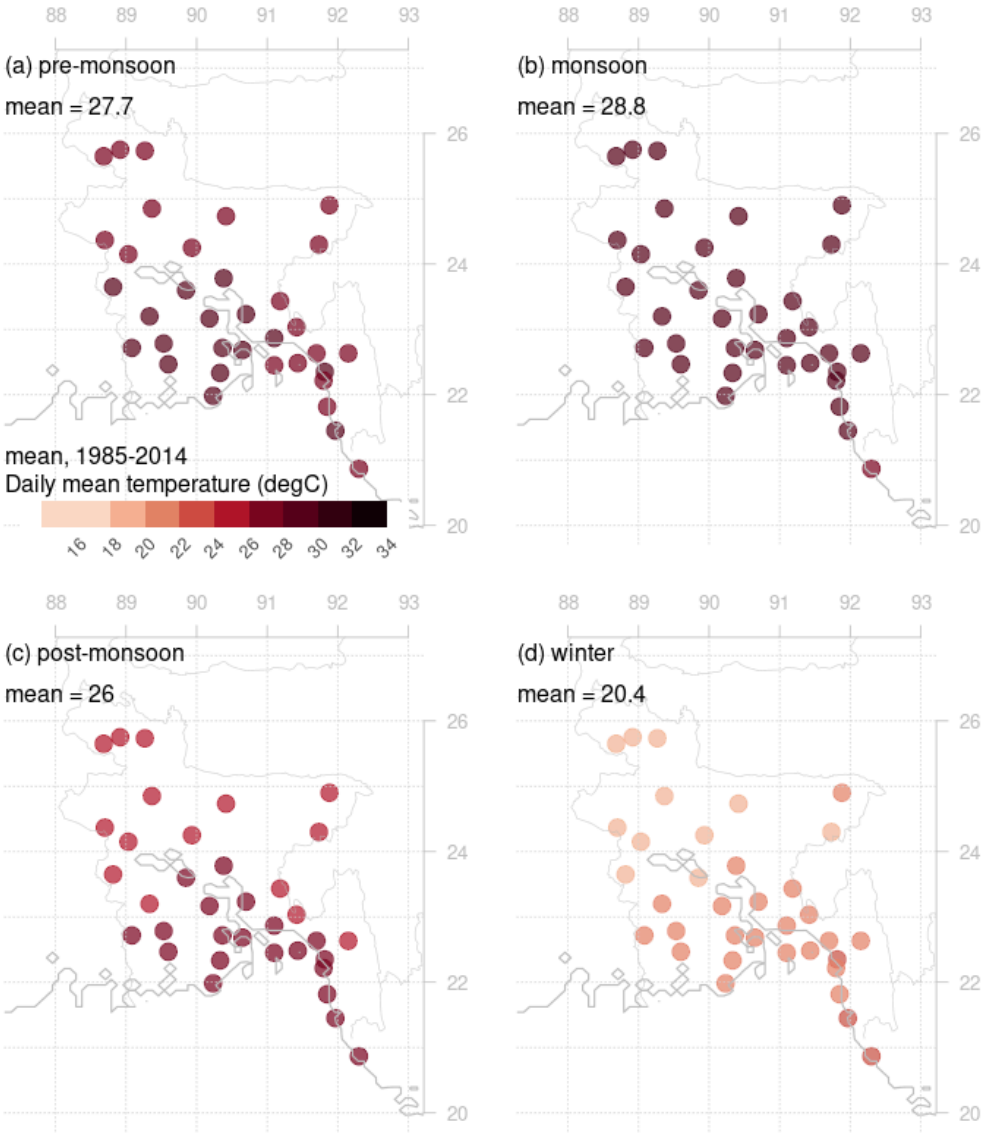


*Figure A1.8 Seasonal average values of the daily mean temperature from surface based observations in Bangladesh for the period 1985–2014 in the a) pre-monsoon (April–May), b) monsoon (June–September), c) post-monsoon (October and November), and d) winter (December–February) seasons. The mean value of each map shows the country average.*

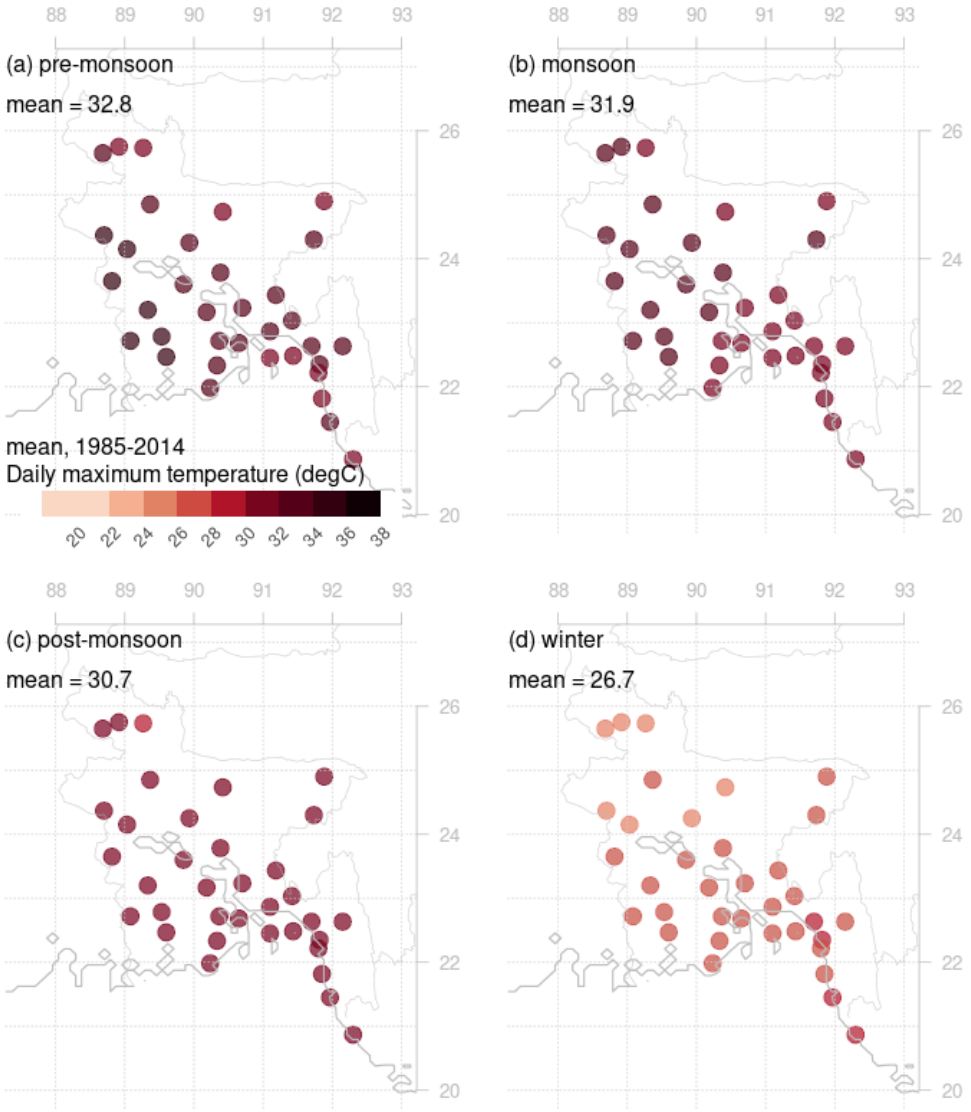


*Figure A1.9 Seasonal average values of the daily maximum temperature from surface based observations in Bangladesh for the period 1985–2014 in the a) pre-monsoon (April–May), b) monsoon (June–September), c) post-monsoon (October and November), and d) winter (December–February) seasons. The mean value of each map shows the country average.*

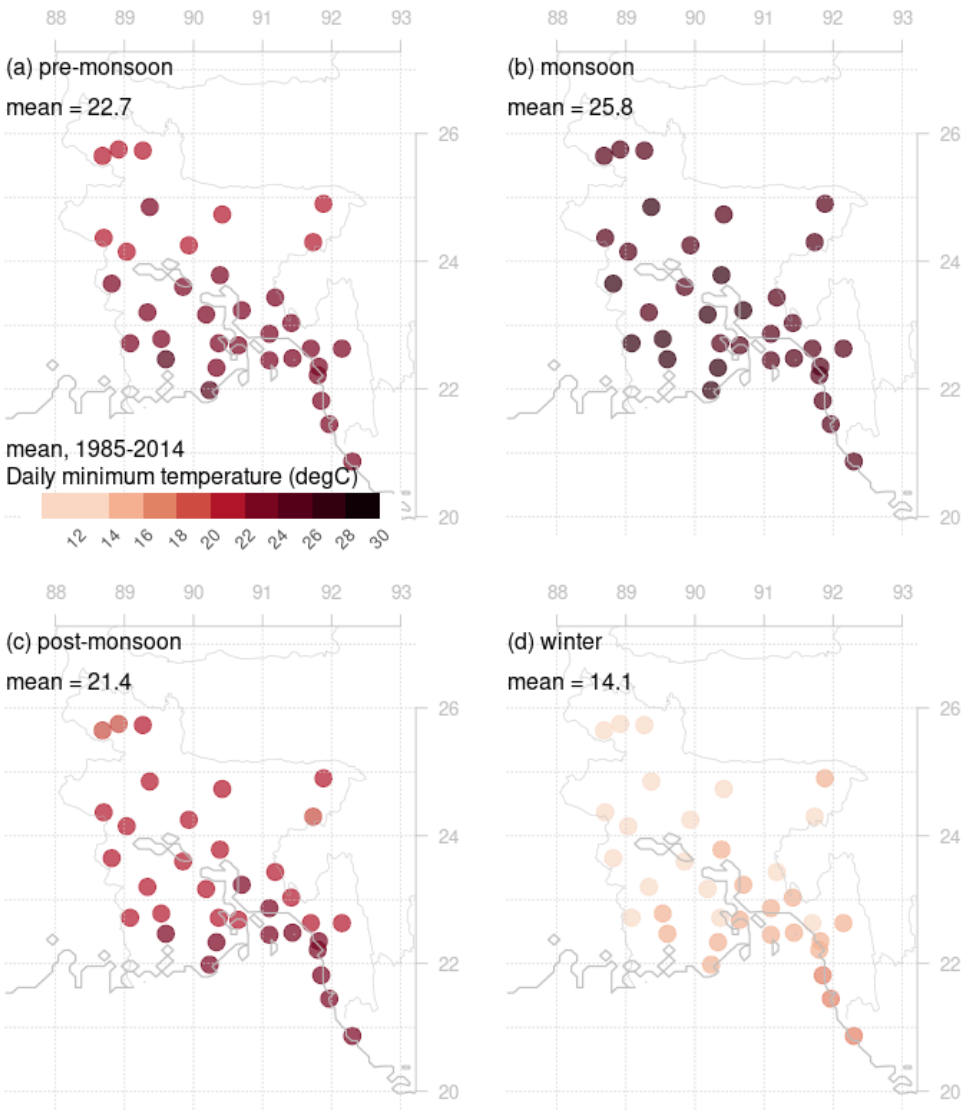


*Figure A1.10 Seasonal average values of the daily minimum temperature from surface based observations in Bangladesh for the period 1985–2014 in the a) pre-monsoon (April–May), b) monsoon (June–September), c) post-monsoon (October and November), and d) winter (December–February) season. The mean value of each map shows the country average.*

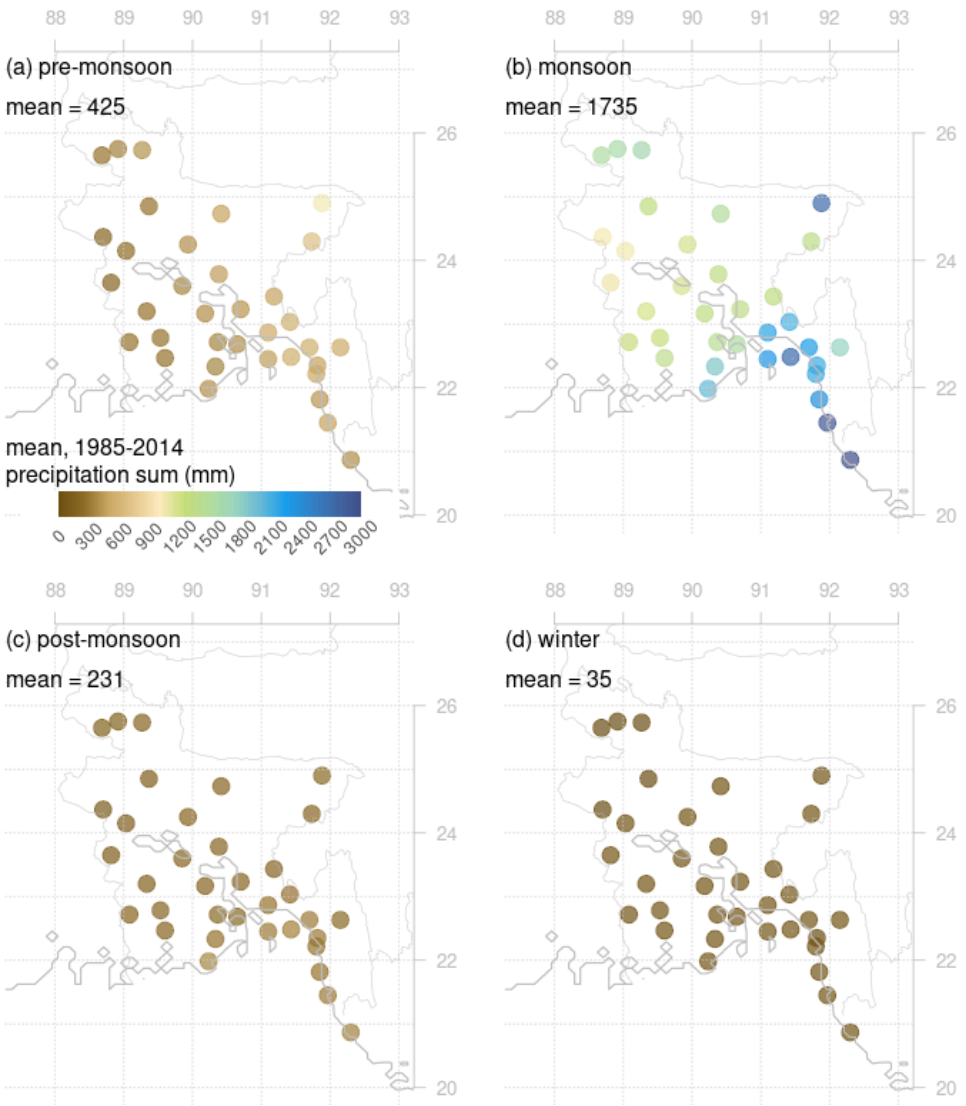


*Figure A1.11 Seasonal average values of the precipitation sum from surface based observations in Bangladesh for the period 1985–2014 in the a) pre-monsoon (April–May), b) monsoon (June–September), c) post-monsoon (October and November), and d) winter (December–February) season. The mean value of each map shows the country average.*

# Appendix 2: Future climate projections for all emission scenarios

Appendix 2 presents future climate projections based on emission scenarios SSP1-2.6, SSP2-4.5, and SSP5-8.5, which are discussed and referenced but not displayed in Chapters 5 and 6 of this report. Figures A2.1–A2.43 show changes in various climate variables from the reference period (1985–2014) to the mid-century (2041–2070) or end of the century (2071–2100), based on the ensemble mean of the NEX-GDDP-CMIP6 projections.

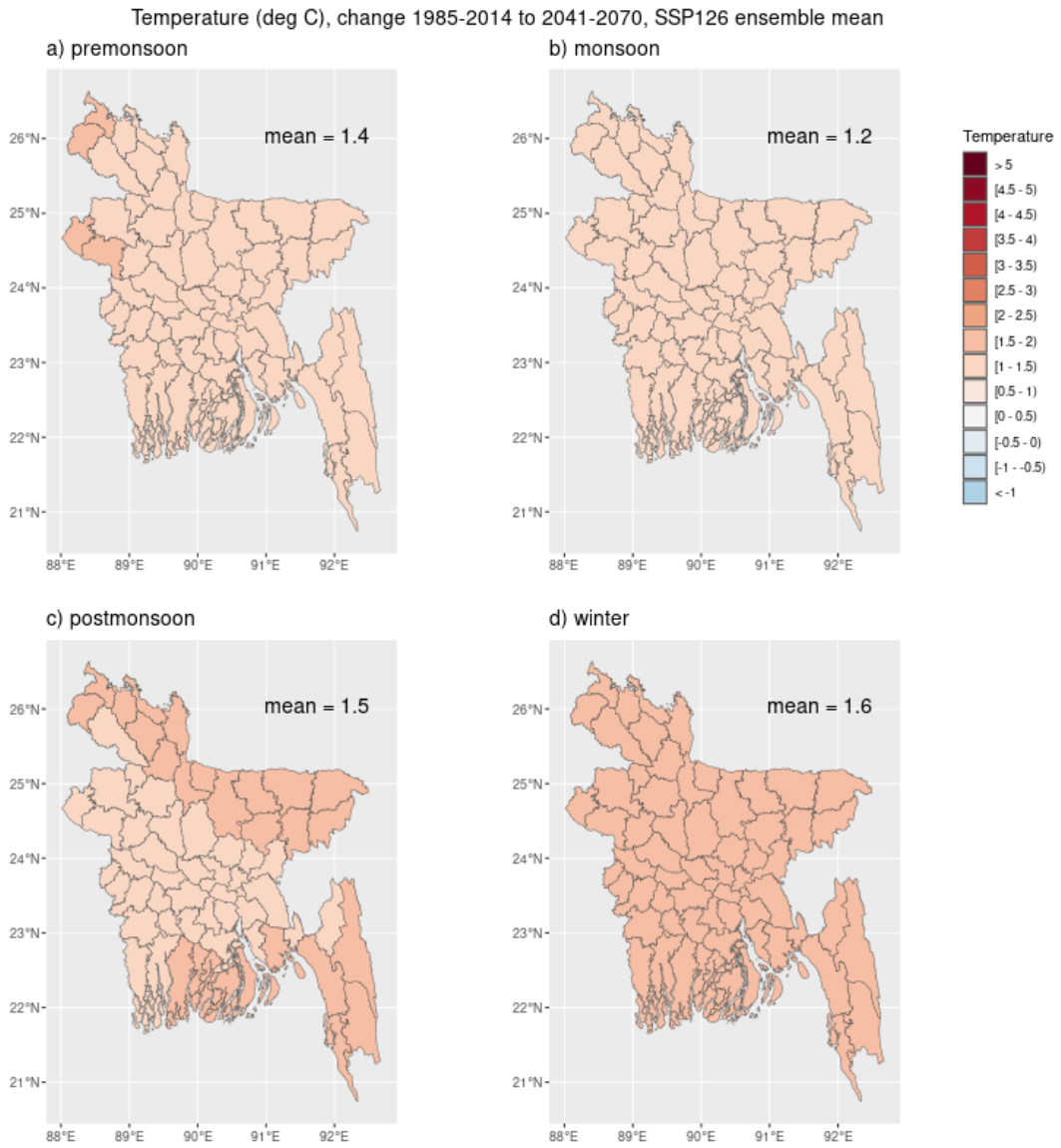


*Figure A2.1 Changes in the daily mean temperature from the reference period (1985–2014) to the mid-century (2041–2070) under emission scenario SSP1-2.6, as estimated by the NEX-GDDP-CMIP6 ensemble mean for the a) pre-monsoon, b) monsoon, c) post-monsoon, and d) winter seasons.The mean value of each map shows the country average.*

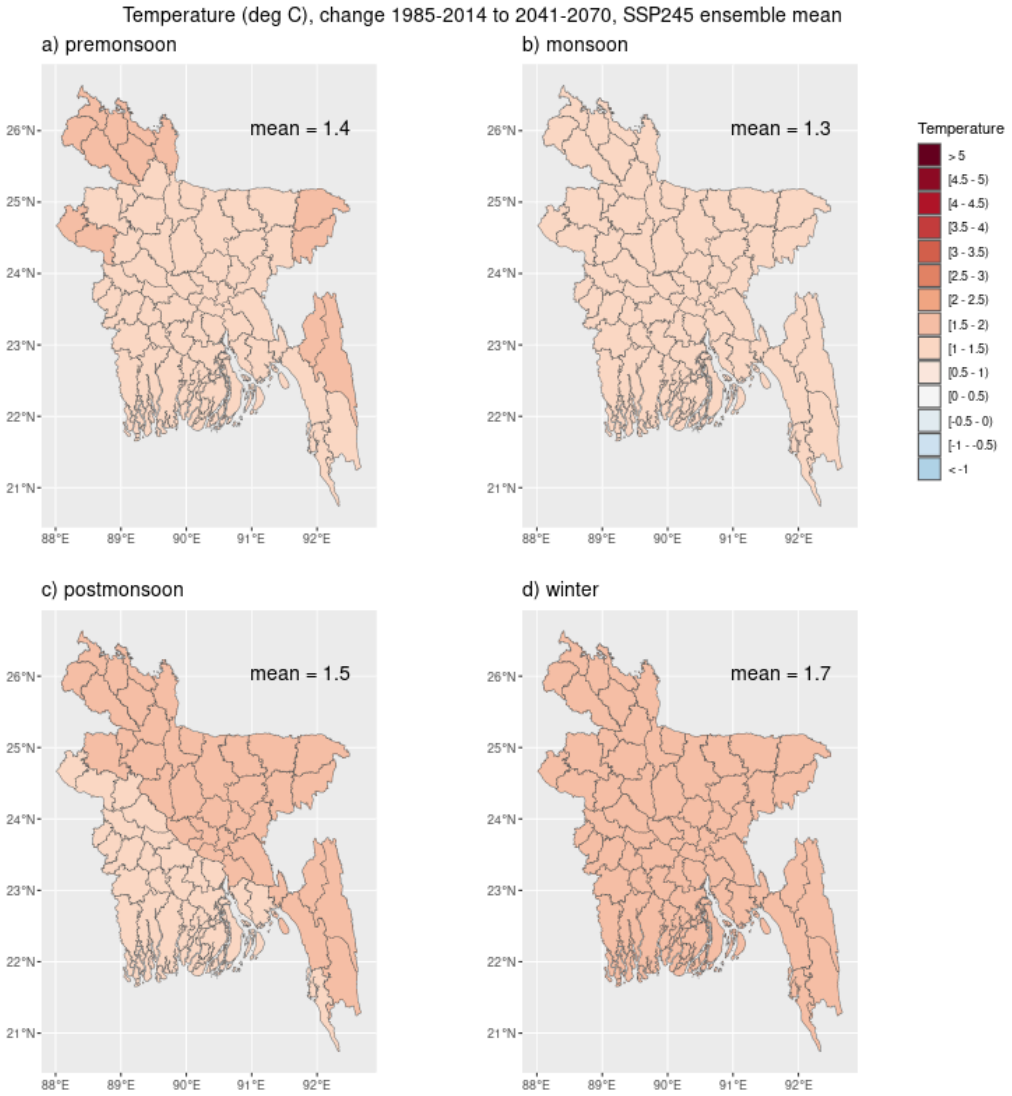


*Figure A2.2 Changes in the daily mean temperature from the reference period (1985–2014) to the mid-century (2041–2070) under emission scenario SSP2-4.5, as estimated by the NEX-GDDP-CMIP6 ensemble mean for the a) pre-monsoon, b) monsoon, c) post-monsoon, and d) winter seasons.The mean value of each map shows the country average.*

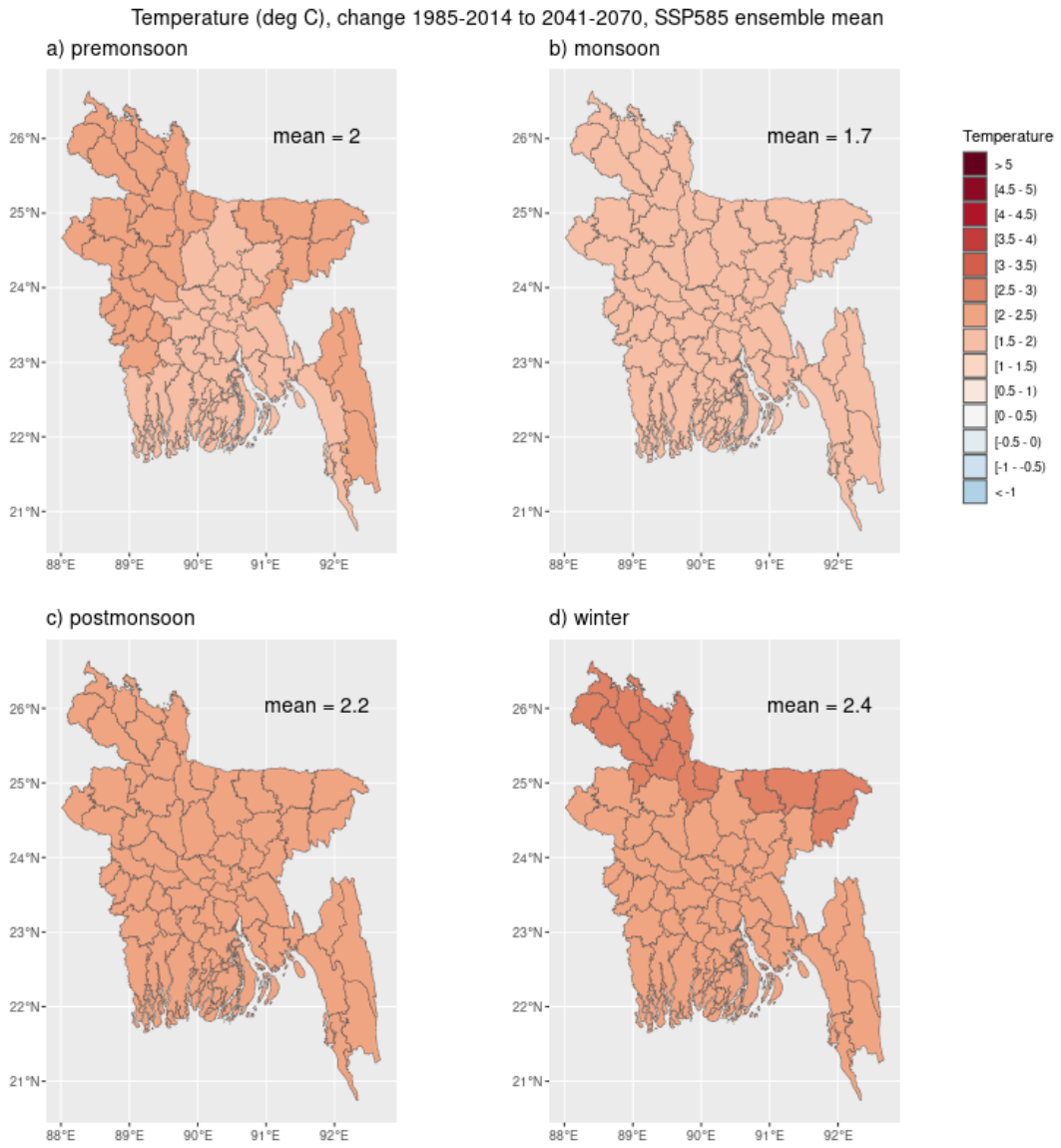


*Figure A2.3 Changes in the daily mean temperature from the reference period (1985–2014) to the mid-century (2041–2070) under emission scenario SSP5-8.5, as estimated by the NEX-GDDP-CMIP6 ensemble mean for the a) pre-monsoon, b) monsoon, c) post-monsoon, and d) winter seasons.The mean value of each map shows the country average.*

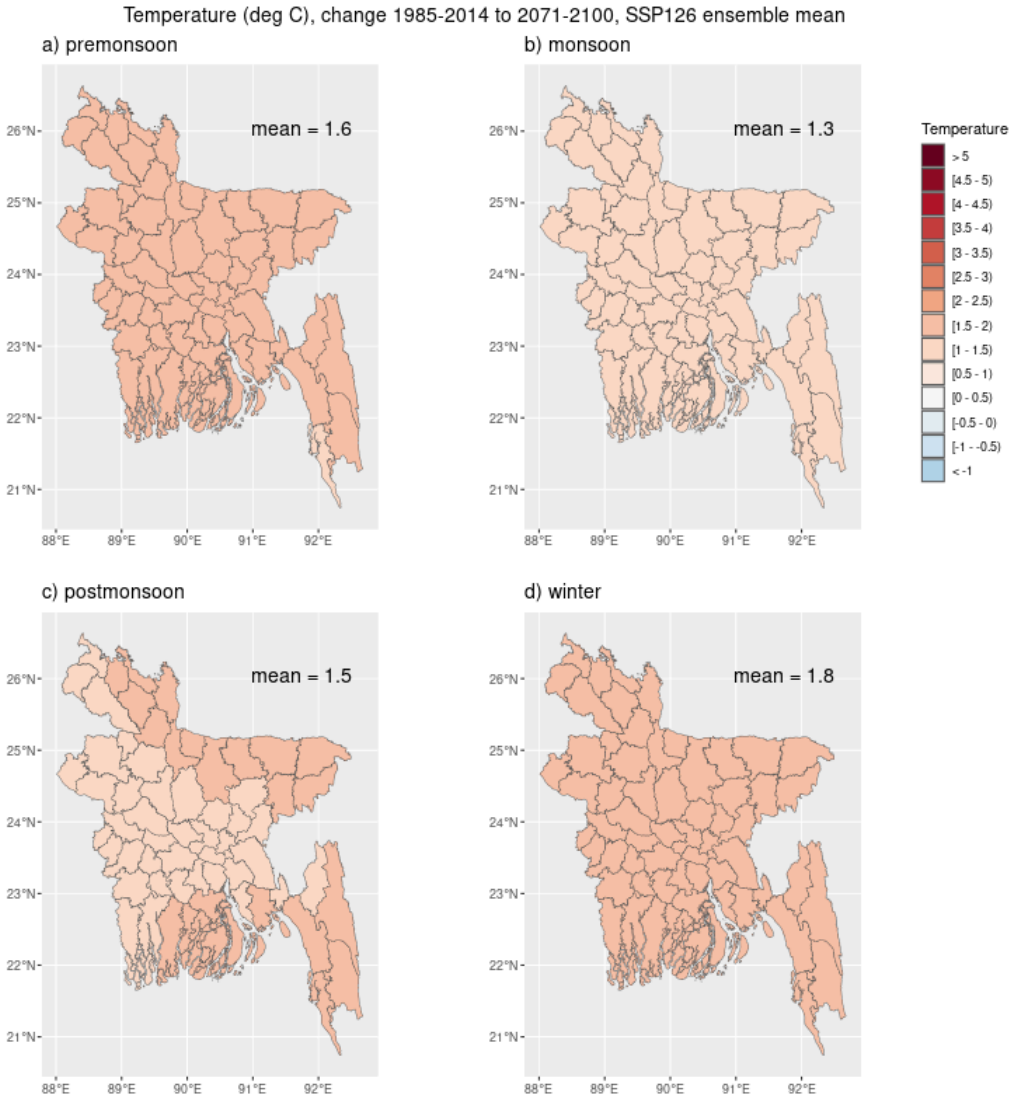


*Figure A2.4 Changes in the daily mean temperature from the reference period (1985–2014) to the end of the century (2071–2100) under emission scenario SSP1-2.6, as estimated by the NEX-GDDP-CMIP6 ensemble mean for the a) pre-monsoon, b) monsoon, c) post-monsoon, and d) winter seasons.The mean value of each map shows the country average.*

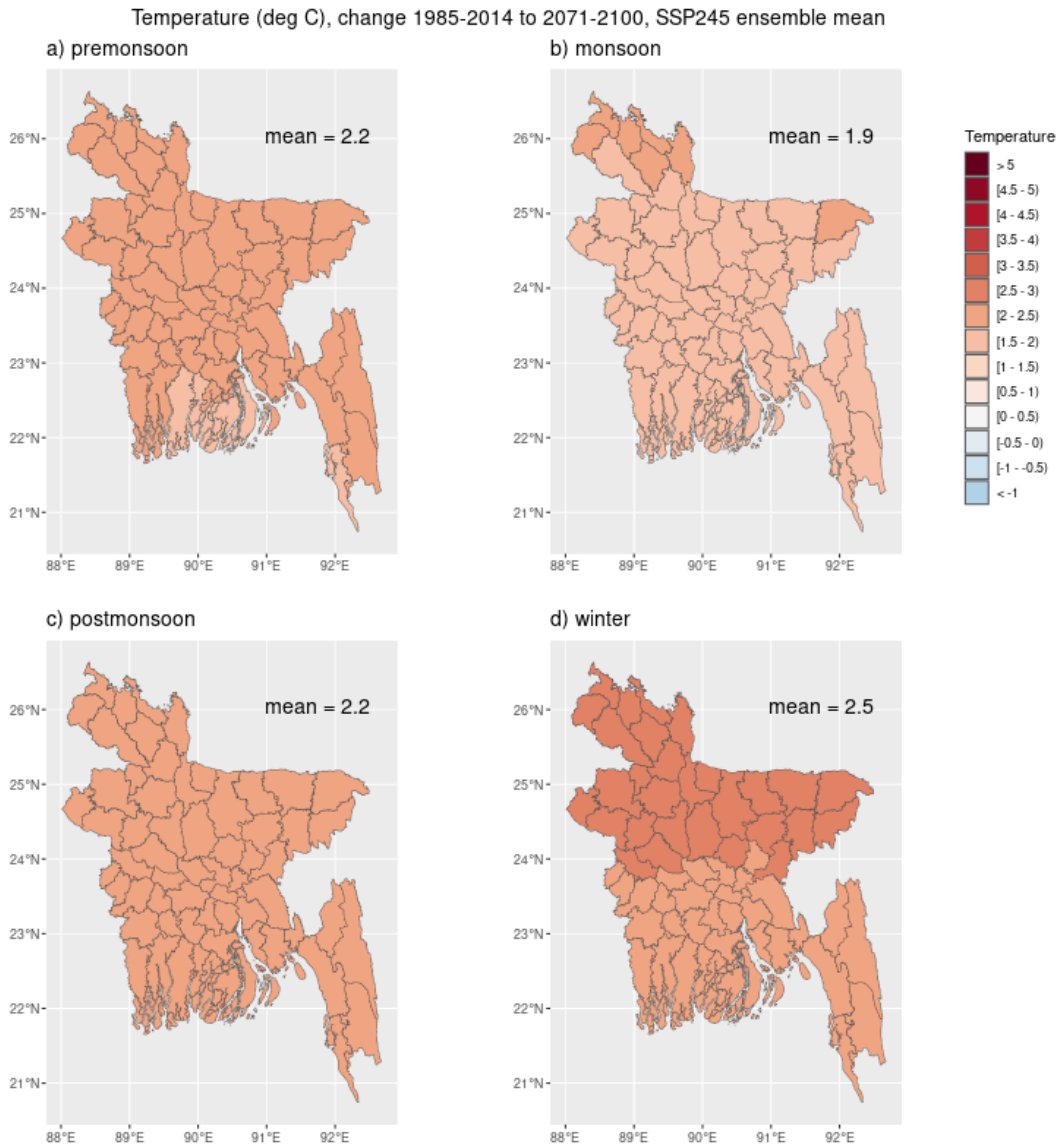


*Figure A2.5 Changes in the daily mean temperature from the reference period (1985–2014) to the end of the century (2071–2100) under emission scenario SSP2-4.5, as estimated by the NEX-GDDP-CMIP6 ensemble mean for the a) pre-monsoon, b) monsoon, c) post-monsoon, and d) winter seasons.The mean value of each map shows the country average.*

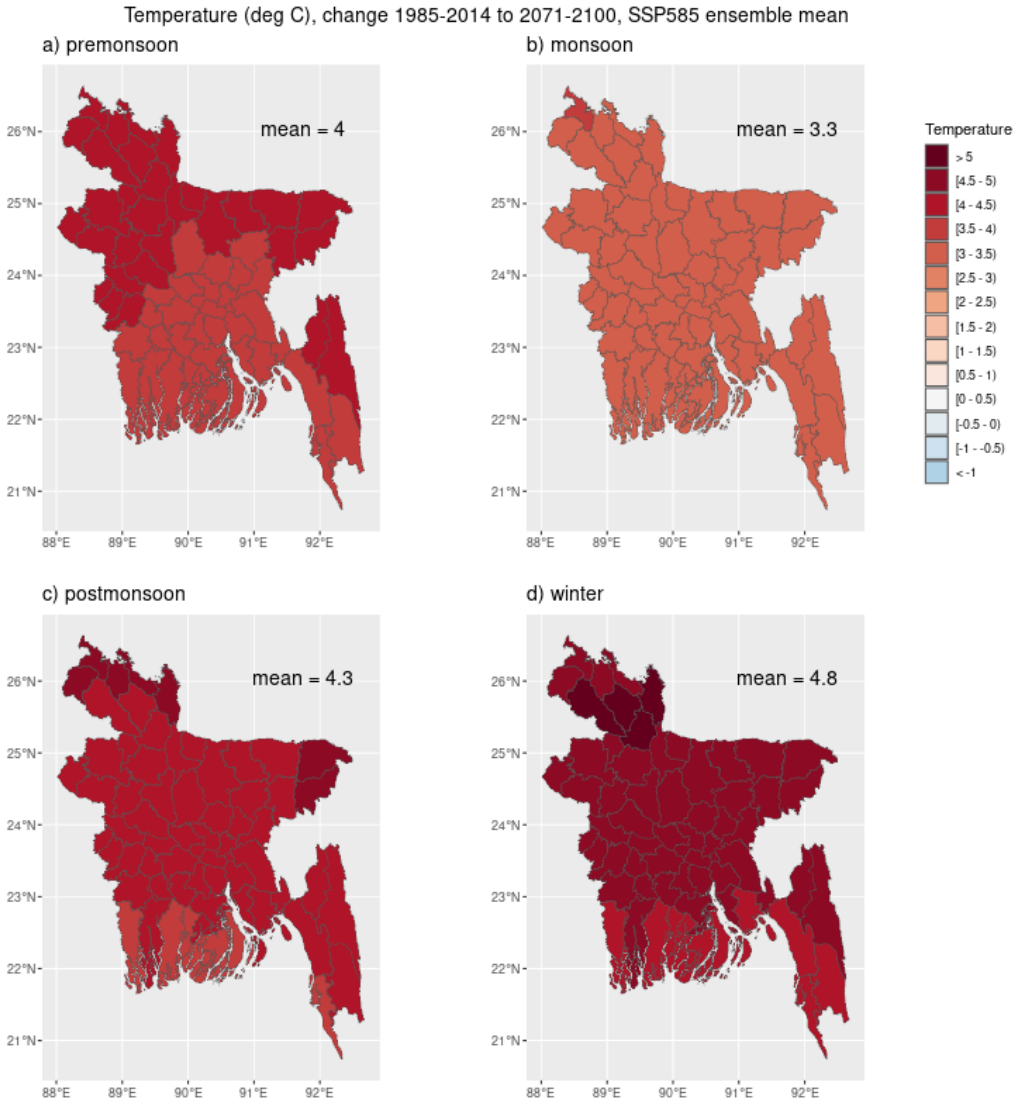


*Figure A2.6 Changes in the daily mean temperature from the reference period (1985–2014) to the end of the century (2071–2100) under emission scenario SSP5-8.5, as estimated by the NEX-GDDP-CMIP6 ensemble mean for the a) pre-monsoon, b) monsoon, c) post-monsoon, and d) winter seasons.The mean value of each map shows the country average.*

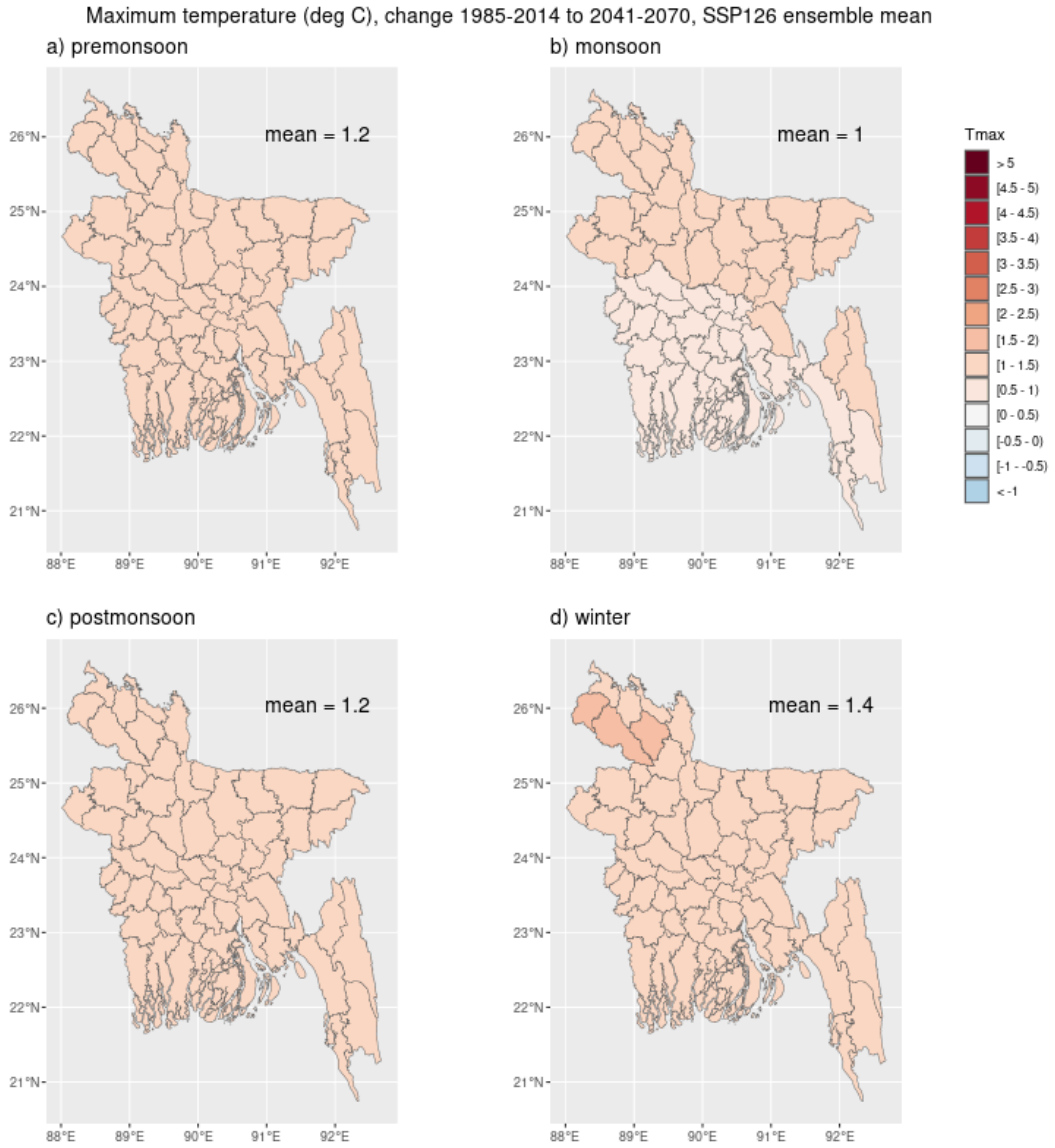


*Figure A2.7 Changes in the daily maximum temperature from the reference period (1985–2014) to the mid-century (2041–2070) under emission scenario SSP1-2.6, as estimated by the NEX-GDDP-CMIP6 ensemble mean for the a) pre-monsoon, b) monsoon, c) post-monsoon, and d) winter seasons.The mean value of each map shows the country average.*

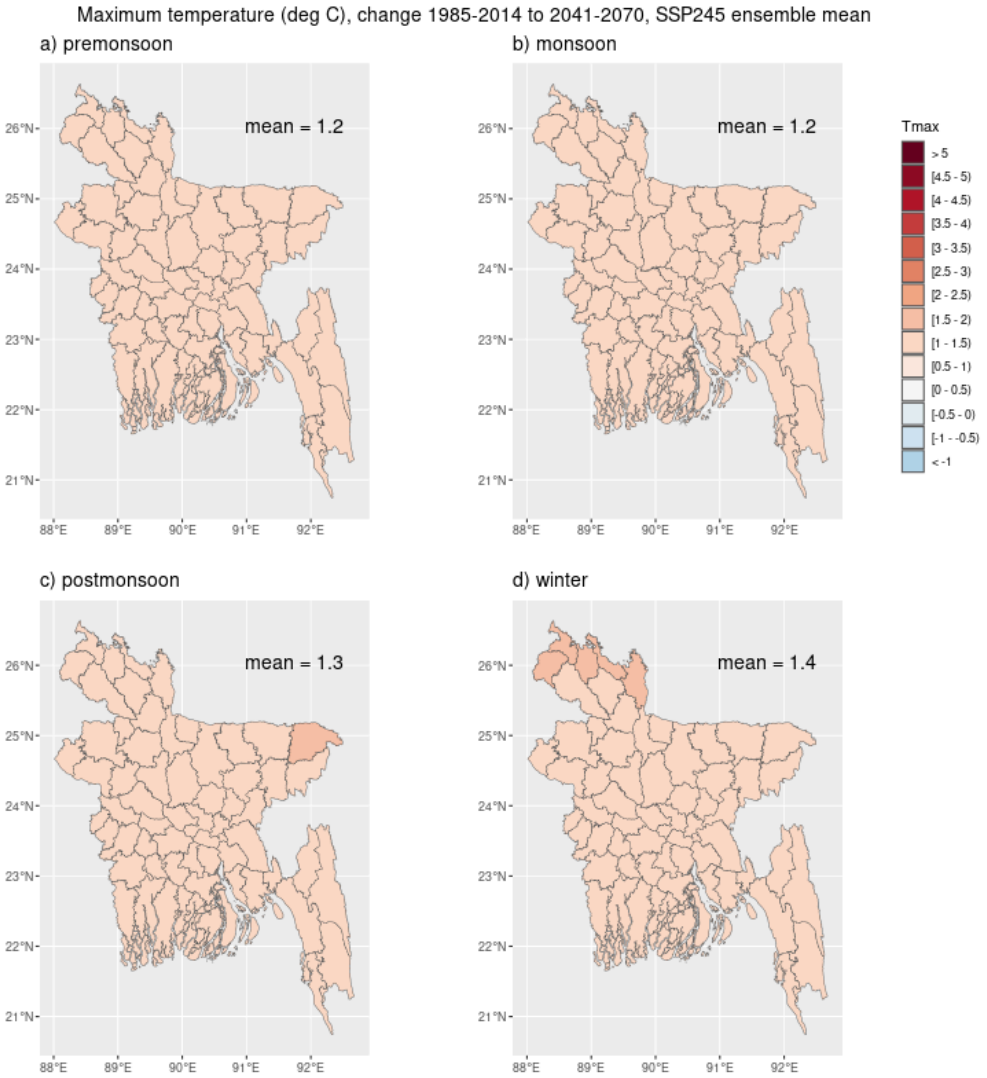


*Figure A2.8 Changes in the daily maximum temperature from the reference period (1985–2014) to the mid-century (2041–2070) under emission scenario SSP2-4.5, as estimated by the NEX-GDDP-CMIP6 ensemble mean for the a) pre-monsoon, b) monsoon, c) post-monsoon, and d) winter seasons.The mean value of each map shows the country average.*

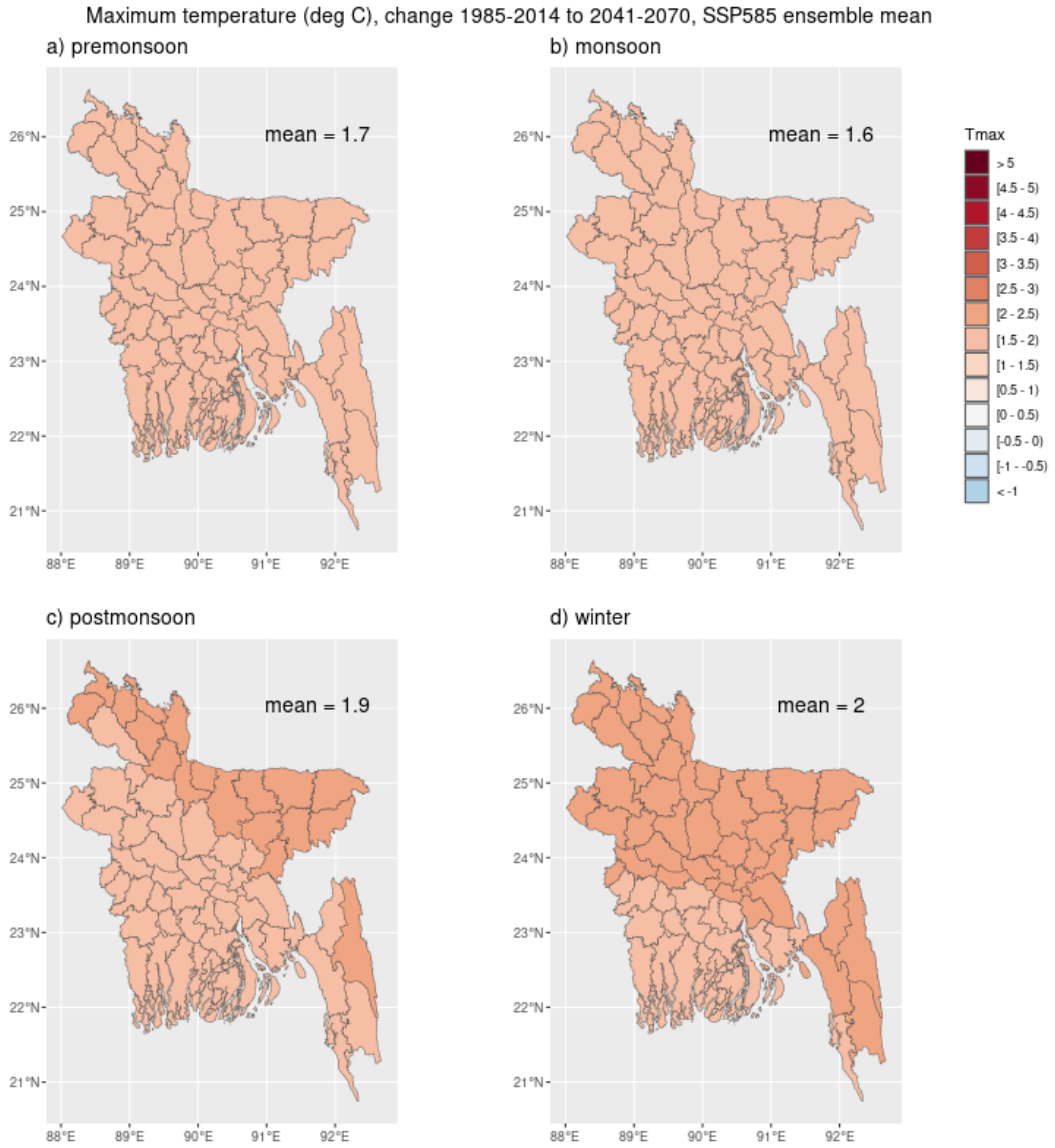


*Figure A2.9 Changes in the daily maximum temperature from the reference period (1985–2014) to the mid-century (2041–2070) under emission scenario SSP5-8.5, as estimated by the NEX-GDDP-CMIP6 ensemble mean for the a) pre-monsoon, b) monsoon, c) post-monsoon, and d) winter seasons.The mean value of each map shows the country average.*

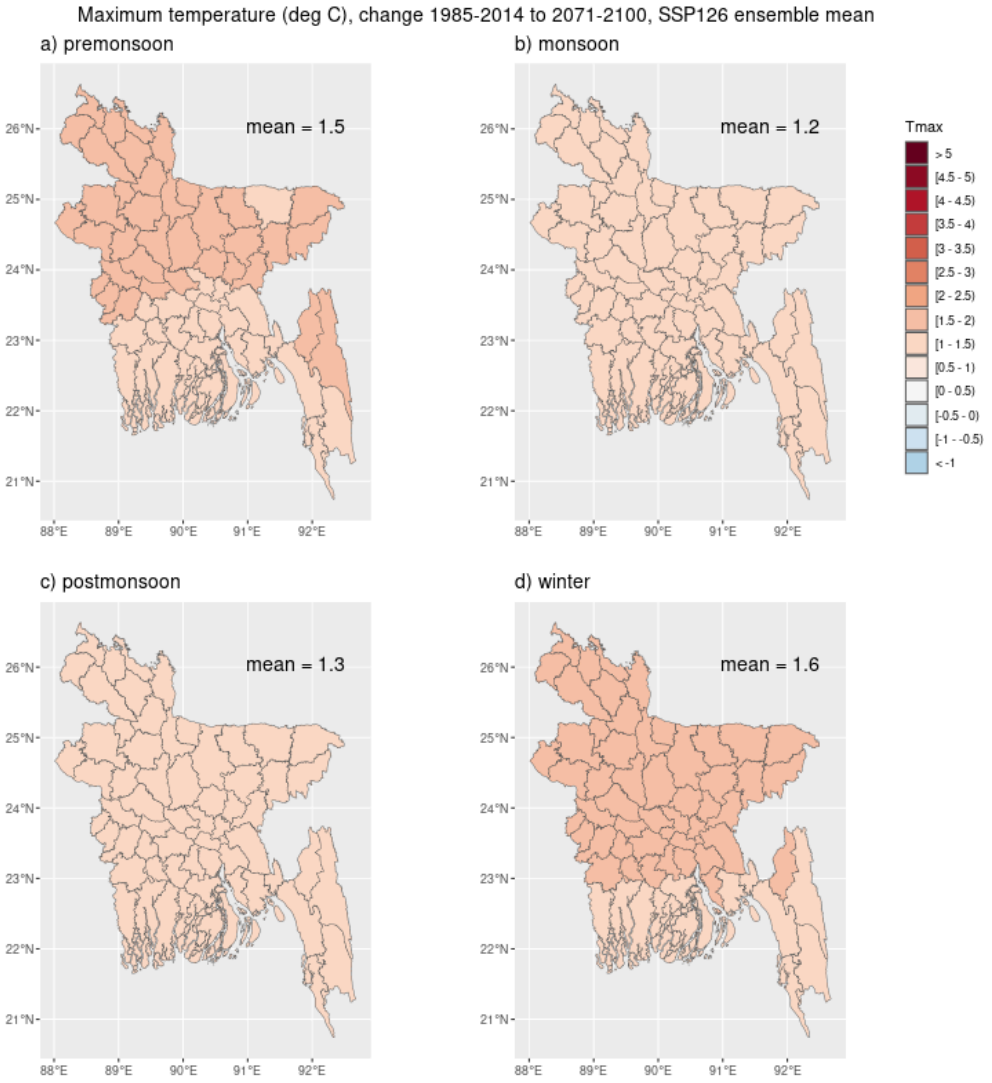


*Figure A2.10 Changes in the daily maximum temperature from the reference period (1985–2014) to the end of the century (2071–2100) under emission scenario SSP1-2.6, as estimated by the NEX-GDDP-CMIP6 ensemble mean for the a) pre-monsoon, b) monsoon, c) post-monsoon, and d) winter seasons.The mean value of each map shows the country average.*

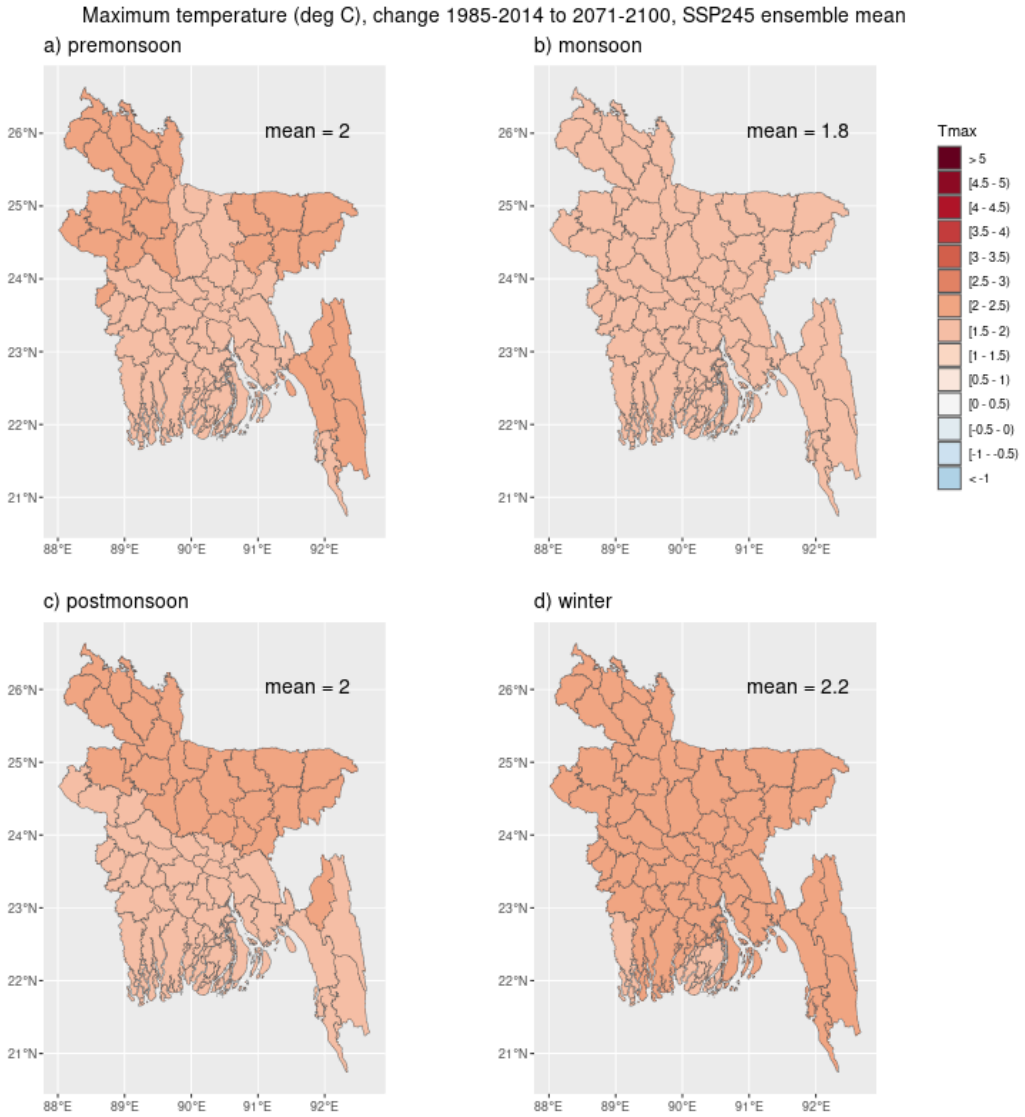


*Figure A2.11 Changes in the daily maximum temperature from the reference period (1985–2014) to the end of the century (2071–2100) under emission scenario SSP2-4.5, as estimated by the NEX-GDDP-CMIP6 ensemble mean for the a) pre-monsoon, b) monsoon, c) post-monsoon, and d) winter seasons.The mean value of each map shows the country average.*

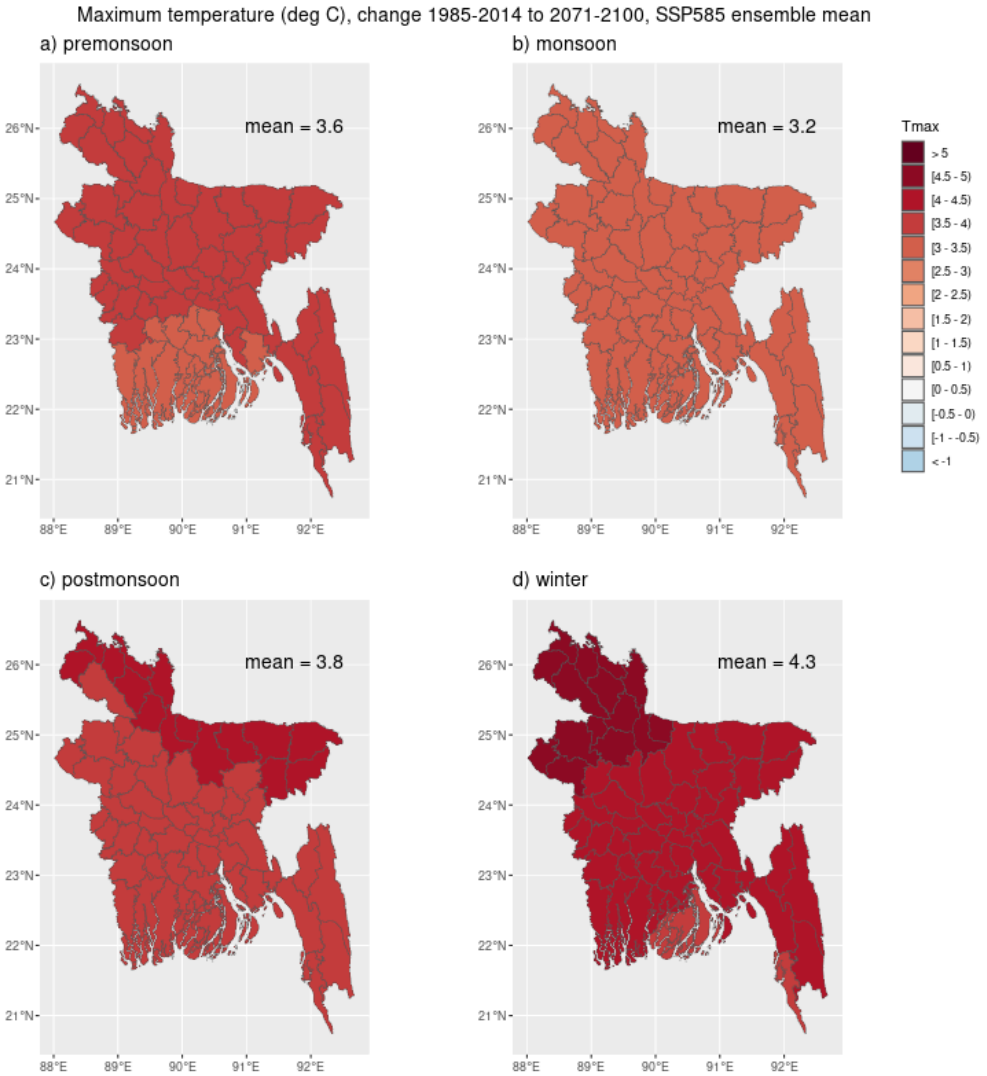


*Figure A2.12 Changes in the daily maximum temperature from the reference period (1985–2014) to the end of the century (2071–2100) under emission scenario SSP5-8.5, as estimated by the NEX-GDDP-CMIP6 ensemble mean for the a) pre-monsoon, b) monsoon, c) post-monsoon, and d) winter seasons.The mean value of each map shows the country average.*

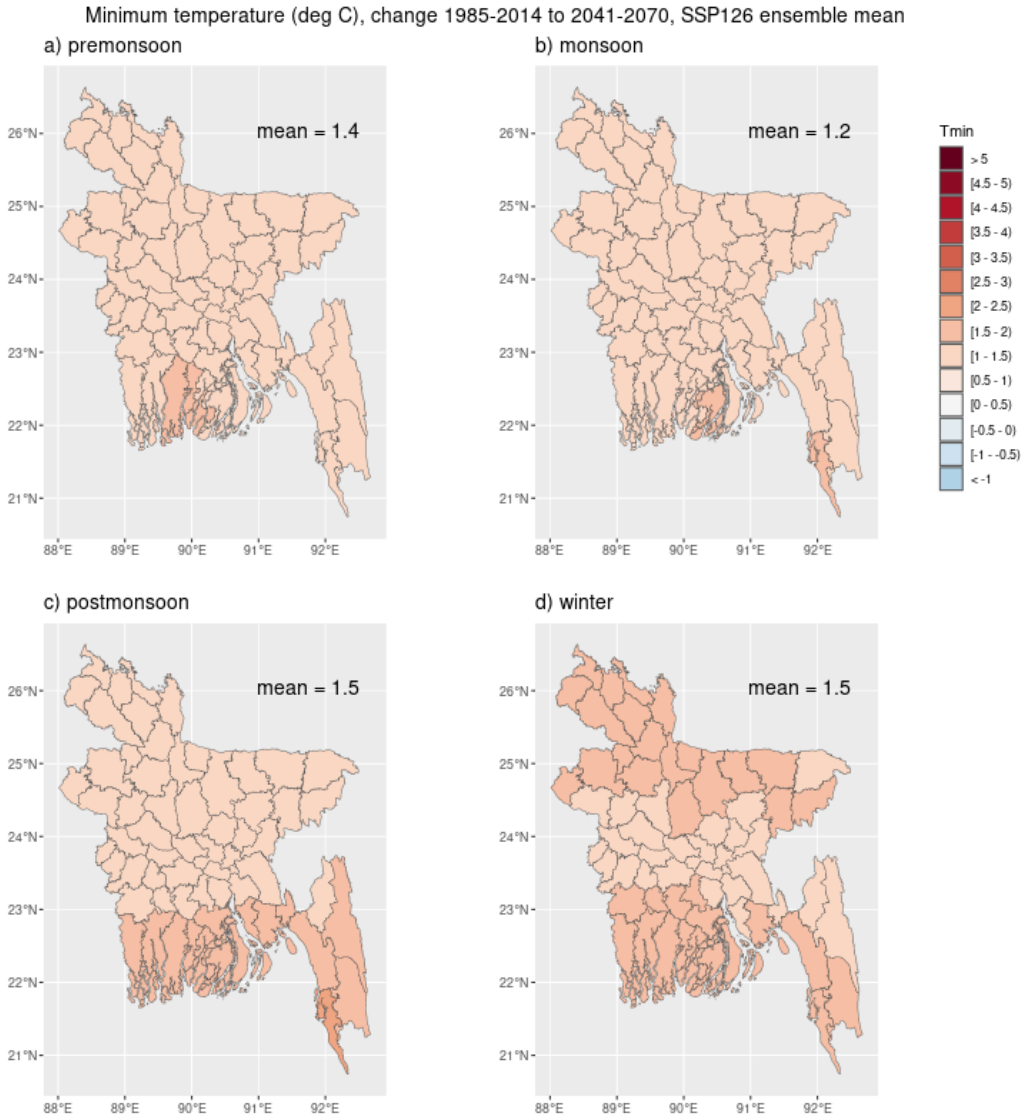


*Figure A2.13 Changes in the daily minimum temperature from the reference period (1985–2014) to the mid-century (2041–2070) under emission scenario SSP1-2.6, as estimated by the NEX-GDDP-CMIP6 ensemble mean for the a) pre-monsoon, b) monsoon, c) post-monsoon, and d) winter seasons.The mean value of each map shows the country average.*

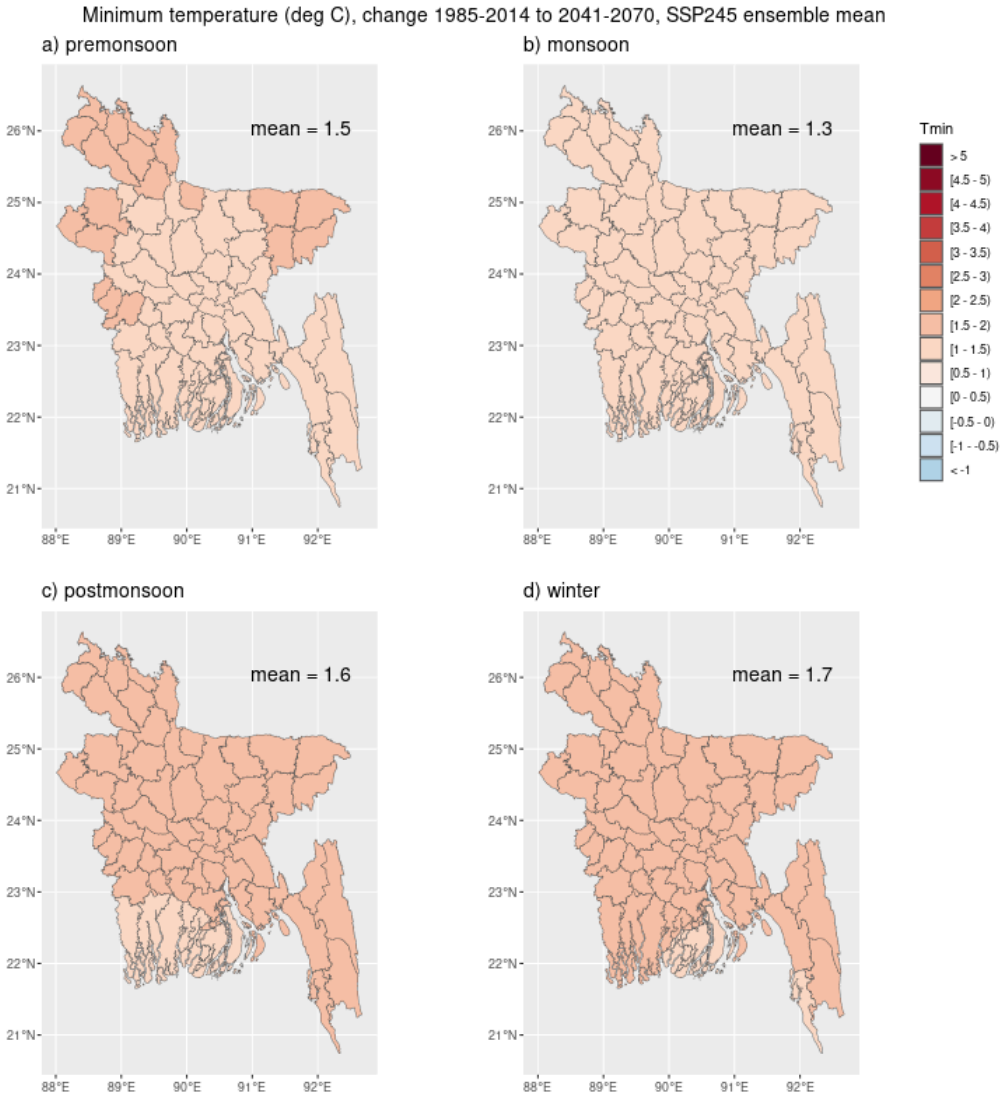


*Figure A2.14 Changes in the daily minimum temperature from the reference period (1985–2014) to the mid-century (2041–2070) under emission scenario SSP2-4.5, as estimated by the NEX-GDDP-CMIP6 ensemble mean for the a) pre-monsoon, b) monsoon, c) post-monsoon, and d) winter seasons.The mean value of each map shows the country average.*

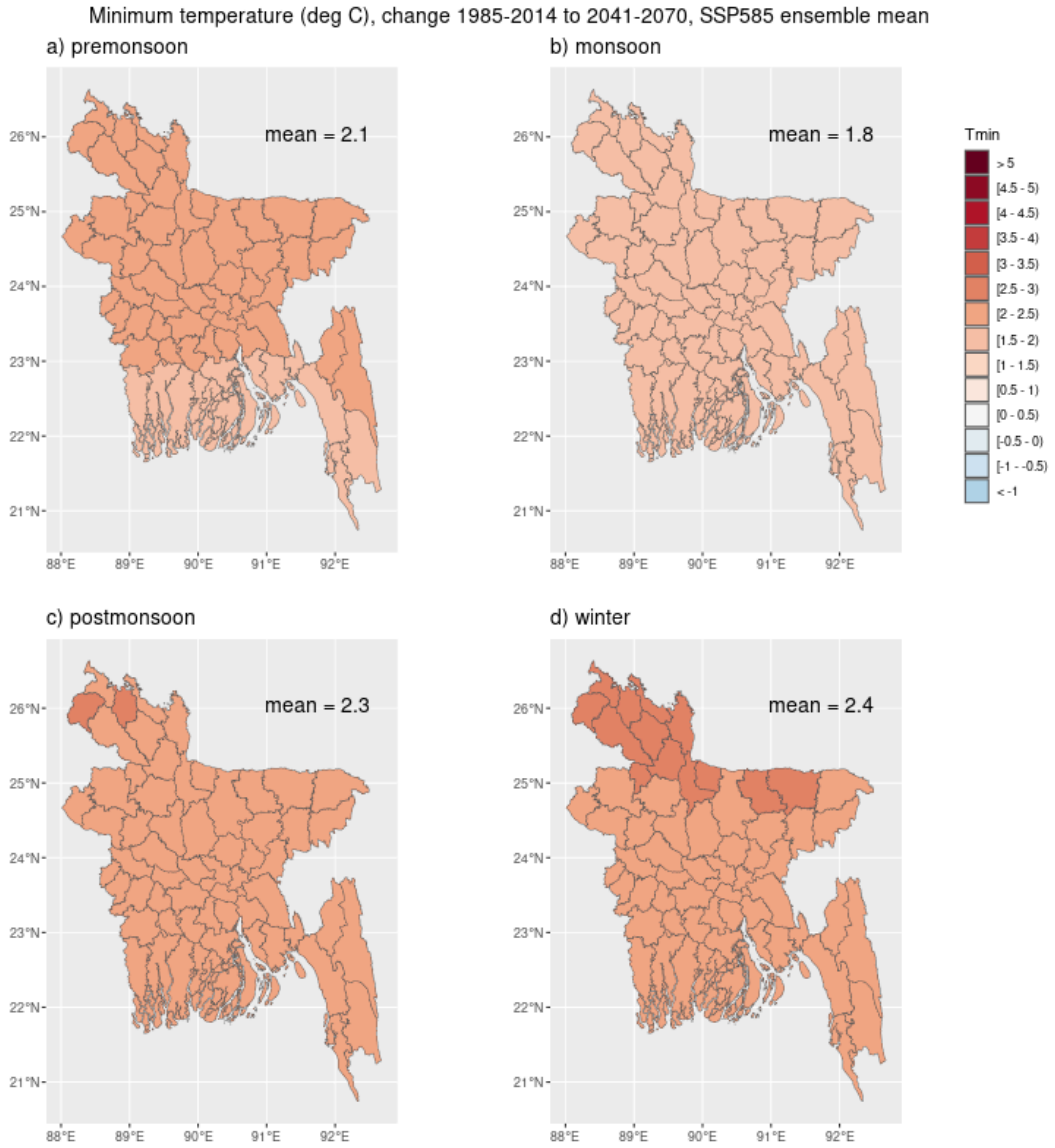


*Figure A2.15 Changes in the daily minimum temperature from the reference period (1985–2014) to the mid-century (2041–2070) under emission scenario SSP5-8.5, as estimated by the NEX-GDDP-CMIP6 ensemble mean for the a) pre-monsoon, b) monsoon, c) post-monsoon, and d) winter seasons.The mean value of each map shows the country average.*

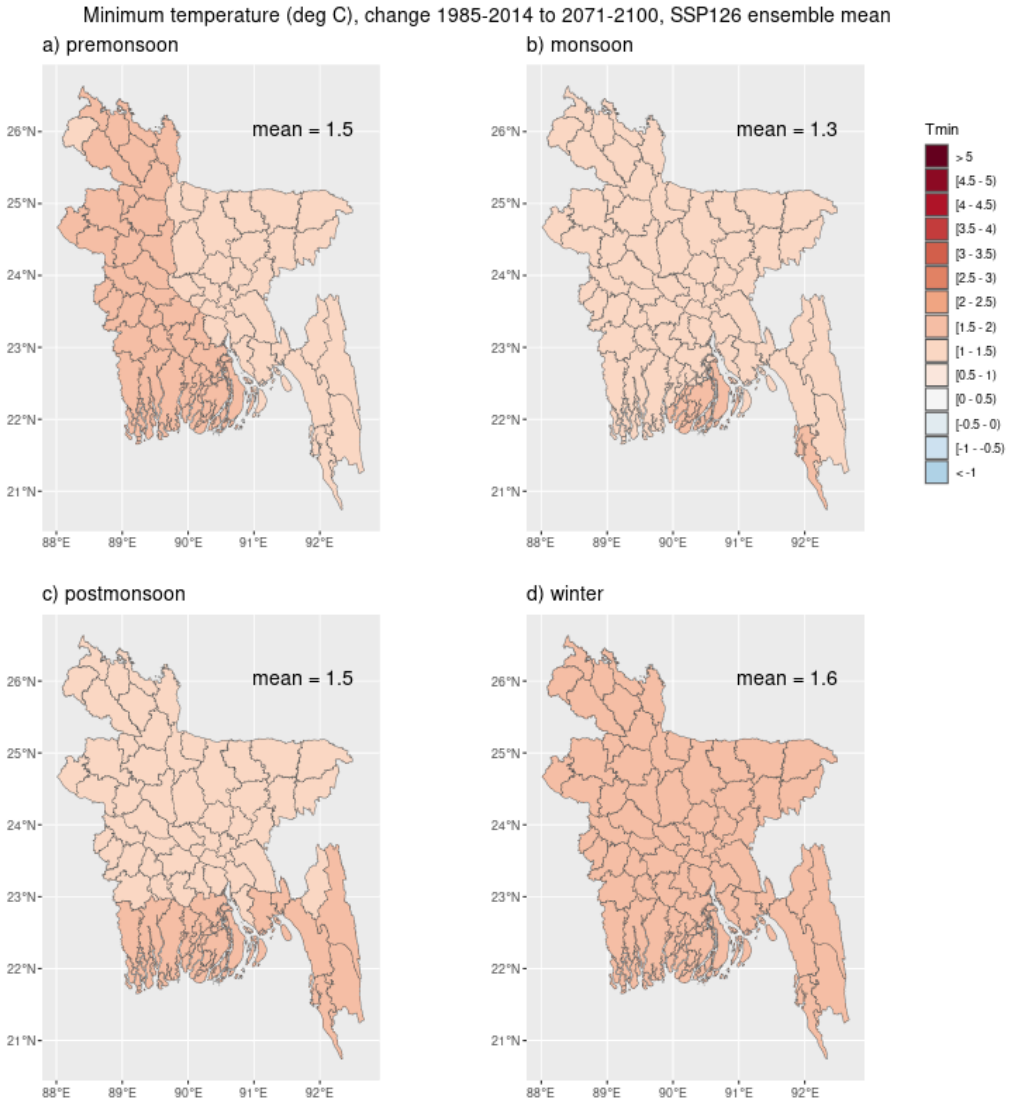


*Figure A2.16 Changes in the daily minimum temperature from the reference period (1985–2014) to the end of the century (2071–2100) under emission scenario SSP1-2.6, as estimated by the NEX-GDDP-CMIP6 ensemble mean for the a) pre-monsoon, b) monsoon, c) post-monsoon, and d) winter seasons.The mean value of each map shows the country average.*

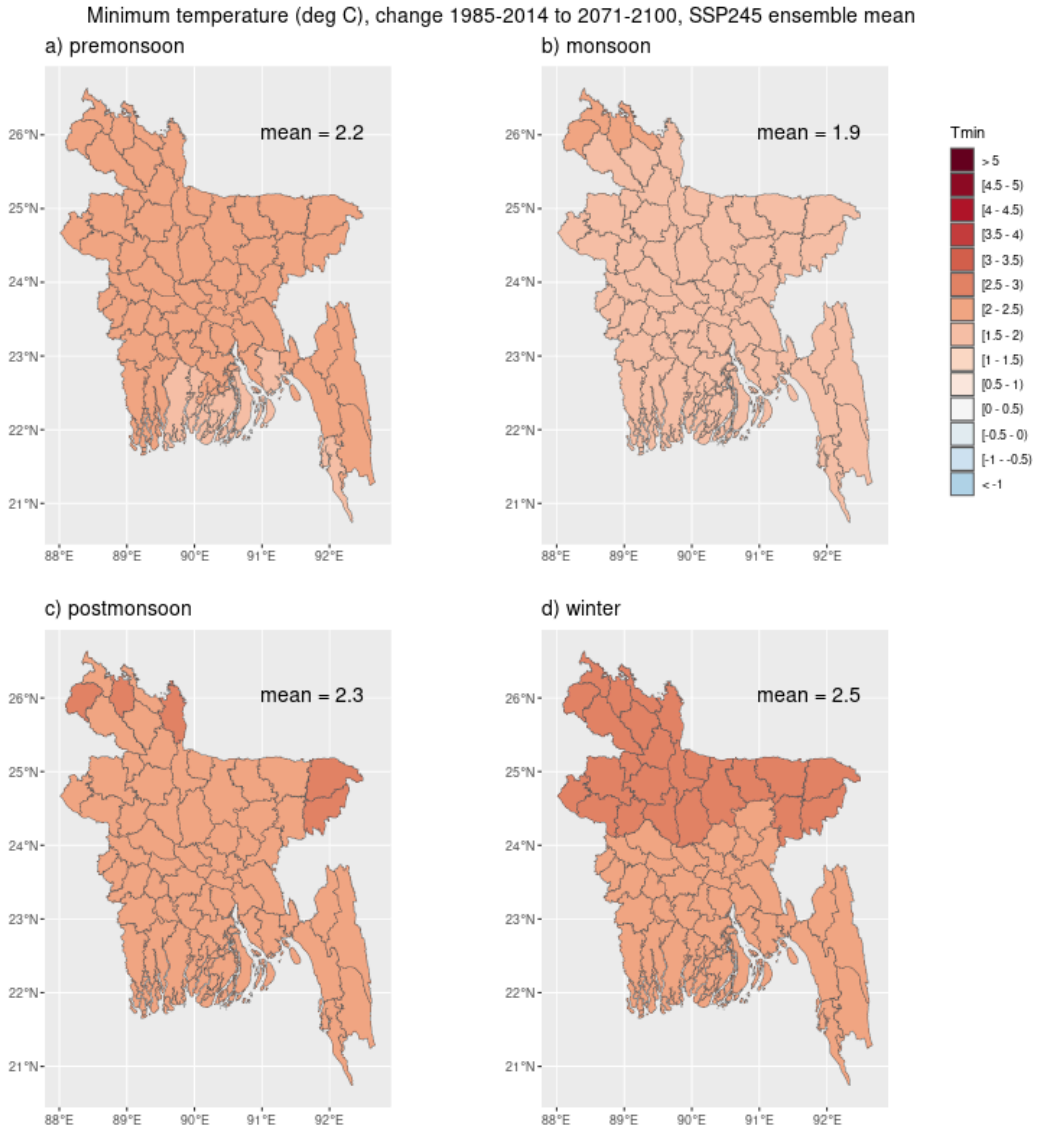


*Figure A2.17 Changes in the daily minimum temperature from the reference period (1985–2014) to the end of the century (2071–2100) under emission scenario SSP2-4.5, as estimated by the NEX-GDDP-CMIP6 ensemble mean for the a) pre-monsoon, b) monsoon, c) post-monsoon, and d) winter seasons.The mean value of each map shows the country average.*

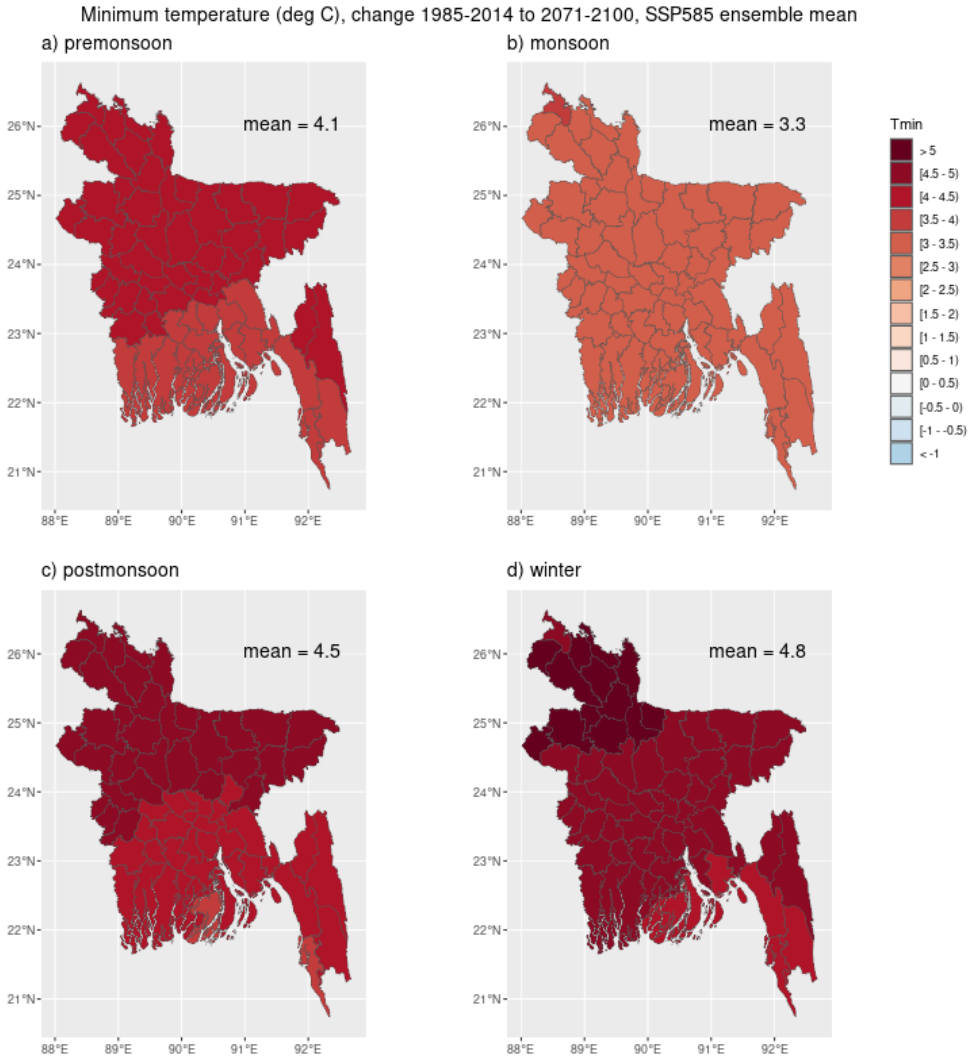


*Figure A2.18 Changes in the daily minimum temperature from the reference period (1985–2014) to the end of the century (2071–2100) under emission scenario SSP5-8.5, as estimated by the NEX-GDDP-CMIP6 ensemble mean for the a) pre-monsoon, b) monsoon, c) post-monsoon, and d) winter seasons.The mean value of each map shows the country average.*

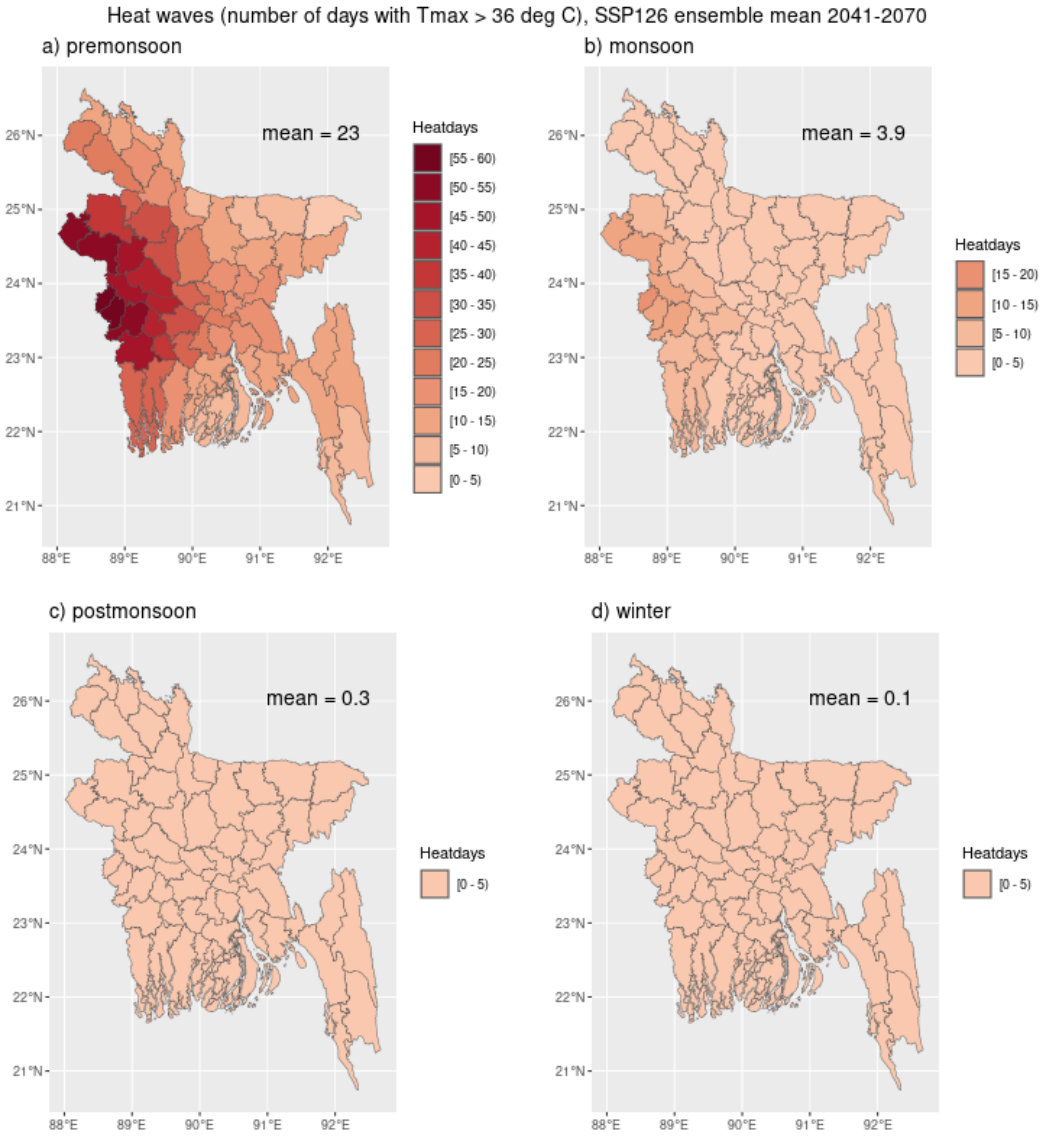


*Figure A2.19 The number of heatwave days (daily maximum temperature > 36 °C) in the* mid-century *(2041–2070) under SSP1-2.6. The estimates are based on the NEX-GDDP-CMIP6 ensemble mean of the daily maximum temperature for the a) pre-monsoon, b) monsoon, c) post-monsoon, and d) winter seasons.The mean value of each map shows the country average.*

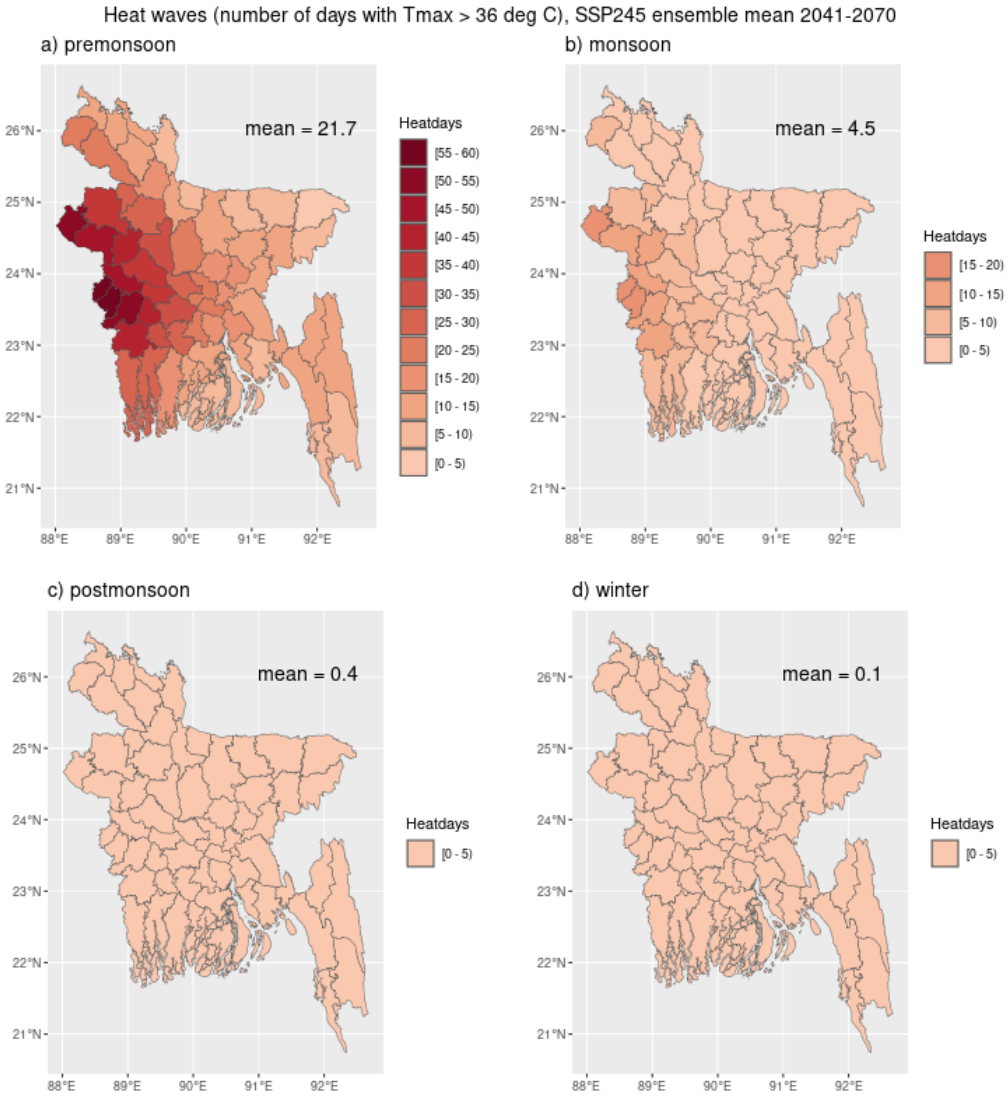


*Figure A2.20 The number of heatwave days (daily maximum temperature > 36 °C) in the* mid-century *(2041–2070) under SSP2-4.5. The estimates are based on the NEX-GDDP-CMIP6 ensemble mean of the daily maximum temperature for the a) pre-monsoon, b) monsoon, c) post-monsoon, and d) winter seasons.The mean value of each map shows the country average.*

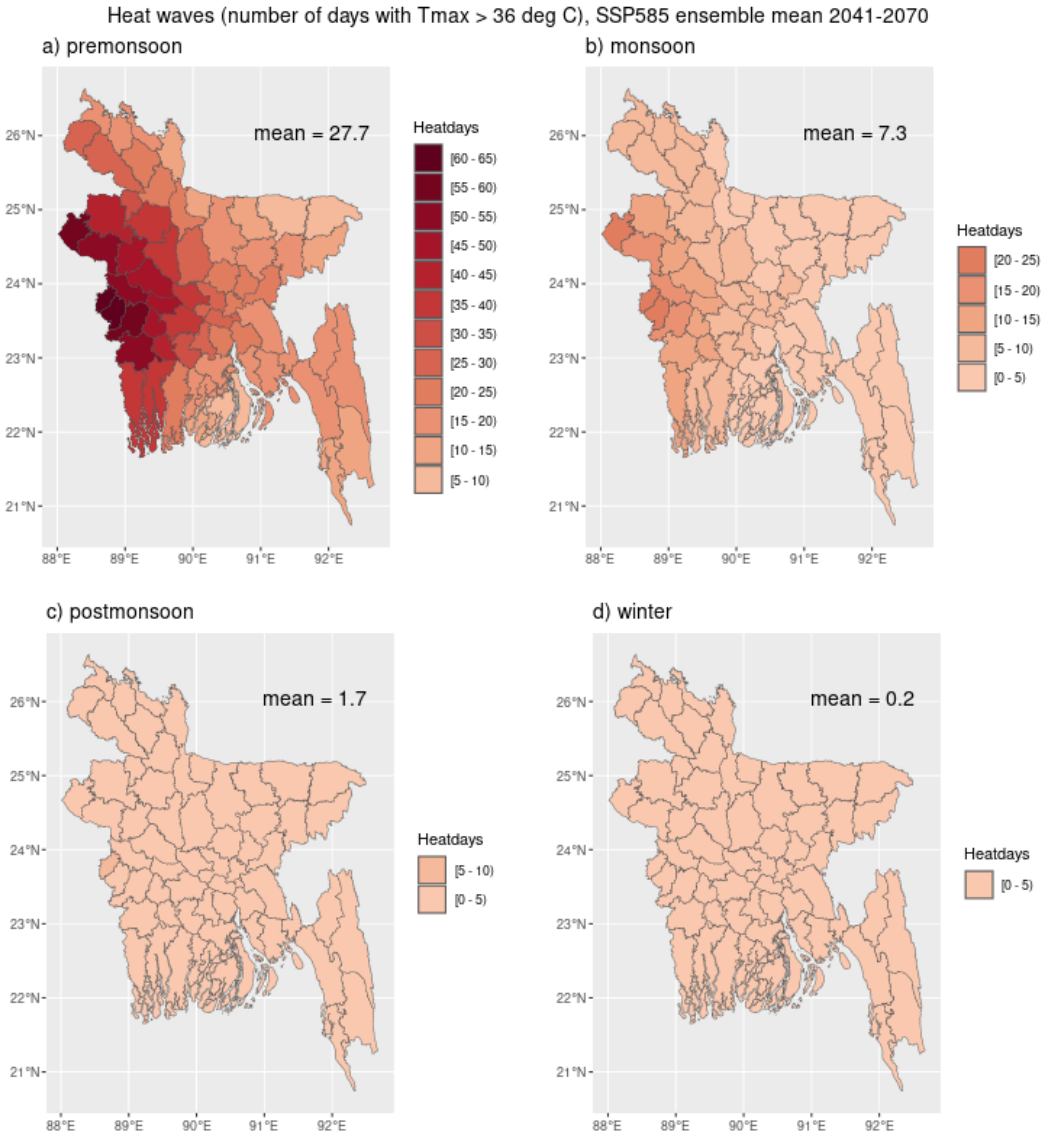


*Figure A2.21 The number of heatwave days (daily maximum temperature > 36 °C) in the* mid-century *(2041–2070) under SSP5-8.5. The estimates are based on the NEX-GDDP-CMIP6 ensemble mean of the daily maximum temperature for the a) pre-monsoon, b) monsoon, c) post-monsoon, and d) winter seasons.The mean value of each map shows the country average.*

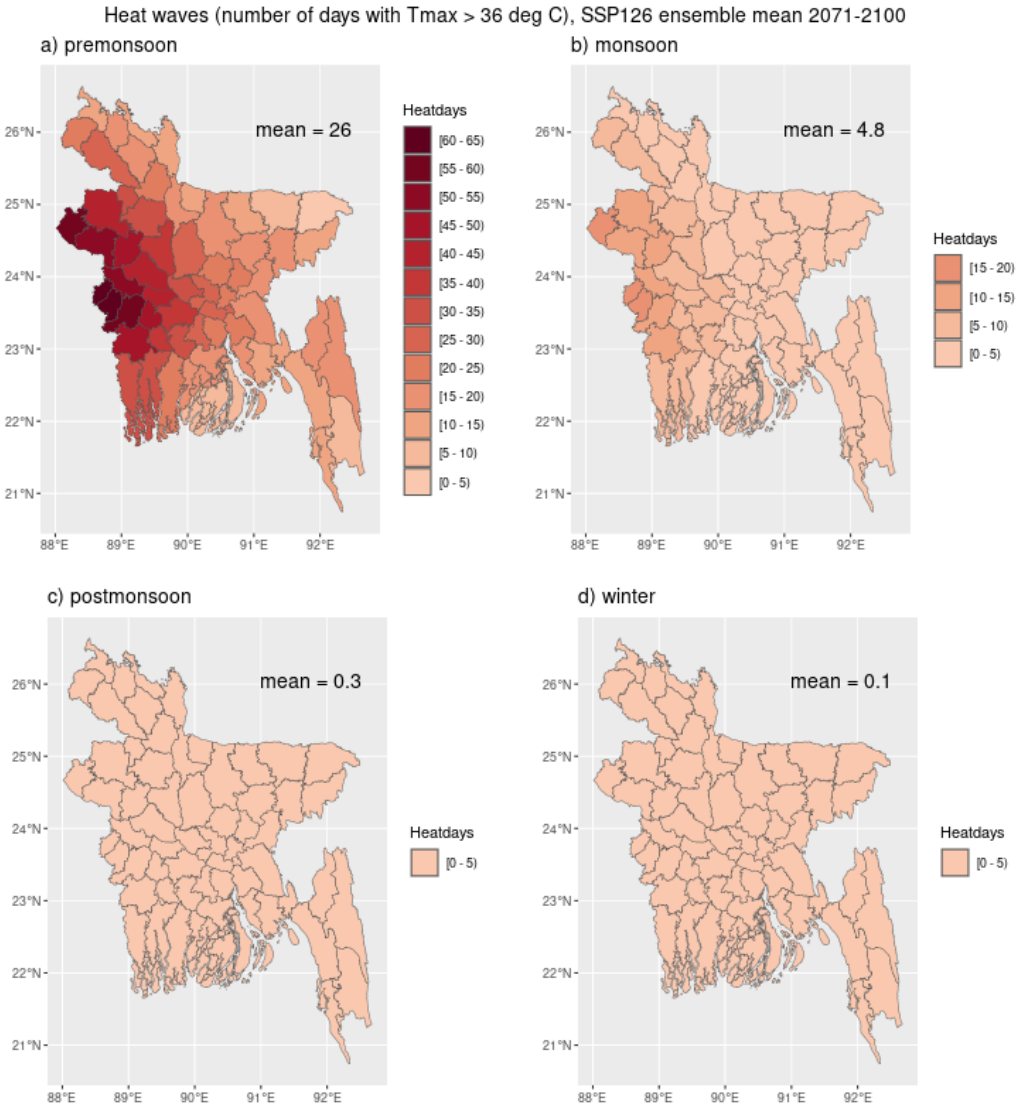


*Figure A2.22 The number of heatwave days (daily maximum temperature > 36 °C) at the end of the century (2071–2100) under SSP1-2.6. The estimates are based on the NEX-GDDP-CMIP6 ensemble mean of the daily maximum temperature for the a) pre-monsoon, b) monsoon, c) post-monsoon, and d) winter seasons.The mean value of each map shows the country average.*

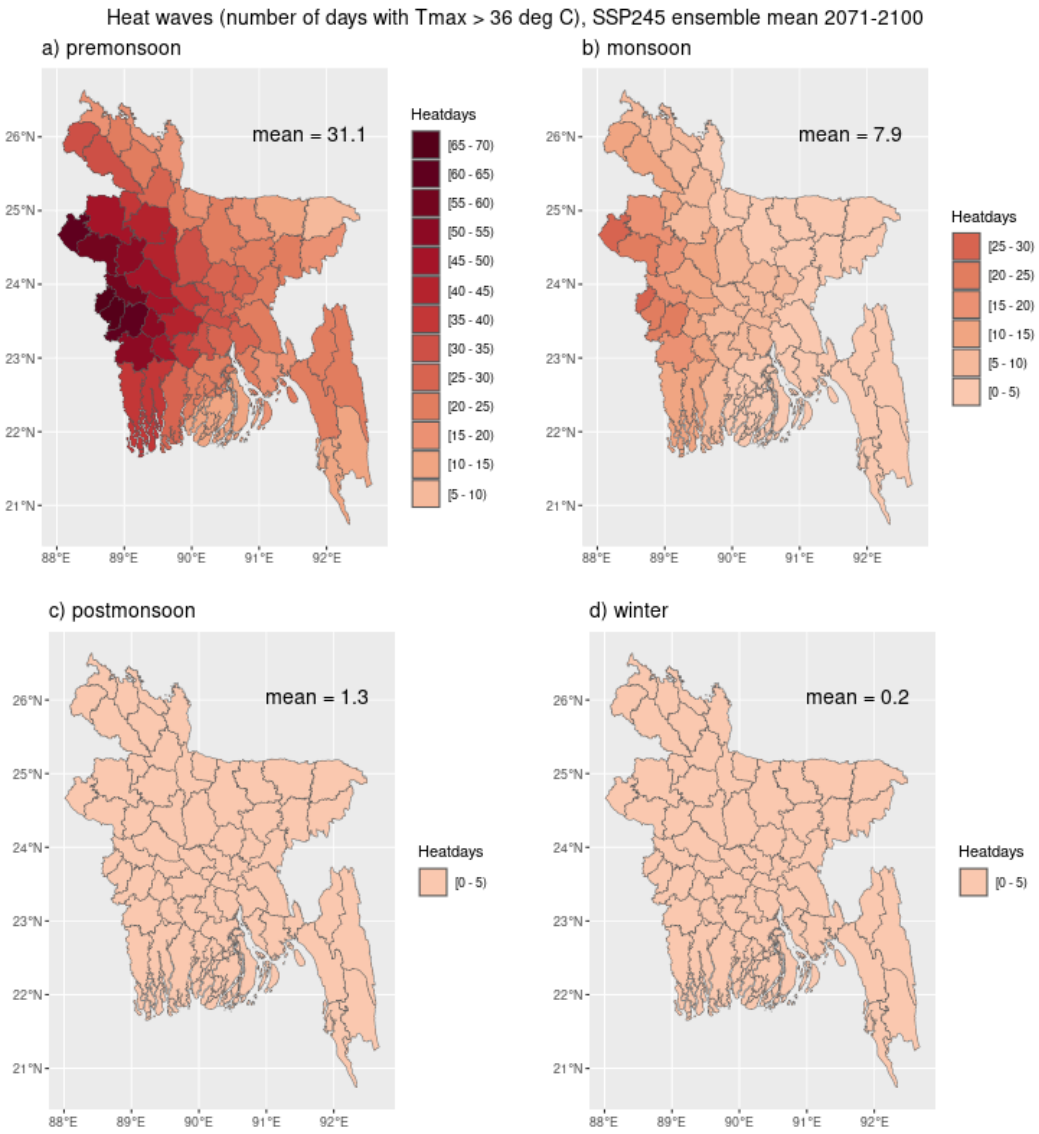


*Figure A2.23 The number of heatwave days (daily maximum temperature > 36 °C) at the end of the century (2071–2100) under SSP2-4.5. The estimates are based on the NEX-GDDP-CMIP6 ensemble mean of the daily maximum temperature for the a) pre-monsoon, b) monsoon, c) post-monsoon, and d) winter seasons.The mean value of each map shows the country average.*

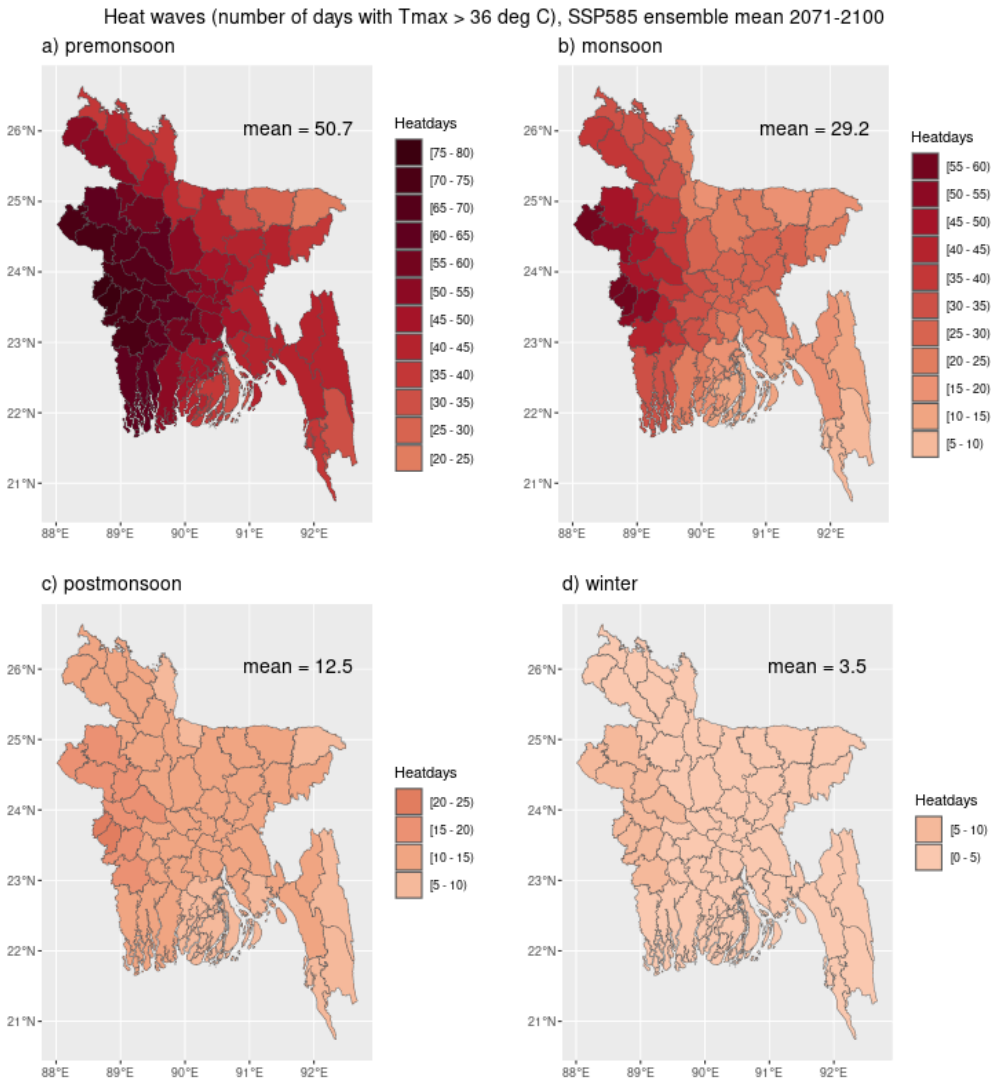


*Figure A2.24 The number of heatwave days (daily maximum temperature > 36 °C) at the end of the century (2071–2100) under SSP5-8.5. The estimates are based on the NEX-GDDP-CMIP6 ensemble mean of the daily maximum temperature for the a) pre-monsoon, b) monsoon, c) post-monsoon, and d) winter seasons.The mean value of each map shows the country average.*

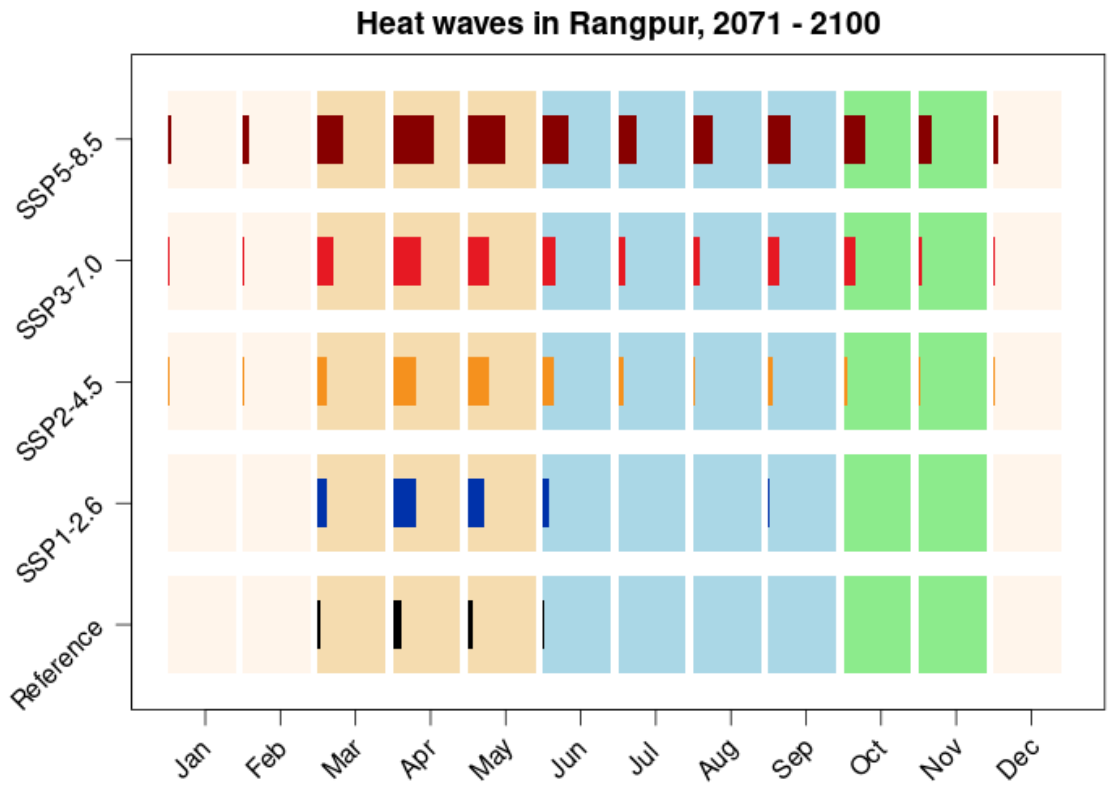


*Figure A2.25 The number of heatwave days (daily maximum temperature > 36 °C) at the end of the century (2071–2100) at Rangpur under different SSPs. The estimates are based on the NEX-GDDP-CMIP6 ensemble mean of the daily maximum temperature.*

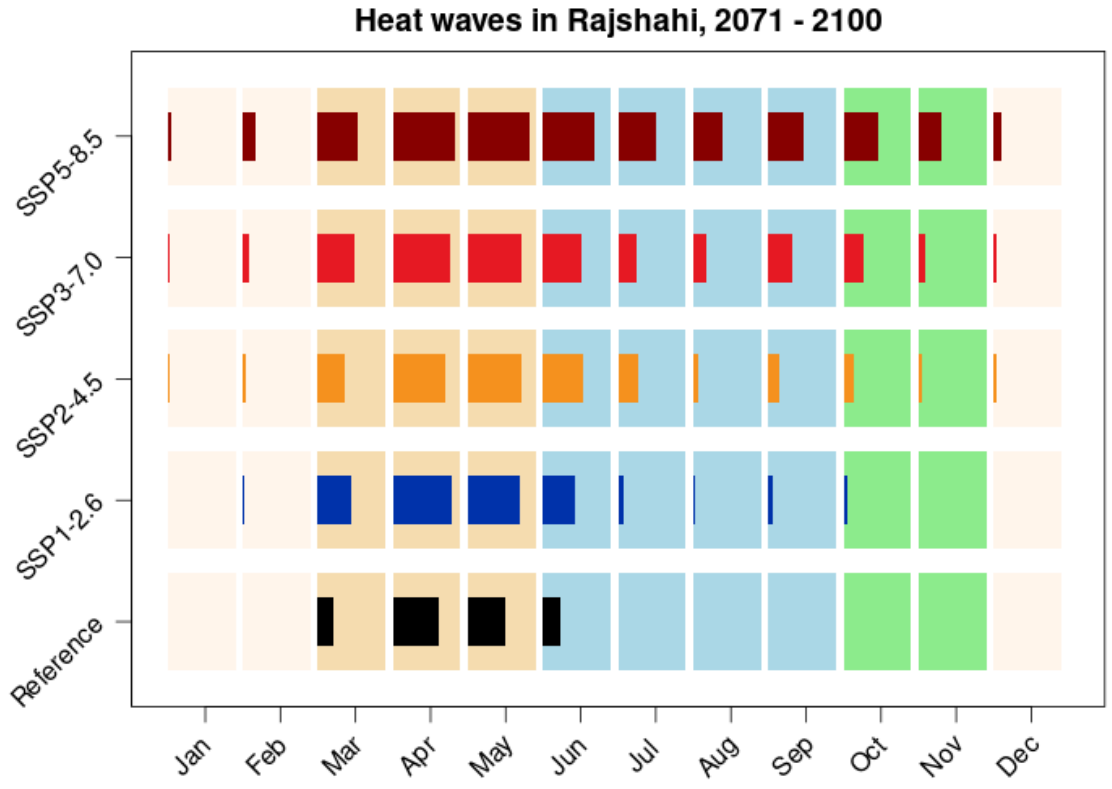

*Figure A2.26 The number of heatwave days (daily maximum temperature > 36 °C) at the end of the century (2071–2100) at Rajshahi under different SSPs. The estimates are based on the NEX-GDDP-CMIP6 ensemble mean of the daily maximum temperature.*

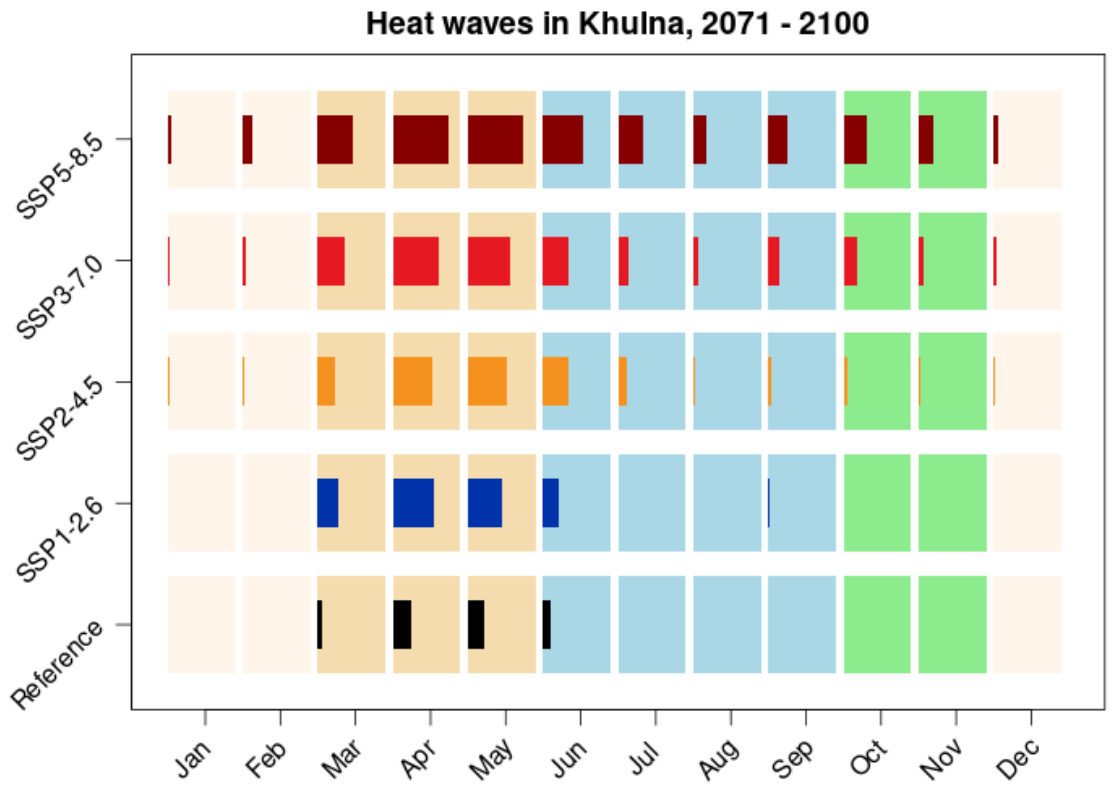


*Figure A2.27 The number of heatwave days (daily maximum temperature > 36 °C) at the end of the century (2071–2100) at Khulna under different SSPs. The estimates are based on the NEX-GDDP-CMIP6 ensemble mean of the daily maximum temperature.*

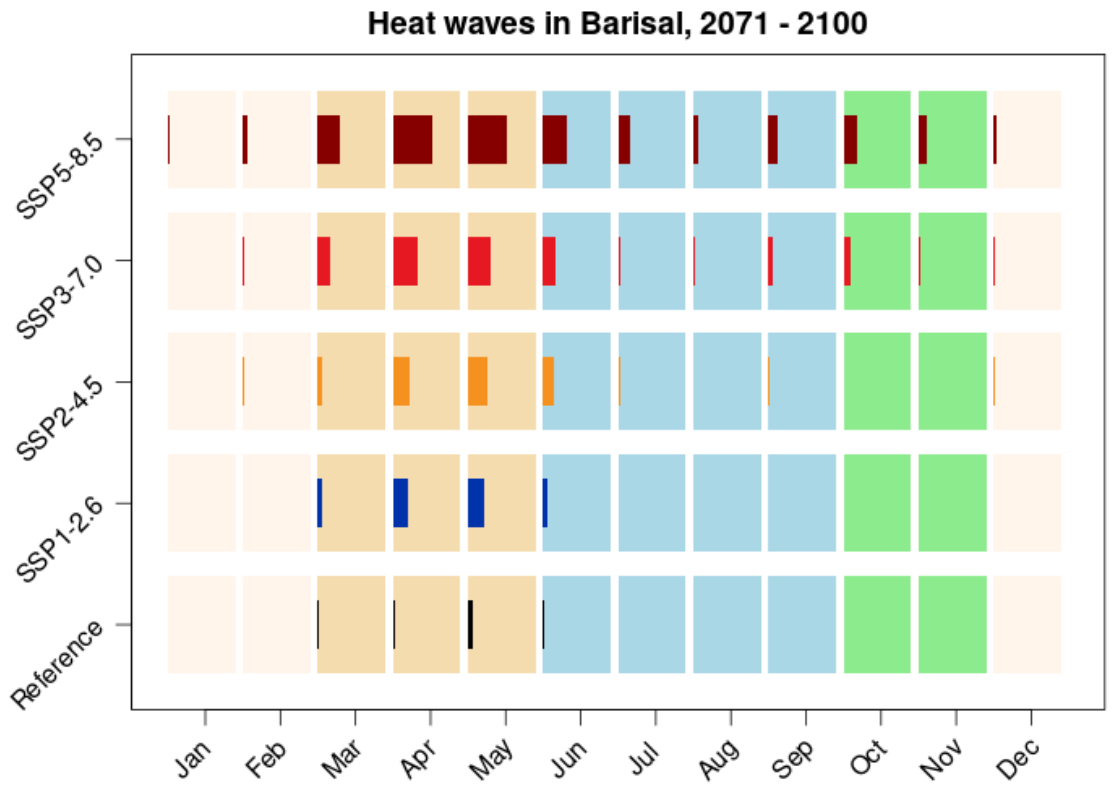


*Figure A2.28 The number of heatwave days (daily maximum temperature > 36 °C) at the end of the century (2071–2100) at Barisal under different SSPs. The estimates are based on the NEX-GDDP-CMIP6 ensemble mean of the daily maximum temperature.*

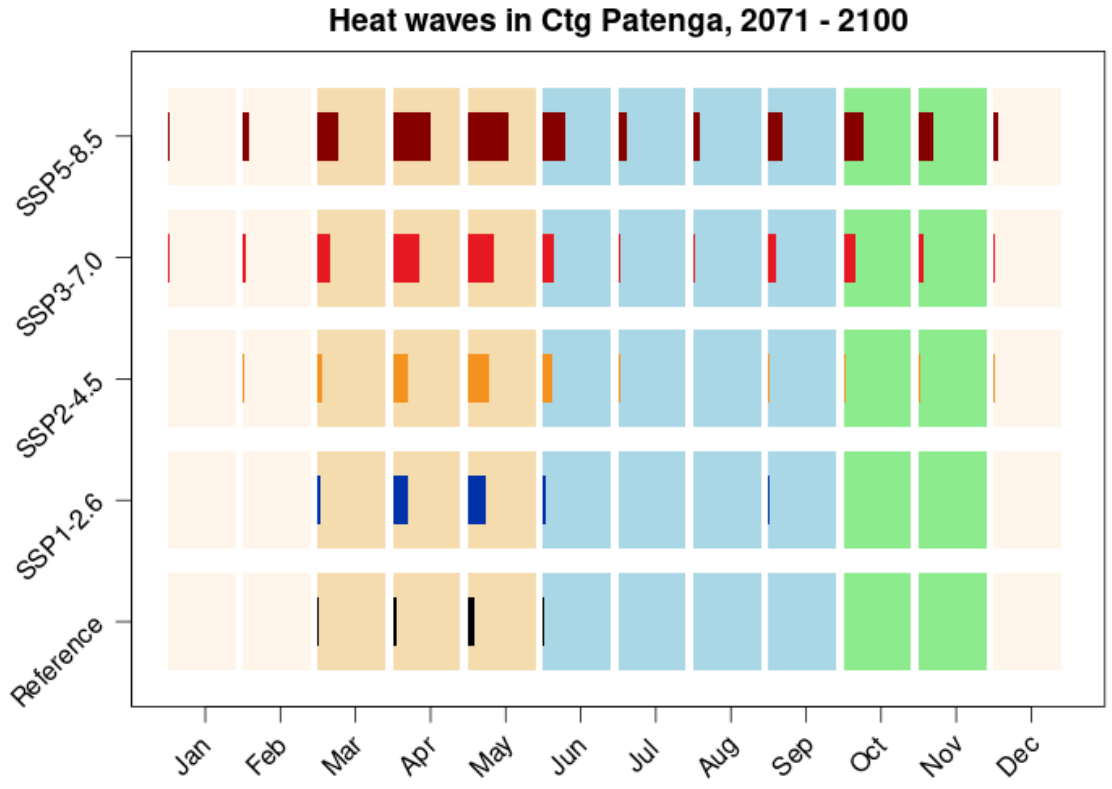

*Figure A2.29 The number of heatwave days (daily maximum temperature > 36 °C) at the end of the century (2071–2100) at Chattogram under different SSPs. The estimates are based on the NEX-GDDP-CMIP6 ensemble mean of the daily maximum temperature.*

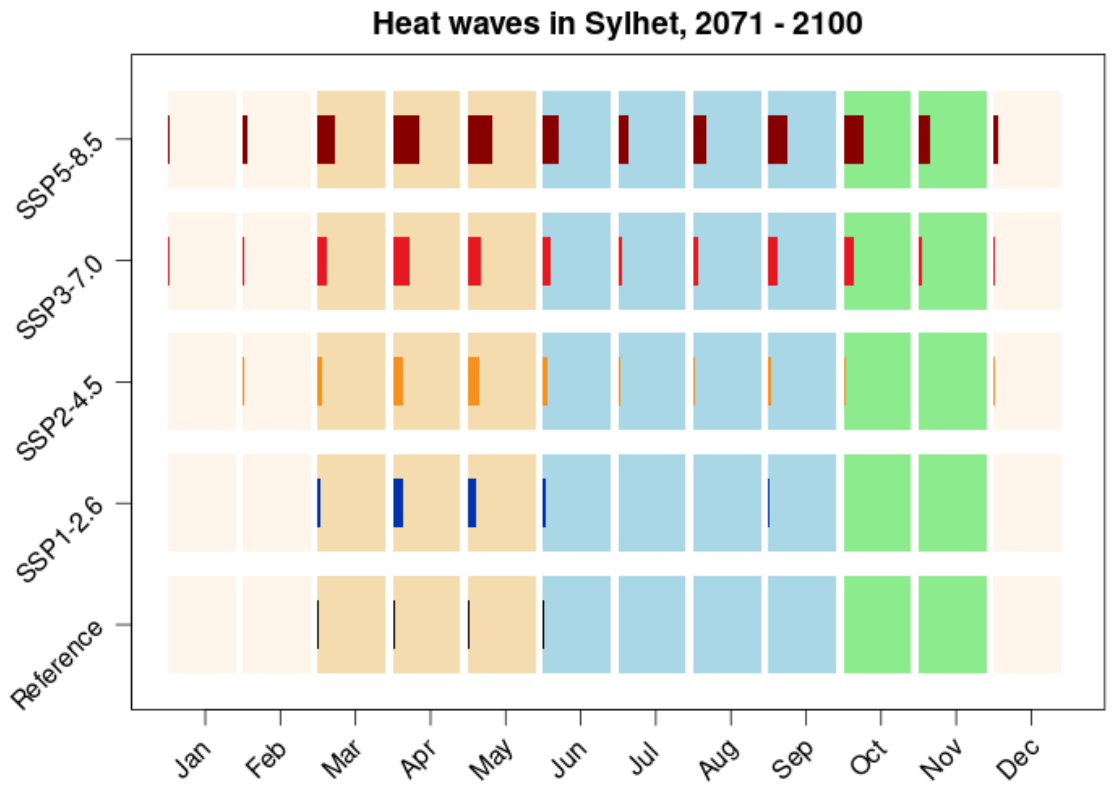


*Figure A2.30 The number of heatwave days (daily maximum temperature > 36 °C) at the end of the century (2071–2100) at Sylhet under different SSPs. The estimates are based on the NEX-GDDP-CMIP6 ensemble mean of the daily maximum temperature.*

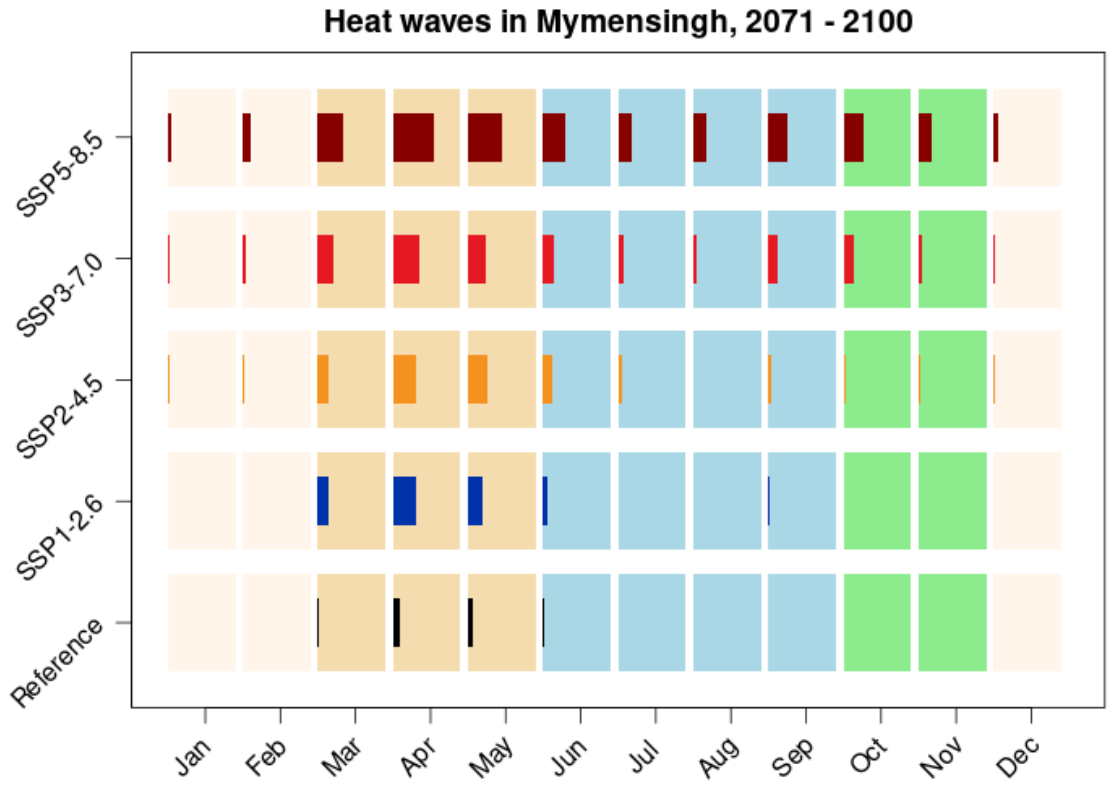


*Figure A2.31 The number of heatwave days (daily maximum temperature > 36 °C) at the end of the century (2071–2100) at Mymensingh under different SSPs. The estimates are based on the NEX-GDDP-CMIP6 ensemble mean of the daily maximum temperature.*

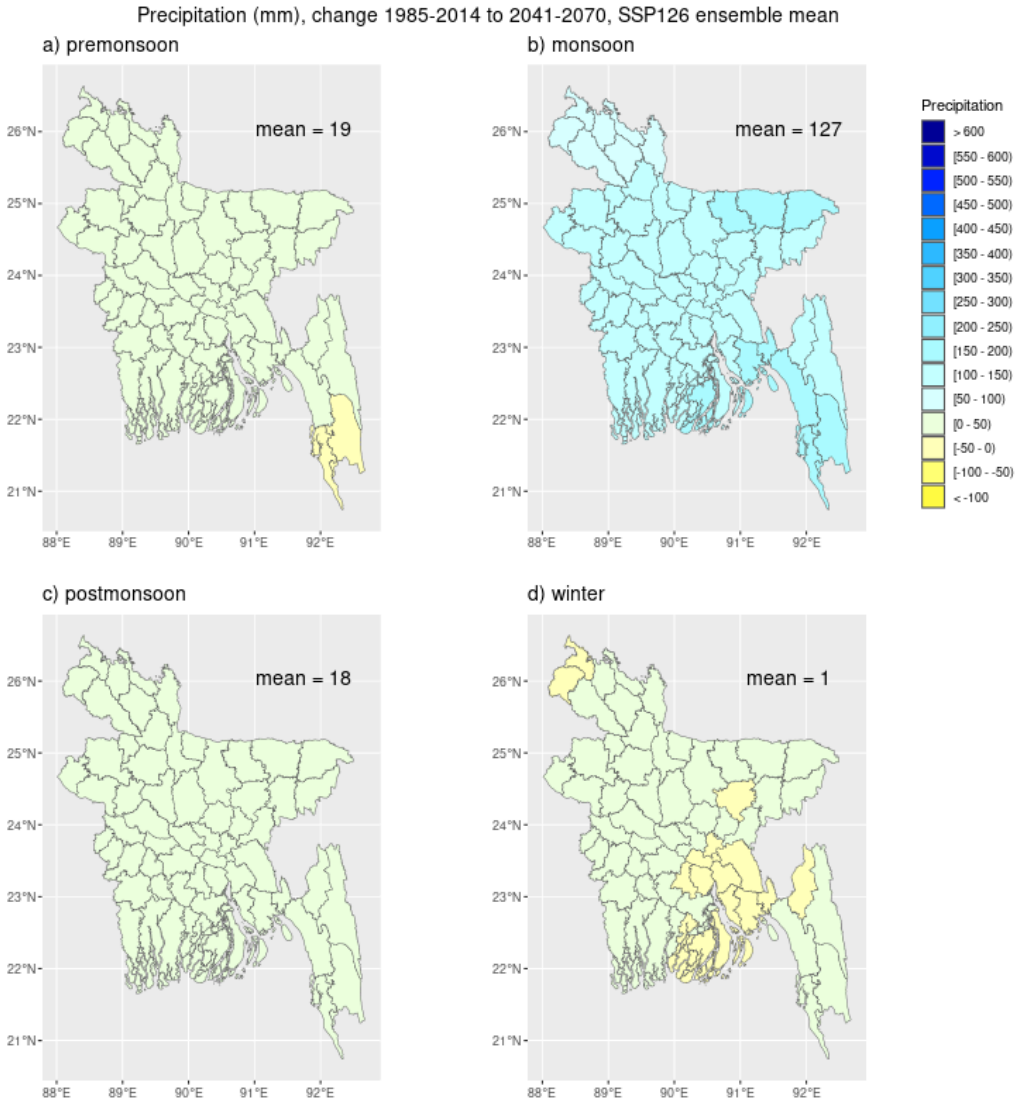


*Figure A2.32 Changes in the seasonal precipitation sum from the reference period (1985–2014) to the mid-century (2041–2070) under emission scenario SSP1-2.6, as estimated by the NEX-GDDP-CMIP6 ensemble mean for the a) pre-monsoon, b) monsoon, c) post-monsoon, and d) winter seasons.The mean value of each map shows the country average.*

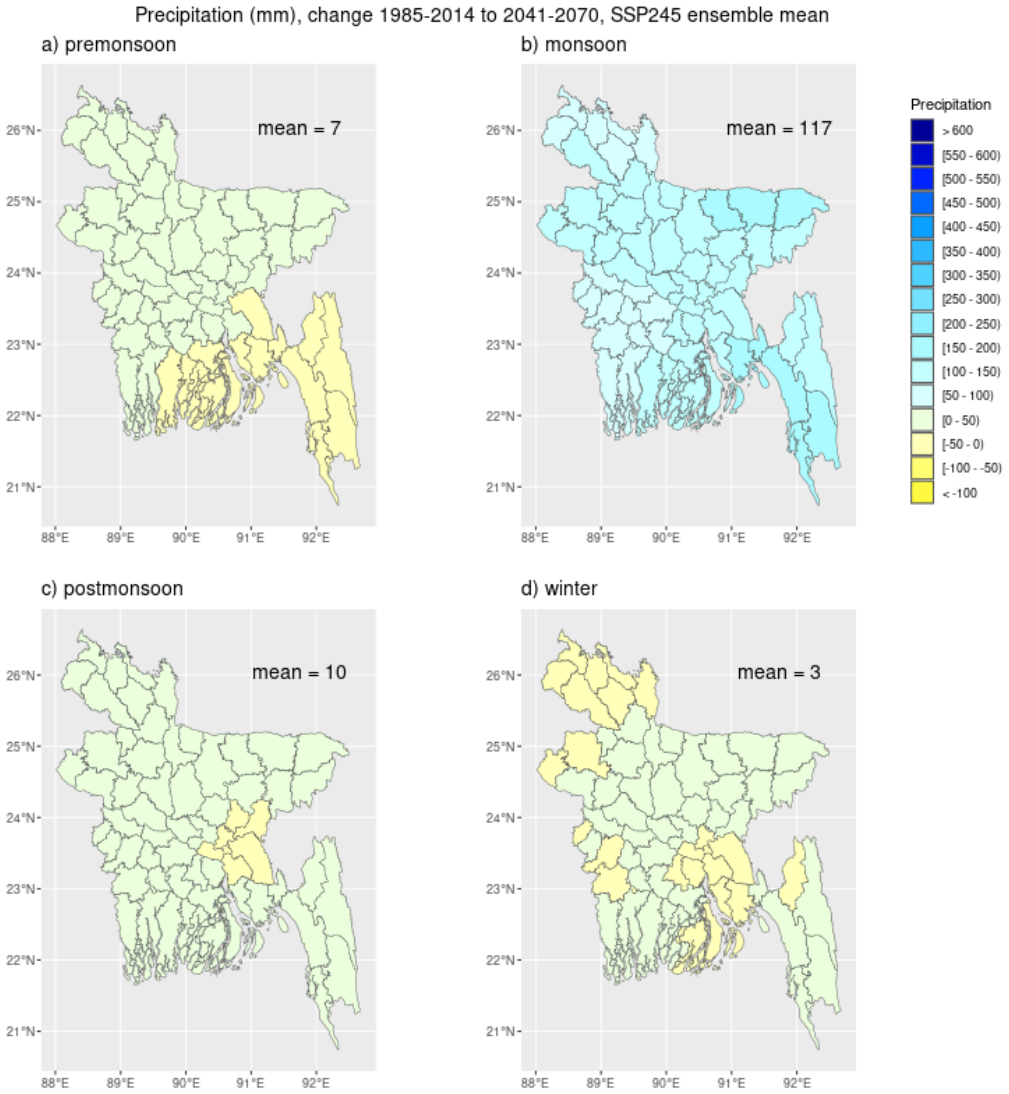


*Figure A2.33 Changes in the seasonal precipitation sum from the reference period (1985–2014) to the mid-century (2041–2070) under emission scenario SSP2-4.5, as estimated by the NEX-GDDP-CMIP6 ensemble mean for the a) pre-monsoon, b) monsoon, c) post-monsoon, and d) winter seasons.The mean value of each map shows the country average.*

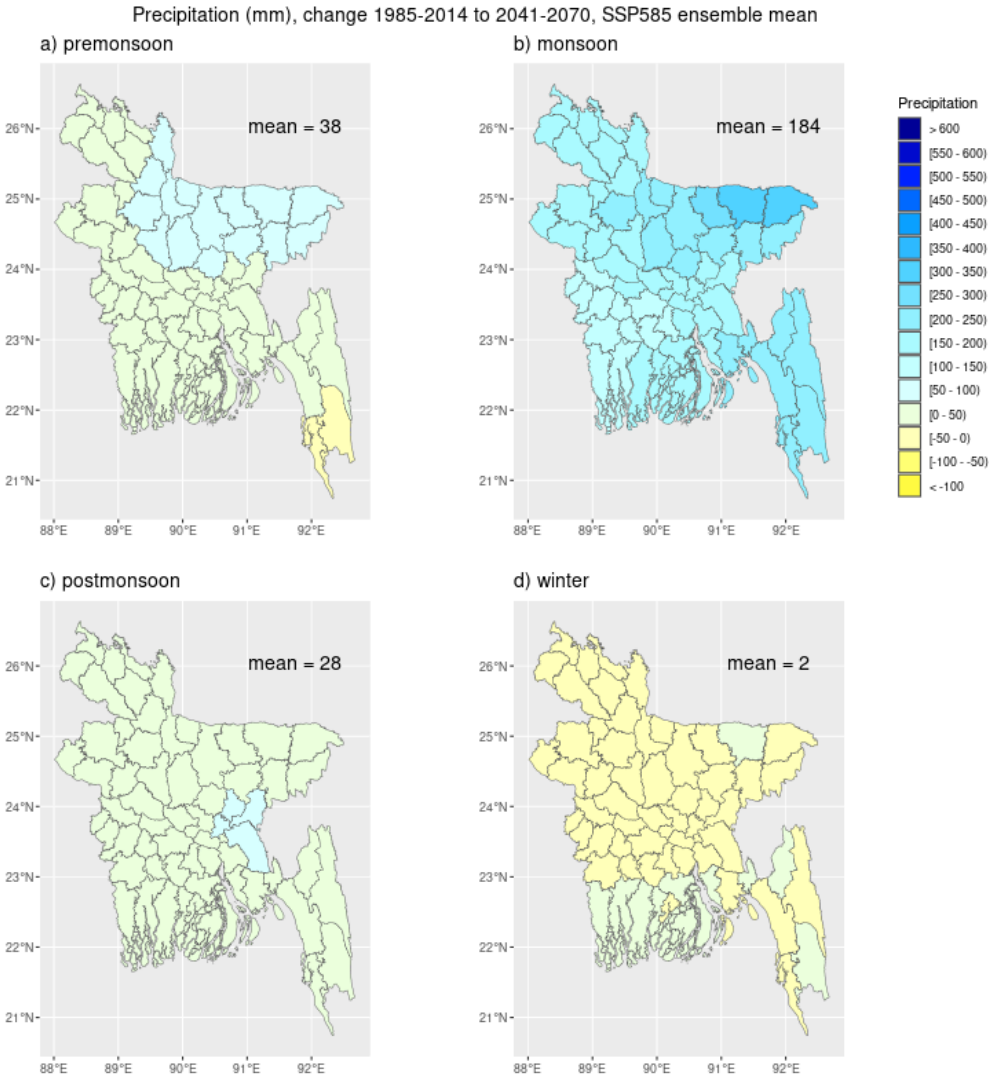


*Figure A2.34 Changes in the seasonal precipitation sum from the reference period (1985–2014) to the mid-century (2041–2070) under emission scenario SSP5-8.5, as estimated by the NEX-GDDP-CMIP6 ensemble mean for the a) pre-monsoon, b) monsoon, c) post-monsoon, and d) winter seasons.The mean value of each map shows the country average.*

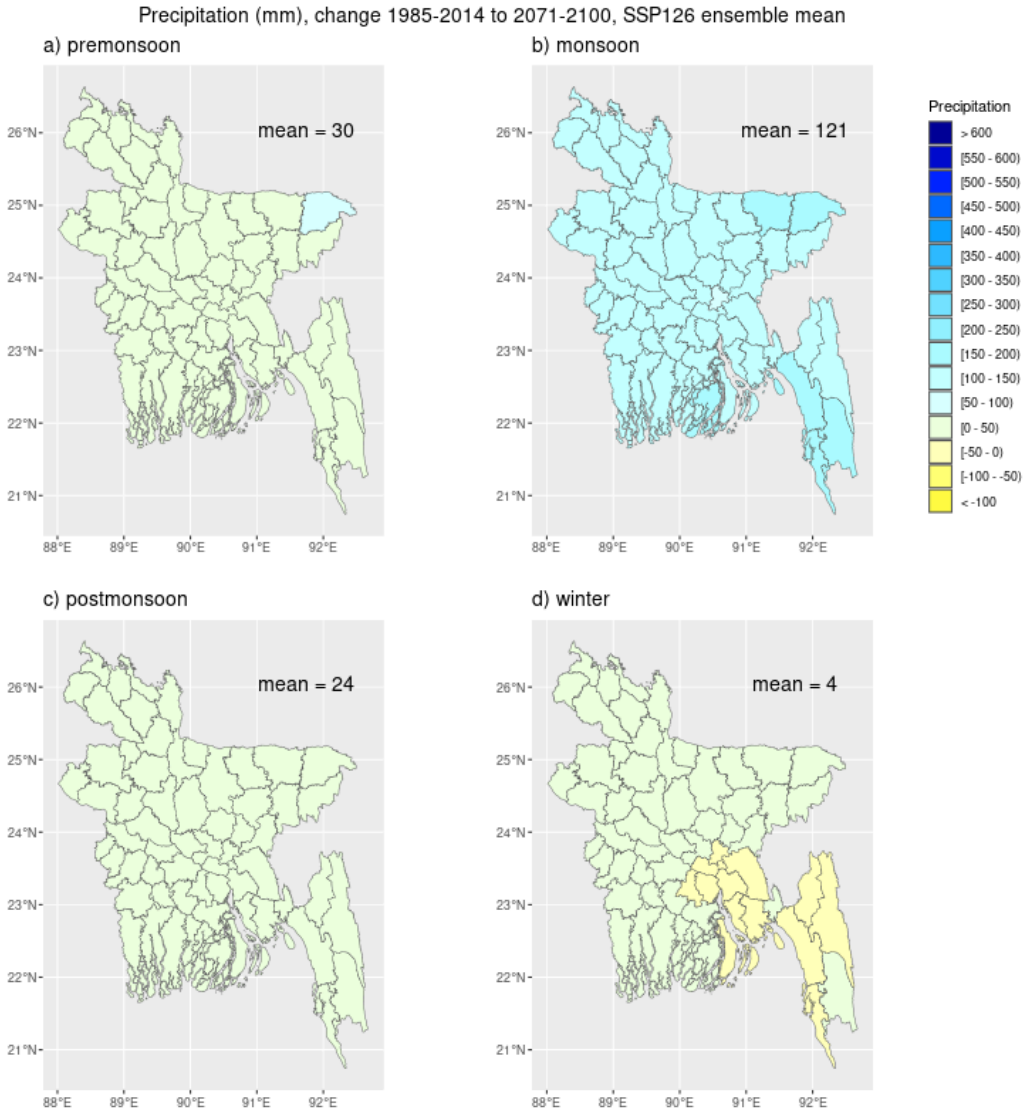


*Figure A2.35 Changes in the seasonal precipitation sum from the reference period (1985–2014) to the end of the century (2071–2100) under emission scenario SSP1-2.6, as estimated by the NEX-GDDP-CMIP6 ensemble mean for the a) pre-monsoon, b) monsoon, c) post-monsoon, and d) winter seasons.The mean value of each map shows the country average.*

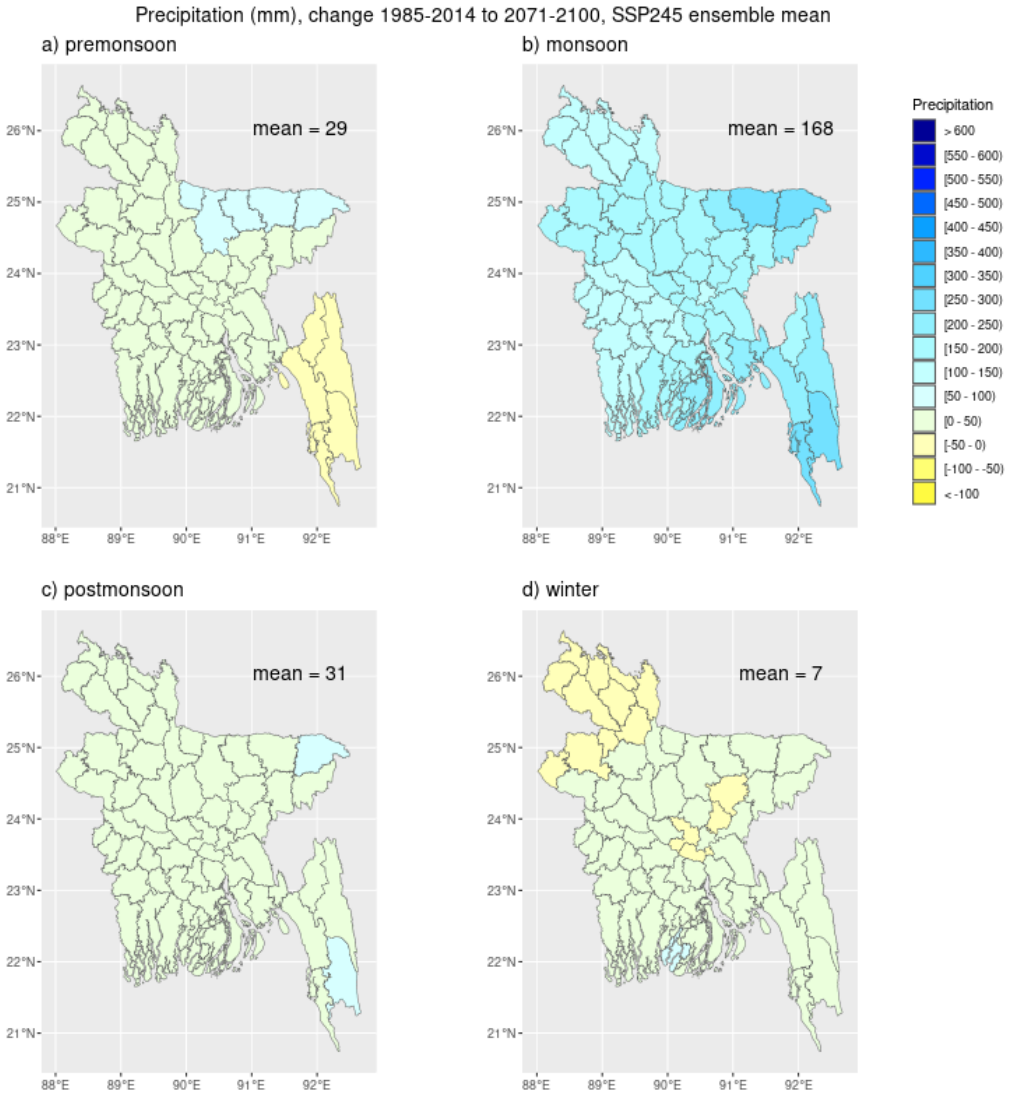


*Figure A2.36 Changes in the seasonal precipitation sum from the reference period (1985–2014) to the end of the century (2071–2100) under emission scenario SSP2-4.5, as estimated by the NEX-GDDP-CMIP6 ensemble mean for the a) pre-monsoon, b) monsoon, c) post-monsoon, and d) winter seasons.The mean value of each map shows the country average.*

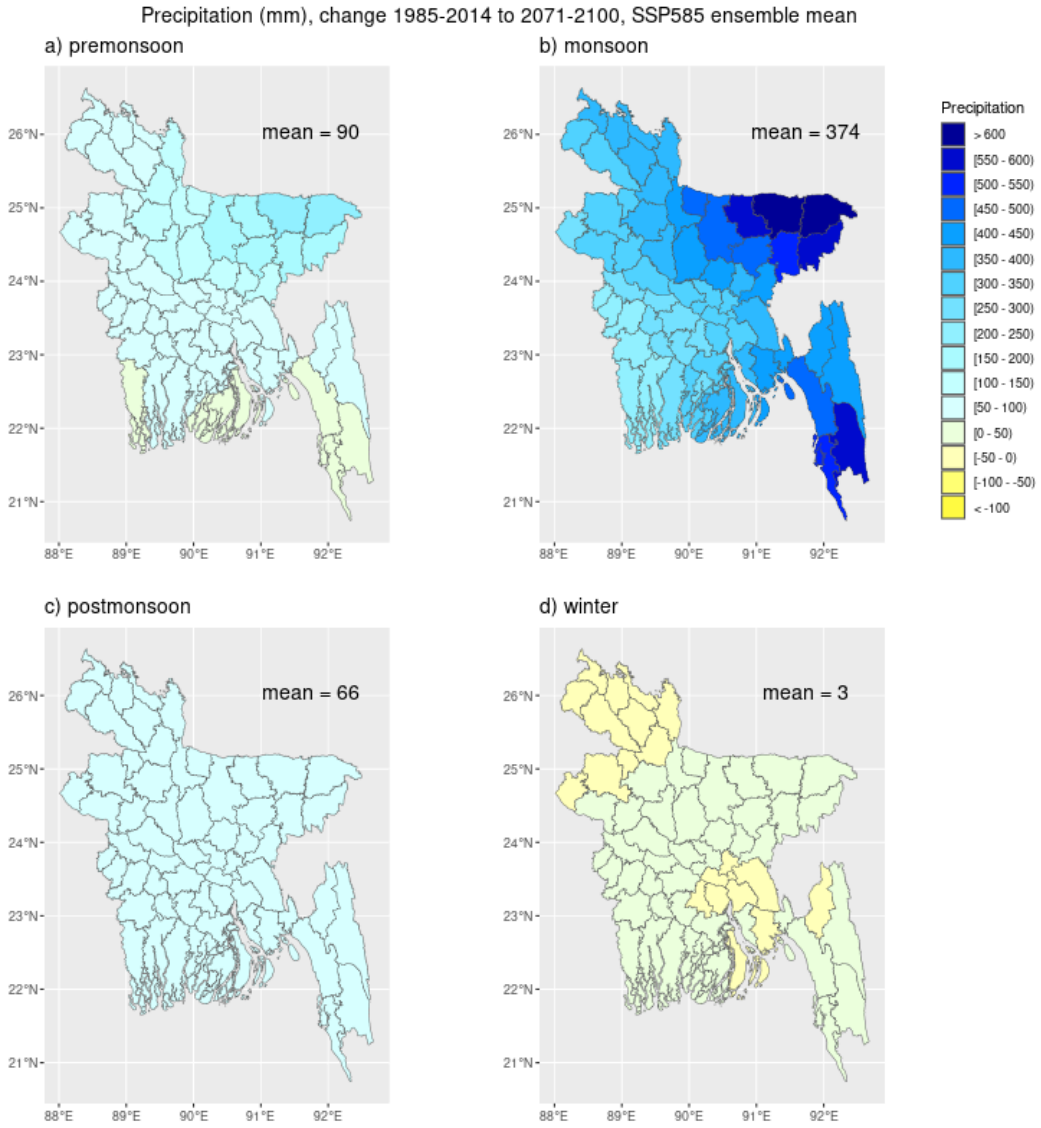


*Figure A2.37 Changes in the seasonal precipitation sum from the reference period (1985–2014) to the end of the century (2071–2100) under emission scenario SSP5-8.5, as estimated by the NEX-GDDP-CMIP6 ensemble mean for the a) pre-monsoon, b) monsoon, c) post-monsoon, and d) winter seasons.The mean value of each map shows the country average.*

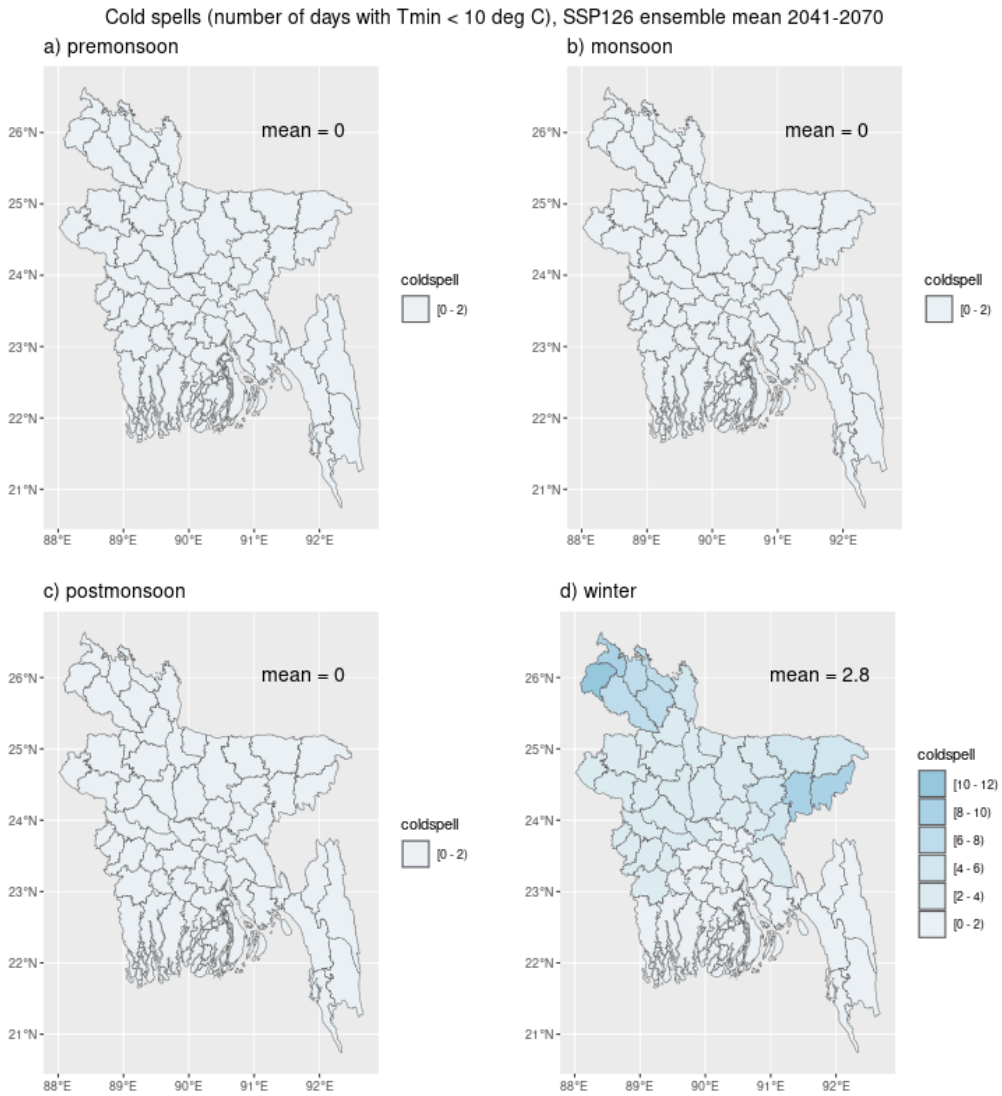


*Figure A2.38 The number of cold spell days (daily minimum temperature < 10 °C) in the* mid-century *(2041–2071) under SSP1-2.6. The estimates are based on the NEX-GDDP-CMIP6 ensemble mean of the daily minimum temperature for the a) pre-monsoon, b) monsoon, c) post-monsoon, and d) winter seasons.The mean value of each map shows the country average.*

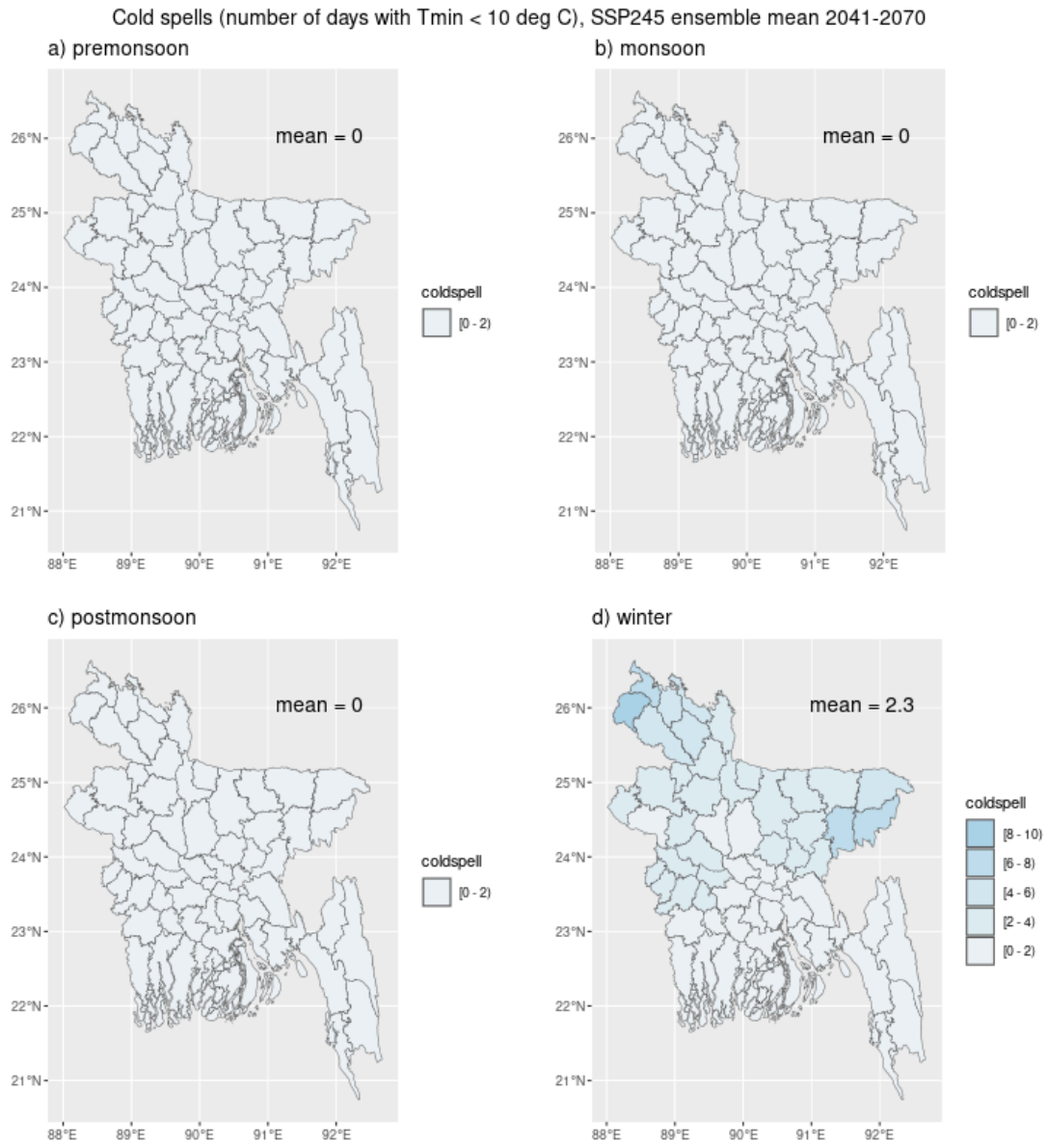


*Figure A2.39 The number of cold spell days (daily minimum temperature < 10 °C) in the* mid-century *(2041–2071) under SSP2-4.5. The estimates are based on the NEX-GDDP-CMIP6 ensemble mean of the daily minimum temperature for the a) pre-monsoon, b) monsoon, c) post-monsoon, and d) winter seasons.The mean value of each map shows the country average.*

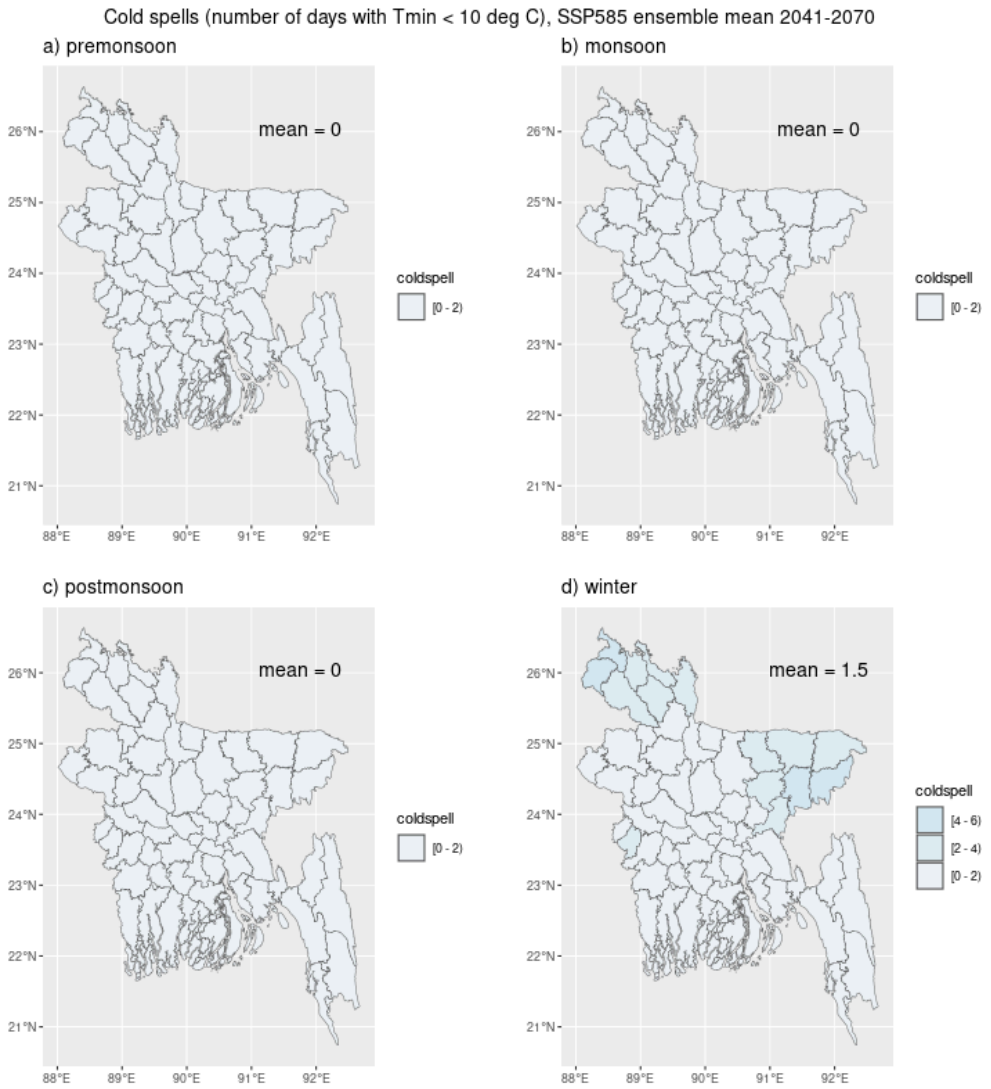


*Figure A2.40 The number of cold spell days (daily minimum temperature < 10 °C) in the* mid-century *(2041–2071) under SSP5-8.5. The estimates are based on the NEX-GDDP-CMIP6 ensemble mean of the daily minimum temperature for the a) pre-monsoon, b) monsoon, c) post-monsoon, and d) winter seasons.The mean value of each map shows the country average.*

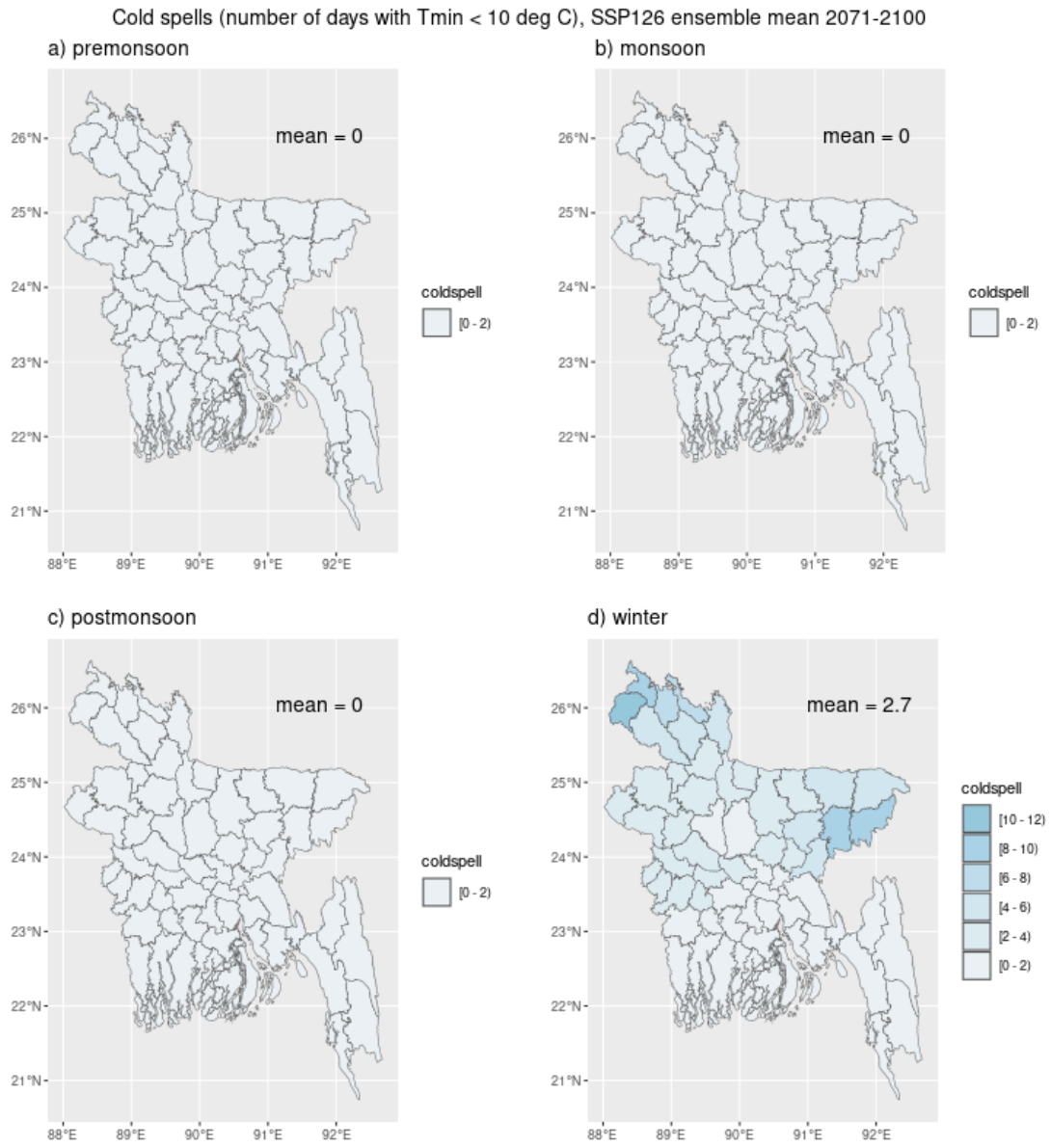


*Figure A2.41 The number of cold spell days (daily minimum temperature < 10 °C) at the end of the century (2041–2071) under SSP1-2.6. The estimates are based on the NEX-GDDP-CMIP6 ensemble mean of the daily minimum temperature for the a) pre-monsoon, b) monsoon, c) post-monsoon, and d) winter seasons.The mean value of each map shows the country average.*

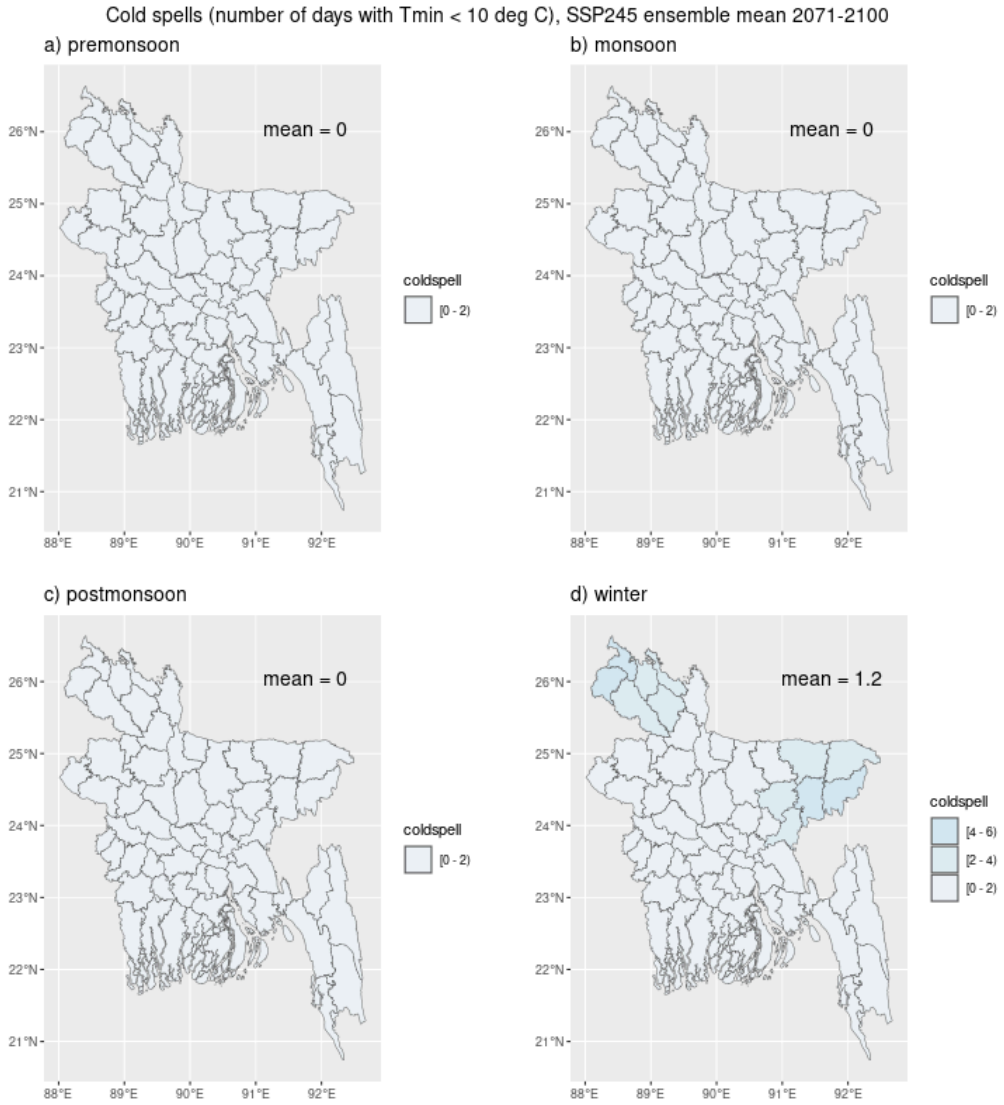


*Figure A2.42 The number of cold spell days (daily minimum temperature < 10 °C) at the end of the century (2041–2071) under SSP2-4.5. The estimates are based on the NEX-GDDP-CMIP6 ensemble mean of the daily minimum temperature for the a) pre-monsoon, b) monsoon, c) post-monsoon, and d) winter seasons.The mean value of each map shows the country average.*

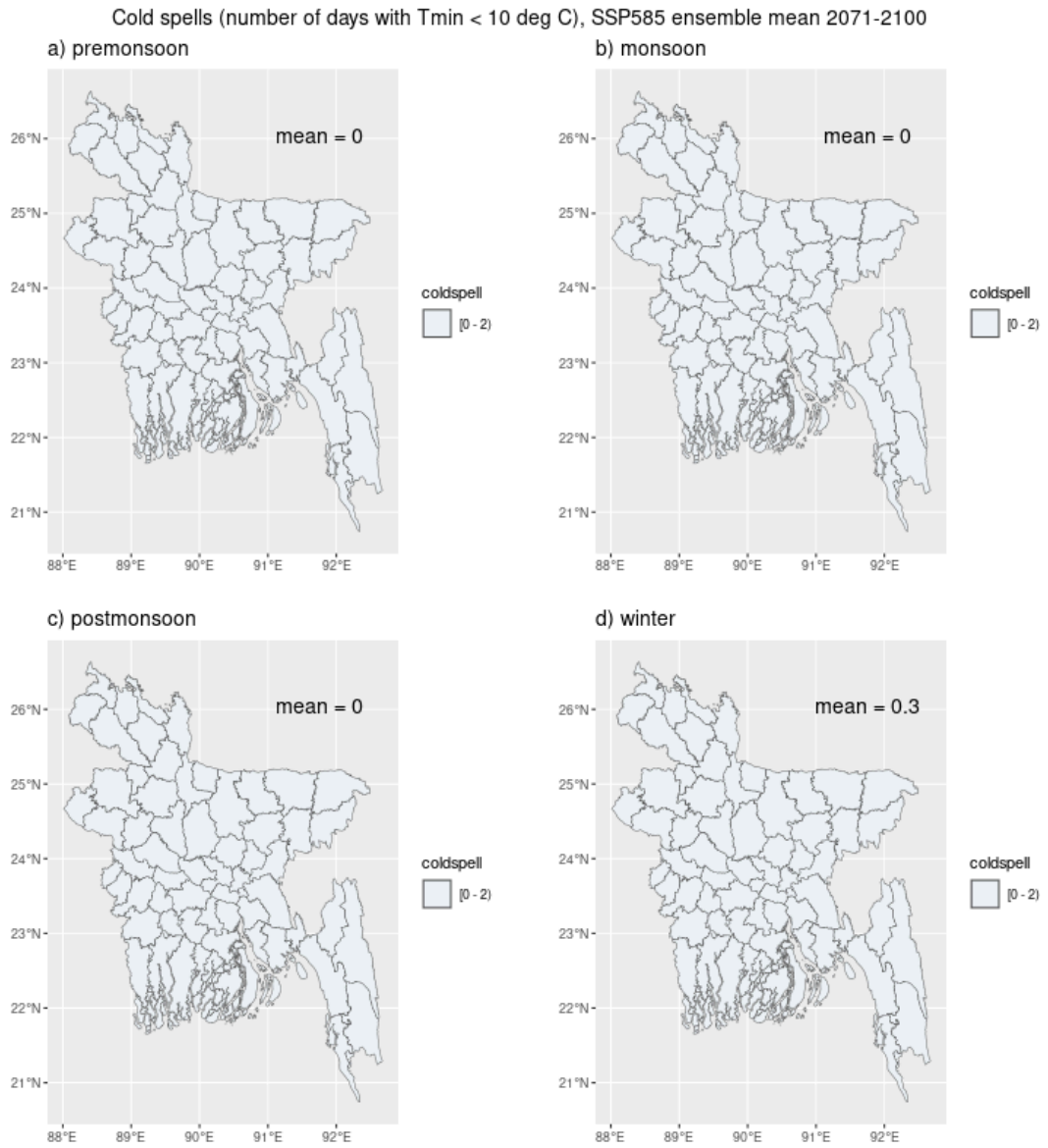


*Figure A2.43 The number of cold spell days (daily minimum temperature < 10 °C) at the end of the century (2041–2071) under SSP5-8.5. The estimates are based on the NEX-GDDP-CMIP6 ensemble mean of the daily minimum temperature for the a) pre-monsoon, b) monsoon, c) post-monsoon, and d) winter seasons.The mean value of each map shows the country average.*


Save the Children

RIMES

JAGONARI
জাগোনারী

SKS


german
humanitarian
assistance